POLITECNICO
MILANO 1863

SCUOLA DI INGEGNERIA INDUSTRIALE E DELL'INFORMAZIONE
Dipartimento di Scienze e Tecnologie Aerospaziali

SCHOOL OF INDUSTRIAL AND INFORMATION ENGINEERING
Department of Aerospace Science and Technology

Corso di Laurea Magistrale in
Ingegneria Aeronautica

Master's Degree Program in
Aeronautical Engineering

Theoretical Performance of Candidate Formulations for Micropropulsion Systems

Relatore:
Prof. Christian PARAVAN

Correlatore:
Prof. Tatiana I. GORBENKO

Tesi di Laurea di:

Edoardo SABAINI
Matr. 905533

Anno Accademico 2018/2019

Abstract

The miniaturization of spacecrafts requires the design of very small propulsion devices, and the development of solid propellant microthrusters can be an easy way to achieve large quantities of energy from small volumes. Among the various propellants that can be used for micropropulsion, thermite-based compositions deserve particular attention in light of their high reaction enthalpy. This research provides a wide chemical equilibrium analysis of different thermite formulations suitable for the application to micro-thruster applications. The theoretical performances of different compositions are investigated considering the effects of operating parameters as the oxidizer to fuel ratio. The main observable parameters of interest are the mixture temperature, the gaseous species produced mass fraction and the specific impulse performance. The analysis is performed by two different software (NASA CEA and the Russian counterpart TERRA), thus providing a comparison between the results obtained by different methods toward the chemical equilibrium assessment. The objective is not to find the real performances of the systems, but to obtain a relative grading between all the mixtures involved in this research. In a first part of the analysis, a relative grading between different thermite formulations was performed. Under the tested conditions (chamber pressure of 1.0 MPa, nozzle expansion ratio of 15, shifting equilibrium), Al was considered as fuel, while different oxidizers (PbO, CuO, I_2O_5, Bi_2O_3 and $Bi(OH)_3$) were analysed. Bismuth-based compositions can not be studied with CEA since information about bismuth are not available in the chemical library of the software. For this reason, mixtures involving bismuth have been studied with TERRA. It was not possible to replicate the same operating conditions used for CEA, so the input parameters for TERRA are: chamber pressure 2.0 MPa, nozzle exit pressure 0.03 MPa. In order to be able to perform a relative grading, the best mixtures found with CEA have been further analysed with the same operating conditions used for TERRA, and then they have been compared with bismuth-based compositions.
The mixture Al/I_2O_5 (Ox/Fu = 0.286, $\Phi = 0.955$) was found to be a promising candidate for propulsion applications in light of its high specific impulse (1706 m/s, the highest value achieved in the relative grading between the different formulations, computed with CEA), and relatively low condensed combustion products mass fraction at throat (25.5%).
Thermites are able to release large quantities of heat but producing a small amount of gas. This is unfavorable for propulsion applications where propellant mixture is expanded through the gas dynamic nozzle to produce thrust. For this reason, performances of the thruster can be enhanced by using a mixture made with a heating source (thermite) and a gas-generating agent like HMX, RDX, nitrocellulose, nitroglycerin and ammonium perchlorate. It was found that even just adding a small amount of additive (5-10 wt.%) leads to a significant increase in performances. The mixture Al/I_2O_5/HMX/NC (Ox/Fu = 0.758) with mass composition 9.90/35.10/50.00/5.00 is the best one in terms of specific impulse (2597.0 m/s, computed with CEA) and produces 18.03 % of condensed species, but it is the only one that has been studied without knowing if compatibility between elements is ensured. Another interesting mixture is Al/CuO/HMX/NC (Ox/Fu = 1.428) with mass composition 11.26/33.74/50.00/5.00, it generates a specific impulse equal to 2380.8 m/s and produces 21.24 % of condensed species (computed with CEA). The best mixture in terms of production of condensed species is Al/Bi_2O_3/HMX/NC (Ox/Fu = 2.251) with mass composition 3.15/41.85/50.00/5.00, which produces a specific impulse equal to 2142.5 m/s and only 5.95 % of condensed species (computed with TERRA).

Sommario

La miniaturizzazione di veicoli spaziali richiede la progettazione di sistemi propulsivi molto piccoli, e lo sviluppo di micropropulsori a propellente solido può essere il modo più semplice per ottenere grandi quantità di energia da volumi di tali dimensioni. Tra i vari propellenti che possono essere utilizzati per la micropropulsione, le composizioni a base di termite meritano particolare attenzione alla luce della loro elevata entalpia di reazione. Questa ricerca fornisce una analisi di equilibrio chimico di diverse formulazioni di termite adatte alla micropropulsione. Le prestazioni teoriche delle diverse composizioni vengono investigate considerando gli effetti di parametri operativi come il rapporto tra ossidante e combustibile. I principali parametri di interesse sono la temperatura adiabatica di fiamma, la frazione massica delle specie gassose prodotte e l'impulso specifico. L'analisi è stata condotta con l'utilizzo di due software (NASA CEA e la controparte russa TERRA). L'obiettivo non è quello di trovare le prestazioni reali dei sistemi, ma di ottenere un confronto tra tutte le miscele coinvolte in questa ricerca. In una prima parte di analisi è stato effettuato un confronto tra diverse formulazioni di termite. Sotto le stesse condizioni (pressione in camera di 1 MPa, rapporto di espansione in ugello pari a 15, shifting equilibrium), è stato considerato l'alluminio come combustibile, mentre diversi ossidanti (PbO, CuO, I_2O_5, Bi_2O_3 e $Bi(OH)_3$) sono stati analizzati. Le composizioni a base di bismuto non possono essere studiate con CEA dal momento che le informazioni sul bismuto non sono disponibili nella libreria chimica del software. Per questo motivo le miscele che coinvolgono il bismuto sono state studiate con TERRA. Non è stato possibile replicare le stesse condizioni operative usate per CEA, dunque i parametri di input per TERRA sono: pressione in camera 2.0 MPa, pressione all'uscita dell'ugello 0.03 MPa. Per ottenere un confronto, le migliori miscele studiate con CEA sono state ulteriormente analizzate con le stesse condizioni operative usate per TERRA, e successivamente sono state paragonate alle composizioni a base di bismuto.
Si riscontra che la miscela Al/I_2O_5 (Ox/Fu = 0.286, Φ = 0.955) è un promettente candidato per applicazioni propulsive alla luce del suo alto impulso specifico (1705.6 m/s, il più alto valore ottenuto dal confronto tra le diverse formulazioni, calcolato con CEA), e una relativamente bassa percentuale di specie condensate in gola pari a 25.53 %.
Le termiti sono in grado di rilasciare enormi quantità di calore ma allo stesso tempo producono piccole quantità di gas. Quest'ultimo aspetto è sfavorevole per applicazioni propulsive dove il propellente deve espandere in ugello per produrre la spinta. Per questo motivo le prestazioni del propulsore possono essere incrementate utilizzando una miscela tra una fonte di calore (la termite) e un agente in grado di generare gradi quantità di gas, come HMX, RDX, nitrocellulosa, nitroglicerina e perclorato d'ammonio. I risultati confermano che aggiungendo anche solo una piccola quantità di additivo (5-10 wt.%) le prestazioni ottengono un significativo incremento. La miscela Al/I_2O_5/HMX/NC (Ox/Fu = 0.758) con una composizione di massa 9.90/35.10/50.00/5.00 è la migliore in termini di impulso specifico (2597.0 m/s, calcolato con CEA) e produce il 18.03 % di specie condensate, ma va specificato che è l'unica miscela che è stata analizzata senza sapere se la compatibilità tra i suoi componenti è assicurata. Un'altra miscela interessante è Al/CuO/HMX/NC (Ox/Fu = 1.428) con composizione di massa 11.26/33.74/50.00/5.00, la quale genera un impulso specifico di 2380.8 m/s e produce il 21.24 % di specie condensate (calcolati con CEA). La migliore in termini di produzione di specie condensate è Al/Bi_2O_3/HMX/NC (Ox/Fu = 2.251) con composizione di massa 3.15/41.85/50.00/5.00, la quale genera un impulso specifico di 2142.5 m/s e solo 5.95 % di specie condensate (calcolati con TERRA).

Ringraziamenti

Ringrazio il Professor Christian Paravan per la sua disponibilità, per la costante supervisione e per i suggerimenti che hanno permesso di portare a termine questa ricerca.
Ringrazio la Professoressa Tatiana Gorbenko per la sua professionalità, la sua cordialità e per l'impegno nell'accogliermi costantemente nel suo ufficio per discutere della ricerca.

Ringrazio i miei genitori, che fin dal primo giorno mi hanno supportato senza mai dubitare delle mie capacità. Un ringraziamento speciale va a mia mamma, la mia più grande sostenitrice, che in questi anni mi ha spronato ad andare avanti e mi ha risollevato nei momenti più difficili.

Ringrazio i miei amici dell'università, che ogni giorno mi hanno regalato almeno una risata, rendendo piacevoli le infinite ore passate tra i banchi.
Ringrazio i miei amici di Verona, che ormai considero una famiglia.
Infine ringrazio gli amici di Tomsk, che fin da subito mi hanno fatto sentire a casa e con i quali ho vissuto una delle esperienze più belle della mia vita.

Contents

List of Figures

List of Tables

Nomenclature

Acronyms

AP	Ammonium Perchlorate
ASP	Atmospheric Sounding Projectile
CEA	Chemical Equilibrium with Applications
CHAMP	CHAllenging Minisatellite Payload
DB	Double Base
DSC	Differential Scanning Calorimetry
ES	Electrospray
EURECA	EUropean REtrievable CArrier mission
GAP	Glycidyl Azide Polymer
GRACE	Gravity Recovery and Climate Experiment
HMX	High Melting eXplosive
HTPB	Hydroxyl-Terminated Polybutadiene
ISS	International Space Station
MEMS	Microelectromechanical Sytem
MM	Mechanical Mixing
NASA	National Aeronautics and Space Administration
NC	Nitrocellulose
NG	Nitroglicerine
RDX	Royal Demolition eXplosive
REDOX	REDuction-OXidation reaction
TNT	Trinitrotoluene
USA	United States of America
VST	Vacuum Stability Test

Greek Symbols

γ	Specific Heat Ratio	[-]
λ	Thermal Conductivity	$[W/(m \cdot K)]$
μ	Chemical Potential	$[J/mol]$

μ_f	Dynamic Viscosity	$[Pa \cdot s]$
ν	Stoichiometric Coefficient	[-]
Φ	Equivalence Ratio	[-]
ρ	Density	$[kg/m^3]$

Other Symbols

ΔH_f^0	Standard Enthalpy of Formation	[kJ/mol]
$\Delta_r H$	Standard Enthalpy of Reaction	[kJ/mol]
$\dot{m}$	Mass Flow Rate	$[kg/s]$
$\mathfrak{M}$	Average Molecular Mass	$[g/mol]$
$\mathfrak{R}$	Universal Gas Constant	$[J/(K \cdot mol)]$
A	Area	$[m^2]$
c	Effective Exhaust Velocity	$[m/s]$
c^*	Characteristic Velocity	$[m/s]$
C_F	Thrust Coefficient	[-]
c_p	Specific Heat at Constant Pressure	$[J/(K \cdot mol)]$
D	Diameter	$[m]$
D_c	Characteristic Length	$[m]$
E_a	Activation Energy	$[J]$
F	Thrust	$[N]$
g	Gibbs Free Energy	$[J]$
g_0	Acceleration of Gravity	$[m/s^2]$
h	Convective Coefficient	$[W/(m^2 \cdot K)]$
I_s	Specific Impulse	$[s]$
I_t	Total Impulse	$[N \cdot s]$
k	Specific Heat Ratio	[-]
L	Length	$[m]$
M	Mach Number	[-]
M_W	Molecular Weight	$[g/mol]$
m_f	Inert Mass	$[kg]$
m_p	Propellant Mass	$[kg]$
N	Number of Particles	[-]
Nu	Nusselt Number	[-]
p	Pressure	$[Pa]$
Pr	Prandtl Number	[-]
Q	Heat Flux	$[W]$

R	Gas Constant	$[J/(Kg \cdot K)]$
R_{gain}	Rate of Heat Gain	$[J/s]$
R_{loss}	Rate of Heat Loss	$[J/s]$
Re	Reynolds Number	[-]
S	Entropy	$[J/K]$
T	Temperature	$[K]$
t	Time	$[s]$
U	Internal Energy	$[J]$
V	Volume	$[m^3]$
v	Velocity	$[m/s]$
w	Effective Propellant Weight	$[N]$
Z	Percentage of Condensed Species in Combustion Products	[-]

Chapter 1

Introduction

Nowadays space research is mainly focused on the development of both heavy launchers for space exploration and micropropulsion systems for in-space maneuvering of micro-, nano-, and pico-satellites. This last research field is the main topic of this document. Small satellites are of huge interest for many companies, laboratories and universities. The capability of producing very small systems able to accomplish an enormous variety of tasks, allows to reduce a lot the mission operating costs, making space research more affordable. Small satellites can perform particular activities, such as inspection of large satellites, generation of "swarms" for multiple-point data acquisition, qualifications and tests of new hardware. Moreover, dimensions of the systems and their standard structure allow to easily connect them to the launcher and to deploy more than a single satellite per launch.

1.1 Micro-propulsion Systems: Motivations

Consequence of the miniaturization of satellites is the need of a micro-propulsion system. Satellites, whether large or small, require propulsion units in order to correct their attitude, to control the stability and to perform maneuvers. Microelectromechanical system (MEMS) technology allows to produce thrusters with dimensions of the order of microns, suitable for this kind of problem. The objective is to consider the technology already available for large scale rocket motors and bring it in the microscale world, or to find completely new ways of producing thrust. Many microthrusters have been already produced and tested, many are under development, others are just concepts. Researchers are focusing on different sources of energy: electric, laser and chemical. Each of them has particular characteristics and the objective is to exploit their advantages for micropropulsion.

Chemical propulsion is a consolidated way to produce thrust for large scale rockets. This system exploits the expansion in a nozzle of hot gases generated by the combustion of reactants (typically, condensed phase oxidizer and fuel, though gas systems can be implemented as well as monopropellant rockets). Specific impulse of chemical propulsion systems is much lower with respect to the one of electric propulsion systems, but at the same time the generated thrust is much larger. This, up to now, makes solid and liquid propulsion systems the only ways to bring a payload from ground to orbit. The same differences can be noticed also for micropropulsion. Electric microthrusters can potentially generate very high specific impulses but with very low thrust (less than 0.1 mN). Thus, the choice of the type of microthruster depends on the requirements of the mission.
It is worth noting that using liquid propellants for propulsion in space is quite complex, due to the emergence of problems like sloshing and leakage. Thus, research interest is more focused on solid propellants. The concept of chemical microthruster is very simple. The system consists of a combustion chamber, a nozzle, and an igniter. The most important aspect is the choice of the propellant. Many researches have been carried on to study thermite systems as propellant for microthrusters. Thermite is a mixture of a solid metal fuel and a solid oxidizer. The reaction between these two components releases a huge amount of heat, but usually with a low amount of gas. For this reason the main idea is to mix thermite as a heat source with gas-generating additives in order to enhance the properties of the propellant.

1.2 Objective of the Research

This document collects the most interesting thermite systems studied for micropropulsion. The aim of this work is to study with chemical equilibrium programs, like NASA CEA and the Russian counterpart TERRA, characteristics and performances of these mixtures making a relative grading. Thus, the objective is not to obtain realistic performances of these mixtures, even because CEA and TERRA do not allow to obtain them. The aim is to put the mixtures in the same conditions and see which one shows the best theoretical characteristics and performances. This kind of preliminary analysis allows to understand which mixture would be the best choice for a chemical microthruster before facing with real experiments.
Setup, analysis, results and considerations about these interesting mixtures are reported in the following chapters.

1.3 Presentation Plan

This document is divided in different chapters. Chapter 2 describes different aerospace applications in which the characteristics of energetic materials can be exploited. An overview about microthrusters, gas generators, rocket igniters and welding systems is presented.
In Chapter 3 some theoretical concepts required for the understanding of the topic are explained.
Chapter 4 describes the way in which chemical equilibrium software like NASA CEA and TERRA work. The approximations applied to the simulation and their effects on the results, and the input parameters required are reported.
In the first part of Chapter 5 all the mixtures studied in this document, followed by their characteristics and the results coming from other scientific papers, are described. Results and their discussion are then reported, before the conclusion in Chapter 6.
Appendix A presents a preliminary analysis about a potential system in which thermite is used as a heat source in a gas propulsion system. Some basic equations of thermodynamics are applied in order to get a general idea on which gas would gain more benefits in terms of propulsion performances by the introduction of a heating chamber warmed by thermite.

Chapter 2

The Use of Thermites in the Aerospace Field

Thermite reaction was discovered in 1893 when Hans Goldschmidt, a German chemist, began to experiment with aluminothermic reactions for the production of high purity chromium and manganese. Metal fuel and metal oxide powders must be mixed and ignited in order to achieve the reaction. Due to the huge amount of heat released and its versatility, thermite reaction was immediately employed in several applications. Rail welding was one of the first important applications that exploited the properties of thermite reaction. The ease of use and the enormous availability of components made the thermite a suitable and efficient mixture to join rails.
From then on, this reaction has been the subject of numerous studies aimed at improving its performances and efficiency by changing or adding components to the mixture. Important results have been obtained in both civil and military fields, and in the last decades researchers tried to exploit the enormous potential also for the aerospace. To date, thermite systems in aerospace field are not yet consolidated, so it is difficult to find a state-of-the-art with which to compare the results obtained from experimental research. Most of the comparisons are made with typical compositions used in other fields, trying to analyze more carefully interesting parameters such as pressure peaks generated by the ignition of the mixture, temperature of gas products and specific impulse.
Gas generation, solid rocket motor ignition, welding in space and propellants for micro-thrusters are just some of the possible aerospace applications in which to introduce thermite processes. In the next sections are reported the researches carried out for these special purposes and the related results [1].

2.1 Propellants for Micro-Thrusters

During the last decades, small satellites became very interesting for space missions. Thanks to their small sizes and simplicity, they are relatively cheap and they can be produced with very low weights, usually lower than 500 kg. Different classifications based on mass can be used in order to categorize small satellites. The term minisatellites refers to satellites with a mass between 100 and 500 kg; microsatellites have a mass between 10 and 100 kg; nanosatellites between 1 and 10 kg; picosatellites between 0.1 and 1 kg.
The size of these systems allows to enormously reduce the cost of missions, which can be affordable for a lot of universities or research laboratories. Furthermore, small satellites can perform particular missions that otherwise could not be accomplished with large satellites, such as: in-orbit inspections of large satellites, create formations of satellites in order to get data from multiple points, testing and qualifying new hardware. Thanks to their dimensions, with a single launch it is possible to deploy more than one satellite per mission.
One of the most interesting nanosatellites is CubeSat. CubeSat is a miniaturized satellite used for space research, developed in 1999 by California Polytechnic State University and by Stanford University. It is made by multiples 10x10x10 cm^3 cubic systems called units, each of which has a mass of no more than 1.33 kg. Each unit has a simple structure, with a standardized interface, which allows to easily connect it to the launcher, or to join it to another unit. A single unit is called CubeSat 1U. It is possible to increase the size of the satellite by adding other units along only one direction. Thus, CubeSat 2U is made by

two units, CubeSat 3U is made by three units and so on [2]. Some pictures of CubeSats are reported in Fig. 2.1.

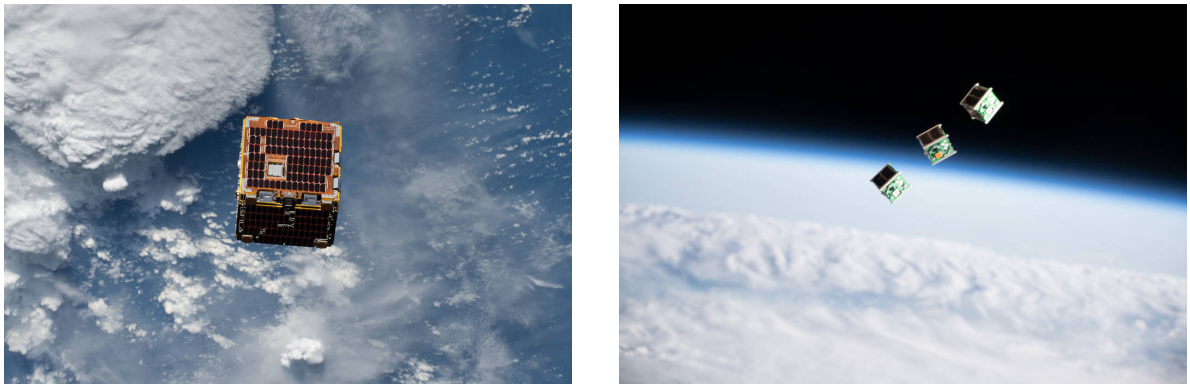

Figure 2.1: CubeSat deployed by ISS for the NanoRacks-Remove Debris investigation (left); three CubeSats ejected outside by the Kibo laboratory module (right) [2]

As large satellites, also small satellites require propulsion systems in order to perform maneuvers and to correct trajectory, attitude and stabilization. Due to the size of the satellite, also propulsion systems have to be adapted to these dimensions. Thus, the use of MEMS technology is of huge interest in order to produce microthrusters for small satellites. Recently, microthrusters became important propulsion units for microsatellites, synthetic aperture radar satellites, and space vehicles to keep orbit, to perform transfer orbit and to control the attitude. The most interesting concepts considered for micropropulsion are: electric thruster, cool gas thruster, laser thruster, and chemical thruster.
Electric thruster is able to provide very high specific impulses ($> 1000\ s$) but with a low thrust ($< 0.1\ mN$). On the contrary, chemical thrusters provide lower specific impulses ($< 200\ s$) but higher thrust (from $0.1\ mN$ to $100\ N$).

Electric propulsion devices can be divided into two major classes: electrostatic thrusters (gridded ion thruster, Hall thruster) and plasmadynamic thrusters (pulsed thruster, continuously operating thruster) [6]. This classification doesn't consider all the existing electric thrust systems, but these two groups are the most interesting for CubeSat applications. Grid ion thrusters are the oldest systems proposed as electric propulsion devices. They generate thrust by accelerating charged particles with an electrostatic field or expelling them while neutralizing the ionized beam with the flux of electrons ejected from a cathode. An anode inside the main combustion chamber supplies a propellant gas, usually xenon, which is ionized at the discharge, while a biased internal mesh extracts ions from the plasma. A second mesh accelerates the extracted ions before they are ejected. An external cathode produces an electron flux which ensures that the plasma exiting from the system is neutral and does not impart a charge on the spacecraft, as shown in Fig. 2.2. The entire process is represented in Fig. 2.3.

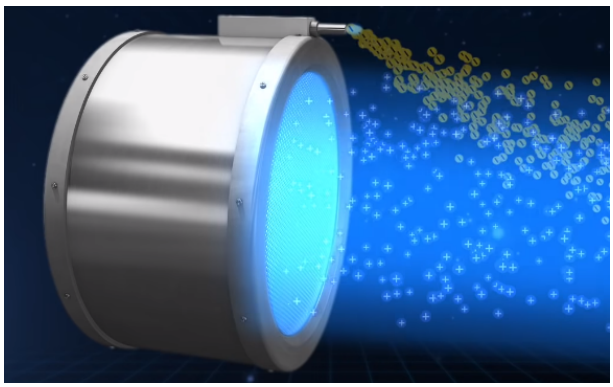

Figure 2.2: Ions flux exiting from the thruster and colliding with electron flux exiting from the external cathode [2].

Figure 2.3: Grid ion thruster operation: electron and neutral atom are released inside the chamber (left); electron and neutral atom collide and ionization occurs (center); positive ion moves towards the electrodes through which it will be accelerated (right) [2].

Hall thruster is another interesting electrostatic thruster considered for micropropulsion. Also in this case, the objective is to accelerate a propellant gas (tipically xenon) supplied in a coaxial channel through a ring-shaped anode. The symmetric axial geometry of the thruster allows to produce a closed Hall current. Electrons supplied by an external cathode are magnetized by a radial magnetic field that intersects an axial electric field, which extends in the direction of the channel length. Electrons trapped in the magnetic field collide with gas supplied by the anode generating ions, which are accelerated through the exit of the chamber at very high speeds, generating thrust. The very high efficiency, simplicity and potential durability make the Hall thruster an interesting system for small satellites propulsion. Fig. 2.4 shows the traditional and the hybrid magnetic systems of a Hall thruster.

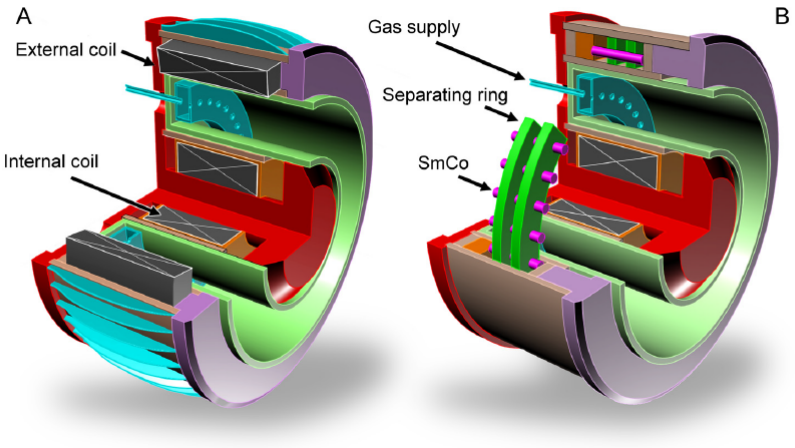

Figure 2.4: Traditional (left) and hybrid (right) magnetic systems of the miniaturized Hall thruster designed and tested at the Plasma Sources and Application Centre/Space Propulsion Centre, Singapore [3].

As mentioned before, another interesting system for micropropulsion is the cold gas thruster. Cold gas propulsion attracts a lot the attention being simple, clean, safe, and robust. For attitude and orbit control systems, extreme stabilisation, pointing precision, and contamination-free operation are important aspects that must be taken into consideration. Cold gas propulsion includes all that systems that generate thrust by making a propellant rushing out from the thruster in gaseous phase, and meanwhile no combustion should occur. However, thawing and warming up the propellant are allowed. The main characteristics that the propellant should have are the high atom weight (due to the third Newton law) and moderate low boiling and melting temperature. A list of the considered cold gas propellants and their performances is showed in Fig.2.5. Xenon is a potential cold gas propellant since it is an heavy

and inert gas. However, its viscosity increases with temperature, affecting the specific impulse. Helium and nitrogen are much lighter than xenon and their temperatures for storage in liquid or solid form is technically more demanding, but performances are way better. Sulfur hexafluoride (SF_6) is one of the most interesting gases thanks to its molecular weight and it sublimates at -64 °C at a pressure of 1 bar. The storage of the propellant is another important aspect. Storage in solid phase is favorable in comparison to storage in liquid phase. This allows to avoid sloshing problems, which could severely affect the high precision stabilization. The propellant is transformed into gas phase before leaving the storage tank.
Cold gas propulsion systems have been successfully adopted for many missions (e.g. EURECA, CHAMP and GRACE). Their characteristics are suitable when reliability, cleanliness and simplicity are the main requirements for the mission. These systems are the simplest form of rocket engine, therefore they are very cheap. The main advantages are: the contamination-free operation, the absence of net charge generation to the spacecraft and low-power operation. In fact, cold gas thrusters do not expel statically charged particles that can be attracted to the satellites surface and the power needed is mainly determined by electric systems and valve actuators. Moreover, it is not required to take care about the impact of electromagnetic force on the satellite.
The main drawbacks of this system are the problems related to the storage of the propellant and the low specific impulse, that imply relatively large propellant mass. Thus, this system is a suitable propulsion device for that missions that require low Δv. Furthermore, it is possible to consider carbon dioxide and sulfur hexafluoride as propellants that can be stored in solid phase, avoiding sloshing problems [4].

M_r = Molecular weight. t_m = Melting temperature. t_b = Boiling temperature. ρ = Density (241 bar, 0°C). $I_{sp,t}$ = Theoretical specific impulse. $I_{sp,m}$ = Measured specific impulse

Cold gas	M_r kg/kmol	t_m (1 bar) °C	t_b (1 bar) °C	ρ (241 bar) g/cm^3	$I_{sp,t}$ [a] s	$I_{sp,m}$ [a] s
H_2	2.0	-259	-253	0.02	296	272
He	4.0	-272	-269	0.04	179	165
Ne	20.4	-249	-246	0.19	82	75
N_2	28	-210	-196	0.28	80	73
Ar	39.9	-189	-186	0.44	57	52
Kr	83.8	-157	-152	1.08	39	37
Xe	131.3	-112	-108	2.74[b]	31	28
CCl_2F_2	121	-158	-29.8	---	46[c]	37
CF_4	88	-184	-128	0.96	55	45
CH_4	16	-182.5	-161.5	0.19	114	105
NH_3	17	-78	-33	Liquid	105	96
N_2O	44	-91	-88	---	67 [c]	61
C_3H_8	41.1	-187.7	-42.1	Liquid	---	---
C_4H_{10}	58.1	-138.3	-0.5	Liquid	---	---
CO_2	44	---	-78 (S)	Liquid	67	61
SF_6	146.1	---	-64(S)	---	---	---

[a] At 25°C. Assume expansion to zero pressure in the case of the theoretical value.
[b] Likely stored at lower pressure value (138 bar) to maximize propellant-to-tank weight ratio.
[c] At 38°C (560R) and area ratio of 100.
(S) Sublimation

Figure 2.5: List of cold gas propellants and their performances [4].

Finally, the remaining device to be described as a potential micropropulsion system is the chemical microthruster. Chemical propulsion is the most traditional kind of propulsion used for rockets. The propellant can be liquid or solid, but for microsystems used in space the best choice is the solid one. This because it is better to avoid problems related to leakage, friction of moving components and the structure is less complex. Nowadays, thanks to the MEMS technology, it is possible to fabricate innovative solid

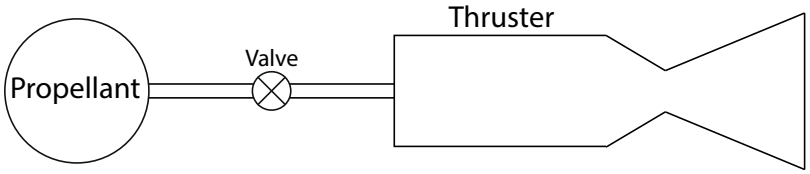

Figure 2.6: Conceptual representation of a cold gas propulsion system.

propellant thrusters suitable for small systems like micro- and nanosatellites. The use of solid propellants confers adequate functionality, simplicity and safety to the propulsion system. The underlying principle of the solid micropropulsion is the same as that for large rocket motors. The combustion of a solid propellant generates a large amount of hot gases, which expand in the nozzle generating thrust. Thus, the system is very simple since the only required components are a combustion chamber, a nozzle and an igniter. It also does not need moving parts and presents good efficiency.
Thanks to this low level of complexity, there are a lot of different geometries that can be adopted in order to produce a solid propellant microthruster. The classical cylindrical combustion chamber can be a solution, but it is common practice to produce a planar or a sandwich structure. Some examples are represented in Fig.2.7 and Fig. 2.8

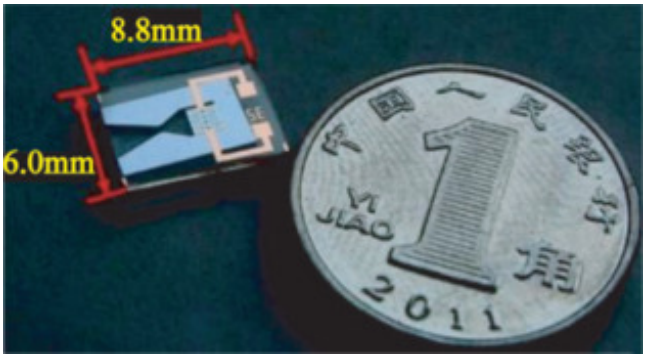

Figure 2.7: Planar structure of a microsolid propellant thruster [5].

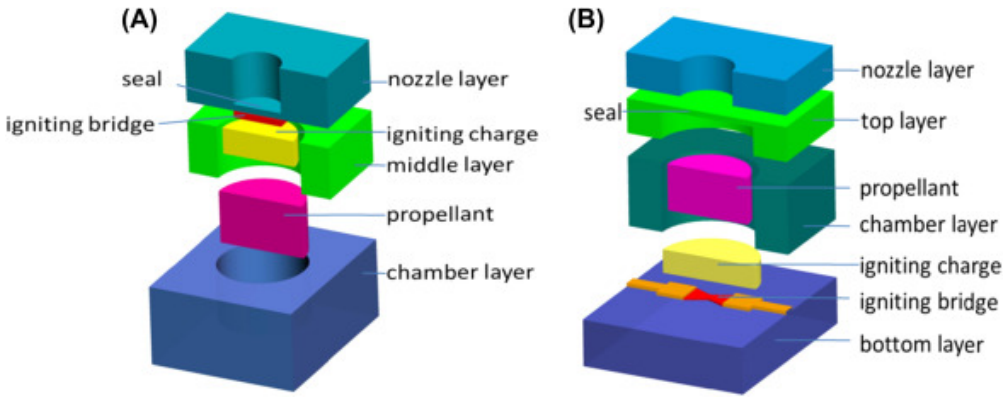

Figure 2.8: Sandwich structure of a microsolid propellant thruster. (A) Igniter on top. (B) Igniter on bottom [5].

The amount of solid propellant stored in microthrusters ranges from micrograms to milligrams. This low quantity leads to a burning time of few milliseconds. Thanks to this short burning time, the exceptional heat transfer and thermal conduction, nozzle and chamber are neither deformed or melted.

Conventional solid propellants used in large rocket motors are glycidyl azide polymer (GAP), ammonium perchlorate (AP) composites, hydroxyl-terminated polybutadiene (HTPB)/AP and gunpowders (75% potessium nitrate, 15% charcoal, and 10% sulfur). However, some of these propellants are not sufficiently sensitive to be used in microthrusters, and their ignition would require a separate ignitor, increasing the complexity of the system. Thus, most of the solid fuels for large rocket engines are not suitable for micropropulsion due to ignition inconsistencies, encapsulation inadequacy and safety.
Propellants should generate a large amount of gas with low average molecular weight and high combustion temperature. For this reason, highly energetic nanothermites and their composite are a good choice for micropropulsion systems. Thermite reactions release an enormous quantity of heat, but generally generating a low amount of gas. Thus, mixtures of termite systems and gas-generating additives (such as HMX, RDX, nitrocellulose and nitroglycerin) are interesting propellants for micropropulsion [5] [6].

2.2 Nano-Energetic Gas Generators

As the name suggests, gas generators are devices used to generate huge amount of gas, typically through a chemical reaction. Among the largest uses of gas generators is space propulsion. The gas is typically used to drive a turbine rather than to provide thrust as in a rocket engine. Liquid rockets require a system able to transfer the liquid propellant from the tanks to the combustion chamber. This task is accomplished by centrifugal pumps, which are activated through a shaft by a gas turbine. Their purpose is to raise the pressure of propellants and deliver them into piping systems. The turbine is driven by hot gases generated by a combustion occurring in a separate gas-generator. This secondary combustion is typically achieved by burning part of the propellant coming from the tanks. The thermal energy is converted in mechanical energy by the turbine, then hot gases are exhausted, so this cycle is open. The higher is the temperature of hot gases entering in the turbine inlet, the lower is the flow of working fluid required by the gas generator, so the higher is the efficiency of the system [7].
Gas generators are widely used for other purposes. Thermite and other energetic materials can be suitable chemical compounds able to achieve very high gas temperatures thanks to their high energy release. Even if one of the typical drawbacks of thermite is the poor capability of generating gas, in some cases it is not. In the last years many researches focused on the evaluation of thermodynamic properties of high-energy nanocomposite materials which have several potential civil and military applications. Among all these compositions, the most widely investigated are Al/Fe_2O_3, Al/MoO_3, Al/CuO, Al/Bi_2O_3 and Al/I_2O_5. The fact that aluminum metal powders appear in all the compositions is due to the fact that they release a huge amount of energy during the combustion. It is demonstrated that Al/Bi_2O_3 and Al/I_2O_5 generate the highest pressure impulse, due to the fact that bismuth and iodine boil at very low temperatures (1560°C and 184°C respectively) with respect to other metal oxides, generating an increase of the released gas pressure [9]. Moreover these mixtures posses optimal reaction characteristics such as fast energy release and high gas discharge and shock wave velocity. Other advantages are:

- reduced ignition delay and reaction times;
- superior heat transfer rate;
- tunability of novel energetic fuel/propellants with desirable physical properties;
- enhanced density impulse.

The attention is also focused on the effects of a decrease of aluminum powders size. The use of micro-aluminum as an additive in solid propellants for space propulsion is well consolidated due to the higher heat release during oxidation, higher combustion temperature, higher density, lower costs and higher safety [8].
Nowadays the challenge is to replace this ingredient with nano-aluminum. Many experiments have been done in this direction and the results are promising. The idea is to replace micro-aluminum with nano-aluminum also in thermite mixtures. Experiments performed on several formulations showed an increase of the combustion temperature leading to an increase of the vaporized reaction products, so a higher pressure peak upon a decrease of the aluminum particles from 70 microns to 100 nanometers [9]. These results are very interesting in order to consider these reactions for gas generation purposes.

2.3 Solid Rocket Motor Ignition

The igniter for a solid rocket motor is that device that produces the required heat and gases for the rocket ignition. Ignition is considered achieved when sufficient grain surface starts burning. If the igniter is not powerful enough the flame extinguishes causing the failure of the mission. Thus, the design of the ignition systems requires a lot of attention in order to produce a very reliable device.
Typical ignition systems for solid rocket motors are pyrotechnic igniters, which use energetic propellants or explosives as heat-producing materials.
There are many requirements for propellants used for ignition systems:

- High heat release and gas generation;
- Small ignition time delay;
- Rapid initiation;
- Low sensitivity to ambient temperature changes;
- Safety (during manufacturing, handling and shipping);
- Minimal degradation with time;
- Low costs;
- Low toxicity and corrosive effects.

There is a variety of consolidated igniter propellants, including black powders and extruded double based propellants. A common igniter formulations is: 20-35% of boron, 65-80% of potassium nitrate and 1-5% of binder (expoxy resins, graphite, nitrocellulose). Another formulation can be a mix of magnesium and fluorocarbon, called Teflon, which produces hot particles and hot gases [7].
Ignition systems require high specific energy, so typical pyrotechnic mixtures include metallic fuels (aluminum, magnesium, boron, zinc, carbon) and metallic oxides (NH_4ClO_4,CuO,Fe_2O_3,BaO,BaO_2) [10].
Thus, thermite systems as igniters for solid rocket motors are not a novelty. Between 1955 and 1962, Asp (Atmospheric Sounding Projectile) rockets were used several times by USA to study explosion clouds of nuclear bombs. These rockets were ignited by a mixture of aluminum and copper oxide, a high energy formulation that burns rapidly producing very little gas [11].

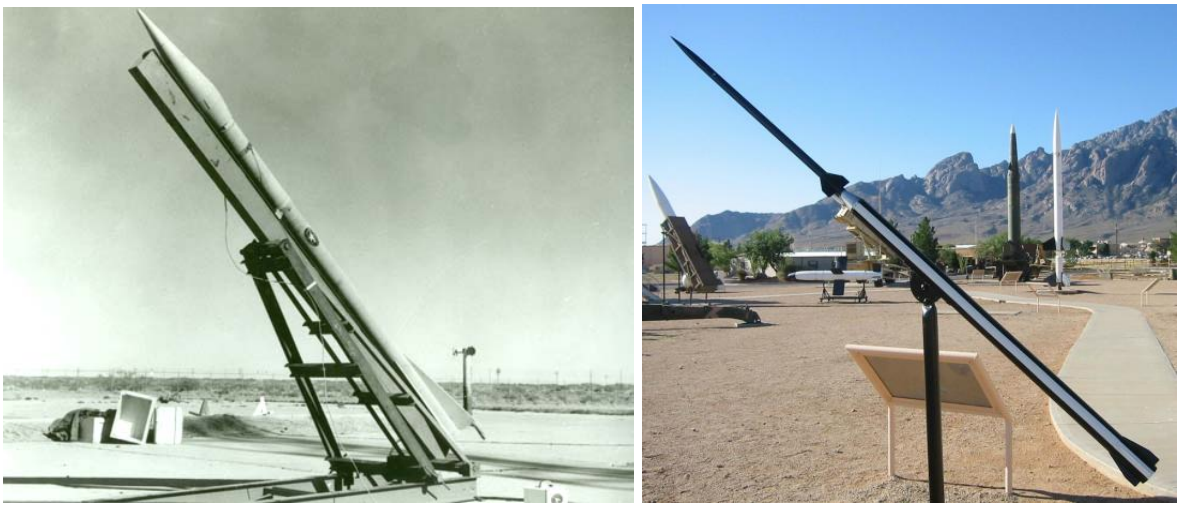

Figure 2.9: Atmospheric Sounding Projectile (left) [12]; Loki-Dart at the White Sands Missile Range rocket museum (right) [13]

Another example is the Super-Loki Dart rocket, an American unguided anti-aircraft rocket adapted to be used as a meteorological sounding rocket, which was ignited by Al/CuO mixture [14]. Pictures of ASP

and Loki-Dart are reported in Fig. 2.9.

With respect to ignition compounds in use, thermite possesses a higher energy density and it is cheaper, safer and readily available. One of the most interesting thermite composition is Al/CuO due to its high energy density, high reaction rate, wide availability and low cost [7] [9] [15].

2.4 Welding in Space

Complexities on welding in space are very clear since the first approach to this challenge. In 1969 Russian cosmonauts Georgi Shonin and Valeri Kubasov were the first to deal with the welding in space during Soviet Soyuz 6 mission, using a tool known as Vulkan. They tested three welding processes: electron beam welding, low-pressure compressed arc welding and arc welding with a consumable electrode. They got significant and promising results, but they also experienced the complexity and the danger of welding in space, since Kubasov burned through the hull of the Soyuz 6's living compartment risking to be hurled into space without spacesuit.
From then on, many efforts have been done in order to develop a reliable method for welding in space. This challenge is not easy, due to the many restrictions imposed by the operating environment. Spacecrafts require limited space and need to be as light as possible, but the most critical aspect for welding in space is the microgravity condition [16].
NASA has been working on innovative welding techniques for the past few years, such as:

- Friction stir welding: technique that uses frictional heating to produce strength bonds without defects (Fig. 2.10) [17];
- Ultrasonic stir welding: technique that uses ultrasonic energy to join two metallic alloy pieces. The process is very fast and reduces unwanted forces [18];
- Handheld laser: a compact and efficient tool which provides high accuracy, easy maneuverability, improves user safety and decreases heat-affected zones. This tool can be used only for small welding jobs (Fig. 2.10) [19].

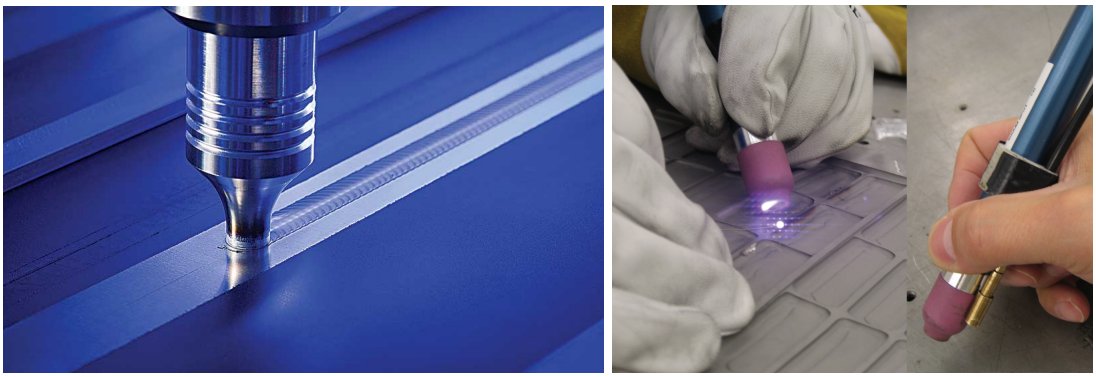

Figure 2.10: Friction stir welding (left) [17]; laser handheld (right) [19].

Thanks to their low energy consumption and self-sustained behaviour of the involved chemical reactions, thermite systems are of great interest for space applications. Many experiments have been carried out in order to use thermite both as a repairing technique and as a fabricating technique in space. For the first one, many experiments tried to investigate the effects of microgravity on the quality of the weld. Unfortunately, results are not promising. Despite the use of springs in order to push the mixture near the welding site, the microgravity condition does not favor the effect of buoyancy forces which lead to the separation of the oxidized metal from the pure metal, generating a weak weld.
However, attention moves also on fabricating techniques. Future exploration of Moon and Mars will require construction of landing/launching pads, radiation shields and other structures. It is possible to create thermite systems using lunar regolith, which is the layer of solid material covering the bedrocks of a planet [20]. Regolith primarily consists of oxides, so the mixture with metal powders like magnesium generates a thermite system [21] [22].

Chapter 3

Theoretical Concepts

Before entering into the details of the use of chemical equilibrium programs (NASA CEA and TERRA), a brief introduction to some important theoretical concepts is required. In order to obtain significant results, these software require many parameters as inputs. Besides the description of the mixture, user must introduce thermodynamic parameters (pressure, standard enthalpy of reaction) and also geometric parameters of the nozzle and the combustion chamber (expansion ratio, contraction ratio). Some of these parameters are described below.

3.1 Standard Enthalpy of Formation and Standard Enthalpy of Reaction

When facing with chemical reactions it is useful to get in mind the definitions of two important concepts: standard enthalpy of formation and standard enthalpy of reaction.
The standard enthalpy of formation ΔH_f^o is the variation of enthalpy as a consequence of the formation of 1 mole of substance starting from its constituent elements, with all substances in their standard states [23]. This value is obtained for an arbitrary temperature (usually $25C$) at standard pressure (1 bar), and it is measured in kJ/mol. The value of ΔH_f^o for a pure element at its standard state, i.e. at its most stable form in standard conditions, is zero. For example, the ΔH_f^o of gaseous oxygen is zero, while for liquid oxygen is non zero.
The standard enthalpy of formation is a thermodynamic state function, so its value depends only on the initial and final conditions of the process, it does not depend on the path followed to arrive at the final state. For a given chemical reaction, the standard enthalpy of formation is evaluated by measuring experimentally the energy release/absorption (measured in kJ) of a single mole of reactants. To further clarify the concept, let's consider the combustion of carbon (graphite) with oxygen (gaseous) forming carbon dioxide (gaseous):

$$\mathrm{C(s) + O_2(g) \rightarrow CO_2(g)} \tag{3.1}$$

Considering what mentioned before, knowing that carbon and oxygen react at their standard state, i.e. their ΔH_f^o is zero, the energy release measured during this reaction is the standard enthalpy of formation of carbon dioxide.
This kind of experiment has been carried out for a lot of substances so today one can find these values in many tables.
The standard enthalpy of reaction $\Delta_r H$ is the enthalpy change that occurs in a system when matter is transformed by a given chemical reaction, when all reactants and products are in their standard states. In order to compute the standar enthalpy of reaction of a chemical reaction one has to know the standard enthalpy of formation of reactants and products.
Given a generic chemical reaction:

$$\nu_A R_A + \nu_B R_B + ... + \nu_M R_M \rightarrow \nu_N P_N + \nu_O P_O + ... + \nu_Z P_Z \tag{3.2}$$

R_i is the i-th reactant, P_j is the j-th product and ν is the corresponding stoichiometric coefficient. The

standard enthalpy of reaction is given by:

$$\Delta_r H = \sum_{j=N}^{Z} \nu_j \Delta H^o_{fj} - \sum_{i=A}^{M} \nu_i \Delta H^o_{fi} \tag{3.3}$$

A negative value of the standard enthalpy of reaction means that the reaction is exothermic (the process releases energy), while a positive value means that the reaction is endothermic (the process adsorbs energy).
Another example helps to clarify the concept. Let's consider the reaction between pure aluminum and copper oxide, which generates alumina and pure copper:

$$2\mathrm{Al} + 3\mathrm{CuO} \rightarrow \mathrm{Al_2O_3} + 3\mathrm{Cu} \tag{3.4}$$

The standard enthalpy of reaction is:

$$\begin{aligned} \Delta_r H &= \Delta H^o_{f_{\mathrm{Al_2O_3}}} + 3\Delta H^o_{f_{\mathrm{Cu}}} - 2\Delta H^o_{f_{\mathrm{Al}}} - 3\Delta H^o_{f_{\mathrm{CuO}}} \\ &= -399.09 + 3 \cdot (0) - 2 \cdot (0) - 3 \cdot (38.5) \\ &= -283.59 \frac{kcal}{mole} \end{aligned} \tag{3.5}$$

This means that the reaction of aluminum with carbon dioxide is an exothermic process [23].

3.2 Chemical Potential

The tendency of a substance to react with other substances, or to change its state of aggregation, or to migrate to another place can be described by a single physical quantity: the chemical potential. These processes take place spontaneously because the tendency to change is higher in the initial state than in the final one. Thus, the chemical potential in the initial state is greater than the chemical potential in final state.
Chemical potential refers to a specific substance and it is a function of its temperature, pressure, concentration and state of aggregation (chemical potentials of water and ice at the same pressure and temperature are different).
Let's consider a system which can exchange energy and mass with a tank, and the volume of which can change. The internal energy of the system can change in three ways: heat exchange; expansion/compression of the volume under the action of pressure; exchange of particles. Thus, the variation of internal energy is given by:

$$dU = Tds - pdV + \mu dN \tag{3.6}$$

where T is the temperature of the system, ds is the variation of entropy, p is the pressure acting on the system, dV is the variation of the volume, dN is the variation of the number of particles (all of a single type) and μ is the chemical potential. If volume and entropy of the system do not change, the chemical potential is defined as:

$$\mu = \left.\frac{\partial U}{\partial N}\right|_{s,V} \tag{3.7}$$

so it is measured in J/mol or G, which stands for Gibbs, the scientist who first introduced the chemical potential.
A chemical reaction, a phase change or a migration occur spontaneously when their tendency to a change is more pronounced in the initial state than in the final state, i.e., because the chemical potential of the initial state A is greater than in the final state B, with A and B that can be either pure substances composed by a single atoms, or complex molecules formed by different elements.
Values of chemical potential for each substance are collected in tables. It is not possible to find absolute values since it cannot be measured with such a precision. This is the reason why tables contain the difference between the potential of the substance and the potentials of the elements that compose the substance. The values usually refer to standard conditions, i.e. at a temperature equal to 298 K and pressure equal to 0.11013 MPa. Potential of chemical elements at their most stable condition or state

of aggregation is 0 J/mol (gaseous argon, solid gold, solid boron). Moreover, the chemical potential of most substances is negative, and this means that these substances are stable, so they do not decompose voluntarily into their constituents.
Thus, chemical potential allows to predict in which direction a chemical reaction proceeds. Let's consider an example:

$$\mathrm{Ca(OH)_2 + CO_2 \rightleftharpoons CaCO_3 + H_2O} \tag{3.8}$$

values obtained from a table of chemical potentials are: $\mu_{\mathrm{Ca(OH)_2}}$ = -897 kJ/mol, $\mu_{\mathrm{CO_2}}$ = -394 kJ/mol, $\mu_{\mathrm{CaCO_3}}$ = -1129 kJ/mol, $\mu_{\mathrm{H_2O}}$ = -237 kJ/mol. Total potential of reactants μ_A must be compared with total potential of products μ_B.

$$\mu_A = \mu_{\mathrm{Ca(OH)_2}} + \mu_{\mathrm{CO_2}} = -1291 \quad kJ/mol \tag{3.9}$$

$$\mu_B = \mu_{\mathrm{CaCO_3}} + \mu_{\mathrm{H_2O}} = -1366 \quad kJ/mol \tag{3.10}$$

Thus, $\mu_A > \mu_B$. This means that the reaction proceeds from left to right [24].

The chemical potential is useful to introduce the concept of minimization of Gibbs free energy. For a mixture of N chemical species the Gibbs free energy per kg of mixture is given by:

$$g = \sum_{j=1}^{N} \mu_j n_j \tag{3.11}$$

where n_j is the number of kilogram-moles of species j per kilogram of mixture, and the chemical potential per kg-mole in this case is defined as:

$$\mu_j = \left.\frac{\partial g}{\partial n_j}\right|_{T,p,n_{i\neq j}} \tag{3.12}$$

The condition for chemical equilibrium is the minimization of the Gibbs free energy, and this is what a chemical equilibrium program does in order to solve problems involving chemical reactions [25].

3.3 Chemical Rocket Propulsion

Among the numerous ways that can be used to classify rocket propulsion systems, one of the most accepted is based on the energy source type (chemical, electric, nuclear, solar). Chemical propulsion is the most common way to produce thrust for a rocket or for a space vehicle. It generates thrust by exploiting the thermodynamic expansion in a supersonic nozzle of hot gases produced by the combustion of a propellant. The discovery of chemical propulsion is not recent. Solid propellants were used over 800 years ago to produce rocket-propelled projectiles during the Chinese Empire era. However, the most significant developments of rocket propulsion systems took place in the twentieth century thanks to the early pioneers K. E. Tsiolkovski and R. H. Goddard. The former, a Russian engineer credited with the fundamental rocket flight equation and his proposal to build rocket vehicles in 1903. The latter, an American engineer credited with the first flight using a liquid propellant rocket engine in 1926 [7].
According to the physical state of the stored propellant, there are different classes of chemical propulsion rockets.
Liquid rocket engines use liquid propellants stored in tanks and fed under pressure into a thrust chamber. The system can be bipropellant or monopropellant. The former uses a liquid oxidizer (e.g., liquid oxygen) and a liquid fuel (e.g., kerosene). The latter is a single liquid that decomposes into hot gases when flowing over a catalyst bed of specific characteristics. Some liquid rockets allow to stop and restart the motor thanks to the use of several precision valves. Due to the presence of valves, pumps, turbines and gas generators, the system is very complex and expensive. However, liquid rocket engines fed by hydrogen and oxygen provides the highest specific impulse among all the chemical rockets. Fig. 3.1 shows the diagram of a liquid propellant rocket engine.
Solid rocket motors store solid propellant directly in the combustion chamber. The typical solid propellant for space applications is a heterogeneous (or composite) propellant. In these systems the reactants

are all in the solid phase, and are mixed in a solid propellant grain. The latter is a composite material featuring an heterogeneous structure (at the micro-scale). The grain is hosted in the case, and it is produced with an internal hollow which can have different geometries. Initial burning takes place in the internal surface of the hollow and the cavity expands as the propellant is consumed. Gas produced with combustion flows through the nozzle generating the thrust. Once ignited, solid rocket motor cannot be stopped until the propellant extinguishes, unless a thrust termination system is activated in case of emergency. However, the system is very simple and highly reliable, it does not require feed systems or valves. Fig. 3.2 shows the section of a typical solid rocket motor.
Hybrid rocket engines use both liquid and solid reactants. Typically, the oxidizer is liquid, while the fuel is solid. If the system uses a liquid oxidizer and a solid fuel, it is called direct hybrid rocket. Hybrid rockets mix some advantages of solid and liquid rockets. For example, as liquid rocket engines they can be shut down easily and the thrust is throttleable, and at the same time they avoid the complexity of liquid systems and the dangers of solid propellants handling, since fuel and oxidizer are stored separately. Theoretical specific impulse of hybrid rockets is higher than that of solid motors, but lower than liquid ones. Fig. 3.3 shows the diagram of a hybrid rocket engine.
Gaseous rocket engines use a high-pressure gas, such as air, nitrogen, or helium, as working fluid. This system provide very low thrust and they were used in many space vehicles for low-thrust maneuvers and for attitude-control. Performances can be improved by heating the gas with electrical energy or with the energy released by combustion of certain propellants. In this case the system is called warm gas propellant rocket. The concept of gas rocket engine is simple, but it requires heavy tanks.

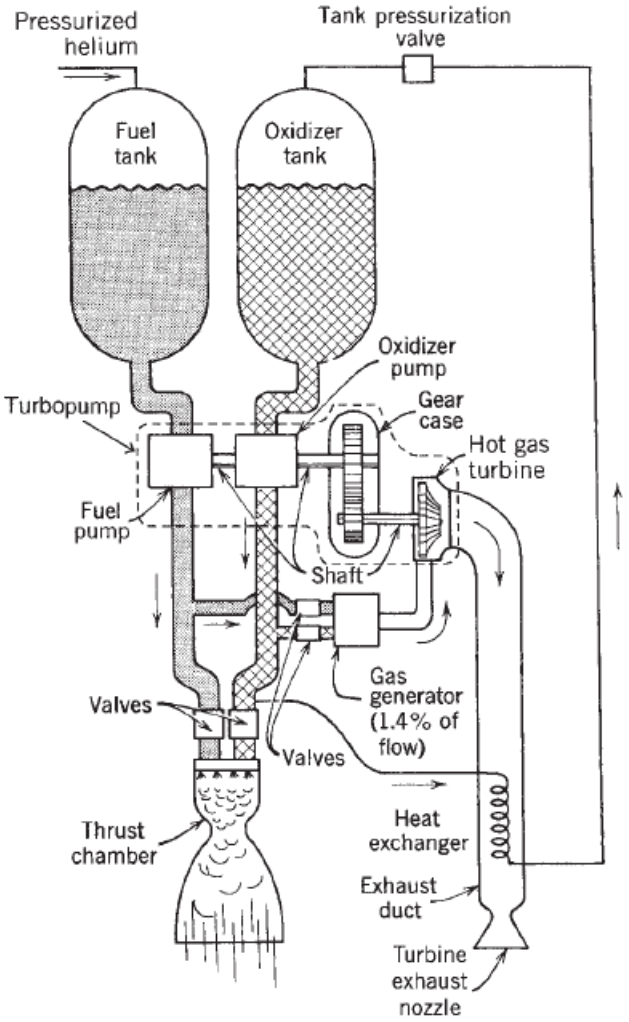

Figure 3.1: Simplified diagram of a liquid propellant rocket engine with one type of turbopump feed system and a separate gas generator, which generates warm gas for driving the turbine [7].

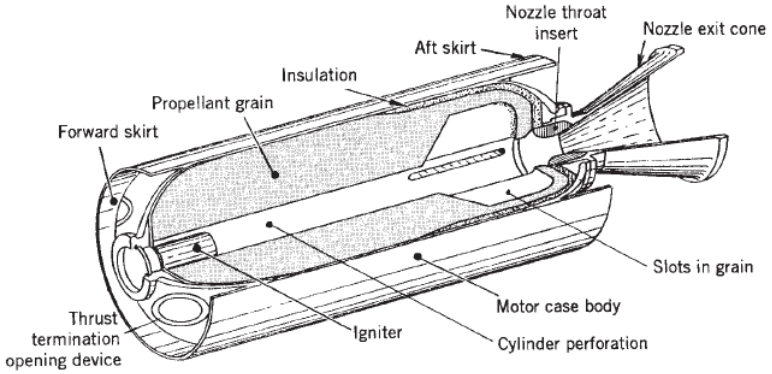

Figure 3.2: Section of a typical solid propellant rocket motor [7].

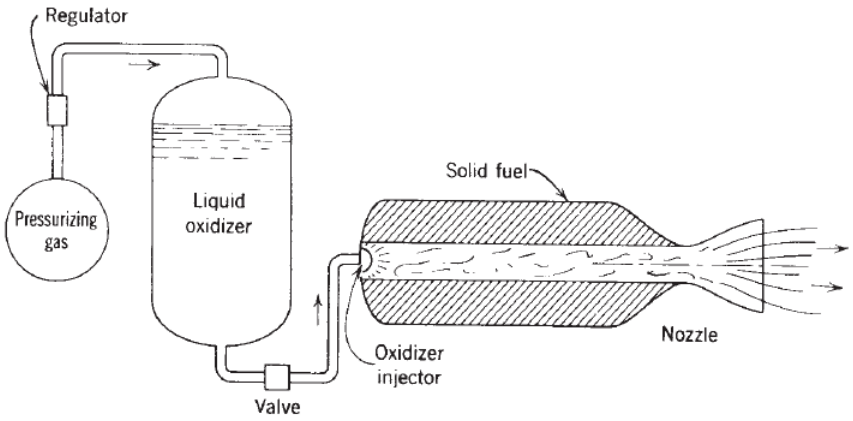

Figure 3.3: Schematic diagram of a typical hybrid rocket engine [7].

In order to evaluate performances for a rocket engine, some definitions and fundamentals about thrust, exhaust velocity, and combustion efficiency are required.
The ejection of hot gases at high velocities through the nozzle generates the thrust, which is a force that acts at the vehicle's center of mass. Thus, thrust is generated by a change in momentum, which is the vector quantity defined as the product of mass times its vector velocity. Under the assumptions of constant, uniform, and purely axial exit gas velocity v_2 (subscripts are shown in fig.3.4) and constant mass flow rate:

$$F = \frac{d(mv_2)}{dt} = \dot{m}v_2 \tag{3.13}$$

This is the total propulsive force only when the nozzle is adapted. When the nozzle is not adapted, a second contribution is given by the pressure of the surrounding fluid. Fig. 3.4 shows the pressures acting on chamber and nozzle walls. Ambient pressure p_3 is uniform, while internal pressure is higher in the combustion chamber (p_1) and decreases in the nozzle until it reaches the exit (p_2). For a fixed nozzle geometry, variations of ambient pressure along the altitude cause imbalances between the exiting gas pressure p_2 and the atmospheric pressure p_3 at the nozzle exit plane. Under the assumption of steady operation in a homogeneous atmosphere, the total thrust is given by:

$$F = \dot{m}v_2 + (p_2 - p_3)A_2 \tag{3.14}$$

Expansion ratios of nozzles A_2/A_t are designed so that the exhaust pressure equals the ambient pressure at a certain altitude. If the nozzle geometry is fixed, this condition occurs only at a certain altitude.

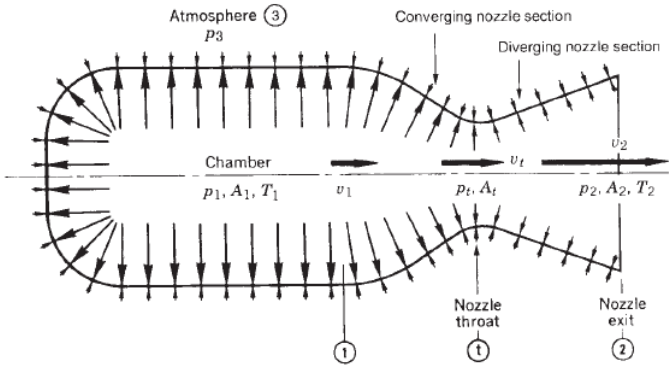

Figure 3.4: Pressure acting on chamber and nozzle walls [7].

The total impulse I_t is the integration of the thrust force F over the time:

$$I_t = \int_0^t F\,dt \tag{3.15}$$

Thus, if the thrust is constant after short start and stop transients:

$$I_t = Ft \tag{3.16}$$

Total impulse is related to the total energy of the propellant.
The specific impulse I_s represents the thrust per unit propellant "weight" flow rate. It is an important parameter for the definition of the performances of the rocket and its value is given by:

$$I_s = \frac{\int_0^t F\,dt}{g_0 \int_0^t \dot{m}\,dt} \tag{3.17}$$

where g_0 is the acceleration of gravity and is the total propellant mass flow rate. Considering average values for F and $\dot{m}$ for short intervals:

$$I_s = \frac{I_t}{m_p g_0} \tag{3.18}$$

where m_p represents the total effective propellant mass expelled. For constant propellant mass flow $\dot{m}$, constant thrust F, and negligible start or stop transients:

$$I_s = \frac{F}{\dot{m} g_0} = \frac{I_t}{w} \tag{3.19}$$

where w is the effective propellant weight $\dot{m}g_0$.
It is difficult to measure the velocity profiles along the exit cross section of the nozzle since the exhaust velocity is not uniform. The effective exhaust velocity c is a uniform axial velocity assumed for one-dimensional problem descriptions. This velocity is the average velocity at which propellant is being ejected from the rocket. It is computed as:

$$c = I_s g_0 = \frac{F}{\dot{m}} \tag{3.20}$$

It is worth noting that c and I_s differ by a constant (g_0), so one of them can be used as a figure of merit for the rocket.
The impulse-to-weight ratio is defined as the ratio between the total impulse I_t and the initial vehicle wight w_0. High values of this parameter mean efficient design. Under the assumptions of constant thrust and negligible start and stop transients, it can be obtained as follows:

$$\frac{I_t}{w_0} = \frac{I_t}{(m_f + m_p)g_0} = \frac{I_s}{\frac{m_f}{m_p} + 1} \tag{3.21}$$

where m_f is the final inert mass of the vehicle and m_p is the propellant mass.

As the altitude increases, the ambient pressure decreases. Thus, thrust and specific impulse increase as the rocket reaches higher altitudes.
Considering equation (3.14) and assuming constant mass flow rate, the exhaust gas velocity can be computed as:

$$c = v_2 + (p_2 - p_3)A_2/\dot{m} = I_s g_0 \tag{3.22}$$

Another parameter typically used is the characteristic velocity c^*, which is defined as:

$$c^* = \frac{p_1 A_t}{\dot{m}} \tag{3.23}$$

Though not a physical velocity, it is used to compare performances of different chemical rocket propulsion system designs and propellants. Since this parameter is independent from nozzle characteristics, it is essentially related to the efficiency of the combustion process.
All these parameters can be further related each other through thermodynamic relations. In this chapter all the passages required to get the final equations are not reported since it would require an extensive description. Considering the principle of conservation of energy, under the assumptions of adiabatic flow, and ideal gas, the total enthalpy per unit mass remains constant through the nozzle. This means that in the converging-diverging nozzle a large fraction of the thermal energy is converted into kinetic energy. Thus, assuming isentropic flow, the nozzle exit velocity can be computed from the equation of conservation of energy, and the relation can be expressed as follows:

$$v_2 = \sqrt{\frac{2k}{k-1} R T_1 \left[1 - \left(\frac{p_2}{p_1}\right)^{\frac{(k-1)}{k}}\right] + v_1^2} \tag{3.24}$$

where k is the specific heat ratio and R is the gas constant and it is equal to the ratio between the universal gas constant $\mathfrak{R}$ and the average molecular mass $\mathfrak{M}$ of the gaseous combustion products. Considering that the entrance velocity v_1 is relatively small, the term v_1^2 can be neglected, and the chamber temperature T_1 differs little from the stagnation temperature T_0. Thus, the exit velocity can be computed as:

$$v_2 = \sqrt{\frac{2k}{k-1} \frac{\mathfrak{R} T_0}{\mathfrak{M}} \left[1 - \left(\frac{p_2}{p_1}\right)^{\frac{(k-1)}{k}}\right]} \tag{3.25}$$

This relation shows that the exit velocity and its corresponding specific impulse are strongly related to the ratio between the stagnation temperature (which is close to the combustion temperature T_0) and the average molecular mass of the exhaust gases, as reported in fig. 3.5. This makes the fraction $T_0/\mathfrak{M}$ an important parameter for the optimization of the mixture ratio of the propellant.

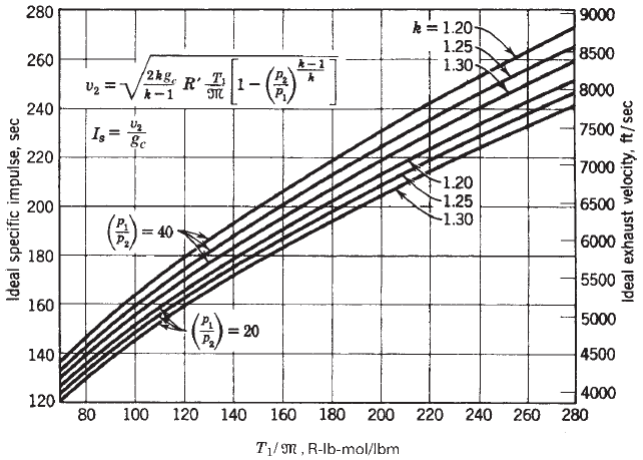

Figure 3.5: Specific impulse and exhaust velocity of an ideal rocket propulsion unit at optimum nozzle expansion as functions of the ratio between the chamber gas temperature T_1 and the molecular mass $\mathfrak{M}$ for several values of k and p_1/p_2 [7].

The ratio between the nozzle exit area A_2 and the throat area A_t is called nozzle expansion area ratio and it is an important nozzle parameter. For a supersonic nozzle the ratio between throat area and any downstream area can be expressed as:

$$\frac{A_t}{A_y} = \left(\frac{k+1}{2}\right)^{1/(k-1)} \left(\frac{p_y}{p_1}\right)^{1/k} \sqrt{\frac{k+1}{k-1}\left[1-\left(\frac{p_y}{p_1}\right)^{(k-1)/k}\right]} \tag{3.26}$$

When $p_y = p_2$, then $A_t/A_y = A_t/A_2$, which is the inverse nozzle exit expansion ratio. This equation shows the relation between the pressure ratio and the expansion ratio.
The last parameter that has to be considered for performances evaluation is the thrust coefficient, which is defined as:

$$C_F = \frac{F}{p_1 A_t} \tag{3.27}$$

It is a dimensionless parameter, useful for performance analysis. It is possible to exploit its dependencies, obtaining the following relation:

$$C_F = \sqrt{\frac{2k^2}{k-1}\left(\frac{2}{k+1}\right)^{(k-1)/(k-1)}\left[1-\left(\frac{p_2}{p_1}\right)^{(k-1)/k}\right]} + \frac{p_2 - p_3}{p_1}\frac{A_2}{A_t} \tag{3.28}$$

The thrust coefficient depends on the specific heat ratio of the gas k, the expansion ratio, and the pressure ratio p_1/p_2, but it is not directly dependent on chamber temperature. This parameter is useful for visualizing effects of chamber pressure and variations of altitude in a fixed nozzle configuration.
All these parameters can be related. The characteristic velocity can be written as:

$$c^* = \frac{p_1 A_t}{\dot{m}} = \frac{I_s g_0}{C_F} = \frac{c}{C_F} = \frac{\sqrt{kRT_1}}{k\sqrt{[2/(k+1)]^{(k+1)/(k-1)}}} \tag{3.29}$$

It is a function of propellant characteristics and combustion chamber properties, so it can be used as a figure of merit when comparing propellants combinations for combustion chamber performances [7].
Combining Eqs. 3.27 and 3.29, a new expression for thrust is obtained:

$$F = \dot{m} c^* C_F \tag{3.30}$$

Some of these parameters can be computed with CEA and TERRA, allowing to compare performances of different mixtures for chemical propulsion or different propulsion systems. Since the mass flow rate of the systems studied in this document is not known a priori, the thrust cannot be evaluated with chemical equilibrium programs. However, it is possible to compare mixtures by computing specific impulse, adiabatic flame temperature and composition of gas products. From the equations listed in this chapter it is clear that a good propellant must produce a very high combustion temperature and the gas generated must have a low molecular mass.

3.4 Thermite Reaction

Thermite is a pyrotechnic composition produced featuring metal fuel reaction with a metal oxide as oxidizing species source. Pyrotechnic mixtures, once ignited, undergo a strongly exothermic reduction-oxidation (redox) reaction. Redox is a chemical reaction in which oxidation states of atoms change. Oxidation occurs when one atom loses electrons, so its oxidation state increases. Reduction occurs when one atom acquires electrons, so its oxidation state decreases [27]. The reduction-oxidation reaction can be written in a generale form as

$$M + AO \rightarrow MO + A + \Delta H \tag{3.31}$$

where M is a metal or an alloy, A is either a metal or a non-metal, MO and AO are the corresponding oxides, and ΔH is the heat released by the reaction [28].
Pyrotechnics, together with explosives and propellants, are high-energy materials. The difference between these 3 categories is related to the nature of the combustion process. Pyrotechnic combustion occurs

by deflagration, i.e. layer-to-layer propagation, in contrast to explosive combustion, which leads to detonation and generation of shock waves. The distinction between solid propellants and pyrotechnics is the particularly powerful evolution of gas in propellants, which is the reason for their application in propulsion devices [29]. On the contrary, typical combustion products of pyrotechnic mixtures are condensed.
A typical example of pyrotechnic combustion is the thermite reaction between iron oxide and aluminum:

$$\mathrm{Fe_2O_3} + 2\mathrm{Al} \rightarrow \mathrm{Al_2O_3} + 2\mathrm{Fe} + Heat \tag{3.32}$$

In this case iron is reduced and gains three electrons, aluminum is oxidized and loses three electrons while oxygen is unchanged.
Thanks to the large heat release, a thermite reaction can generally be initiated locally and than it sustains itself. The mixture undergoes a cycle in which an increase of temperature generates an increase of the number of atoms with energy greater than the activation energy, leading to a further increase of the temperature of the material due to the increase of the reaction rate. This cycle suggests that a slight rise in temperature would lead to the pyrotechnic ignition, but in reality it doesn't work in this way. A huge amount of heat generated by the reaction is lost to the surroundings. Thus, in order to understand the process of a pyrotechnic ignition, two parameters must be introduced: the rate of heat production (R_{gain}) and the rate of heat loss (R_{loss}). The former increases exponentially following the Arrhenius equation:

$$R_{gain} \cong Ae^{BT} \tag{3.33}$$

where A and B are two constants, and T is the temperature. In the range below several hundred Celsius degrees, the rate of heat loss is proportional to the temperature difference between the composition (T) and the sorroundings (Ta):

$$R_{loss} \cong K(T - Ta) \tag{3.34}$$

where K is a constant. Fig. 3.6 shows the behaviours of the rates of heat gain and loss as function of the temperature of the material.

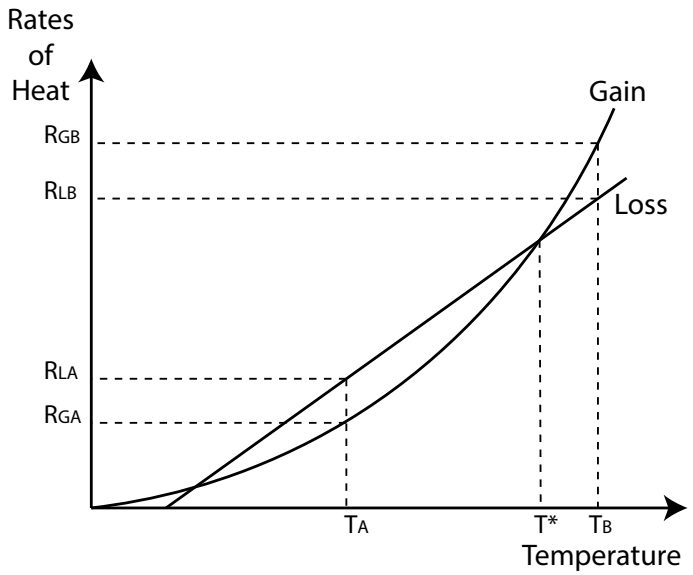

Figure 3.6: Rates of heat gain and loss as functions of the temperature of the material (this figure is adapted from Ref. [27]).

When the temperature reaches the value T_A the rate of heat loss is greater than the rate of heat production, so the temperature of the mixture goes back to the room temperature. When the temperature reaches the value T_B the situation is the opposite, so the temperature of the mixture and the rate of reaction continue to rise. T* is called *thermal run-away temperature* and corresponds to the point of contact between the two lines. This parameter depends on the activation energy, the standard enthalpy of reaction of the mixture and the ease of heat loss.

Another aspect that influences this process is the sample size. Only the heat loss is affected by this factor due to the thermal insulating effects. As the sample size increases the slope of the heat loss line decreases. The risk is to obtain a mixture in which the rate of heat production is always greater than the rate of heat loss, so the mixture spontaneously ignites. Furthermore, as the ambient temperature increases the heat loss line is translated to the right, decreasing the value of the thermal run-away temperature. These two behaviours are shown in Fig. 3.7.
Another important aspect for the ignition of pyrotechnic mixtures is the physical contact between solid fuel and solid oxidizer. After one component melts, it flows over the surface of the other component increasing a lot the number of atoms in physical contact. Thus, more atoms exceeding the activation energy are in contact and the rate of reaction increases, decreasing the thermal run-away temperature. Once a portion of mixture is ignited, the propagation is not guaranteed. Part of the heat generated is dissipated with the surrounding, so only if the heat transferred to the next layer of unreacted composition is enough, burning will continue.
The heat transfer occurs in three ways: conduction, convection and radiation. Conduction consists in the transfer of thermal energy through molecular vibrations along solids. Convective heat transfer occurs between solid and the hot gases which penetrate inside the solid. Thermal radiation is absorbed by incompletely reacted components. It is possible to increase the heat exchange in different ways. Conduction can be improved by producing a more compact mixture, using metal fuels or using metal casing/core wires. Convection can be improved by producing a non-compact granulated mixture. Radiation can be improved by using dark or black components [27].

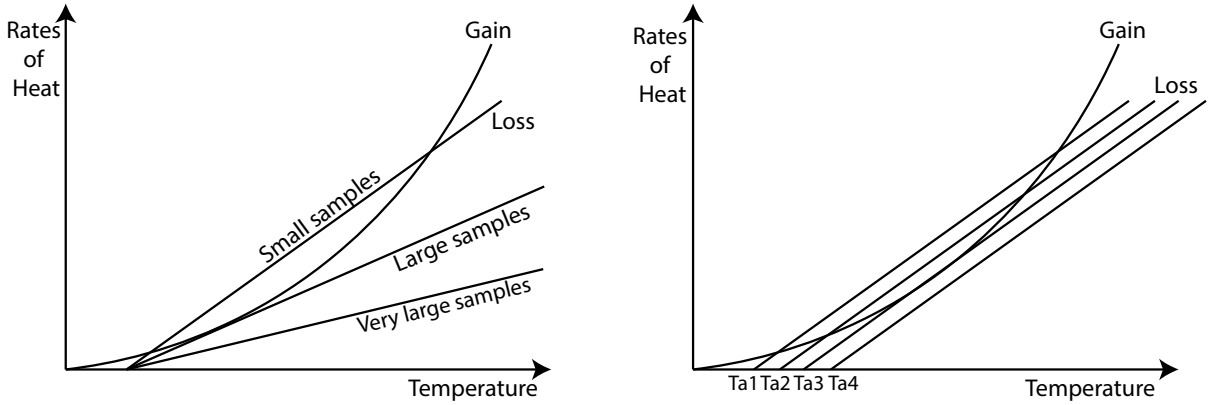

Figure 3.7: Effects of sample size on the slope of the heat loss line (left); effects of ambient temperature on the heat loss line (right) (this figure is adapted from Ref. [27]).

Chapter 4

Setup of the problem

4.1 How Do Chemical Equilibrium Programs Work

Performance analysis of the mixtures considered in this section is carried out with chemical equilibrium programs, and, in particular, by NASA CEA and TERRA. Basically, these two programs allow to perform the same calculations, yet differences arise from the thermodynamic datasets of the softwares as well as in the details of the numerical scheme followed to obtain the results.
The NASA CEA is a computer program developed and revised by NASA Lewis Research Centre more than 40 years ago. Earlier versions aimed at the developing of methods for calculating complex chemical equilibrium compositions and thermodynamic properties. Thanks to the continuous improvement of the code, today CEA is even able to calculate performances for a rocket motor with finite-area combustor [25].
Computer program TERRA represents the new version of the software ASTRA-4, which was developed in Bauman Moscow State Technical University. This program performs chemical equilibrium applying various conditions of balance: achievements of a minimum of Gibbs energy and an entropy maximum. The updated version TERRA works in Windows systems and implements extended possibilities for presentation of calculations [26].
Chemical equilibrium programs as NASA CEA and its Russian counterpart provide reliable data for the evaluation of the ideal performance of systems. The calculated flame temperature is evaluated under the assumption of an adiabatic condition (i.e., all the heat released/absorbed by the reaction provides product mixture heating/cooling, neglecting possible losses). Specific impulse performance for rocket problems are treated under the hypotheses of unit efficiency for the combustion and the expansion process, and also the nozzle shape is not confirmed for the evaluation of 2D-effects [7]. However, experimental activity is required for a identification of the possible influences of actual operating conditions on the system performance (e.g., reactants mixing, residence times).
In this thesis are reported all results obtained simulating the combustion in a rocket motor, so it is required to underline the assumptions and simplifications adopted by the codes. First of all, the simplified system considers a combustion chamber and a convergent-divergent nozzle. Performances are evaluated for a one-dimensional flow, which means that all velocities, pressures and temperatures profiles are considered flat at any normal cross section of the nozzle. It is not possible to estimate the losses for a two-phase flow. More accurate results can be obtained with a 2D- or 3D-analysis, but these would require the knowledge of temperature, pressure, densities and velocities profiles along the nozzle cross section. Yet, the base assumptions of thermochemical equilibrium calculations are suitable for the early stages of a propellant formulation development, since the possibility to achieve a relative grading of different compositions is of significant importance.
To get the results, chemical equilibrium programs have to know a priori some parameters, given as an input by the user. In order to setup the problem, one has to know the composition or propellant mixture, the chamber pressure and at least one parameter between the nozzle area ratio or the exit pressure.
The analytical description of the problem can be divided into two separate parts: combustion process and nozzle gas expansion process. Each part has its own assumptions and simplifications. For the combustion process:

- Reactions occur at constant pressure;
- Gaseous products follow Dalton's law;

- Chemical reactions occur very rapidly;
- Chamber volume is considered large enough and the residence time long enough for attaining chemical equilibrium in the combustion chamber.

For the nozzle gas expansion:

- The gas entropy is assumed constant during the reversible expansion.

NASA CEA allows to select between "frozen" and "shifting equilibrium" conditions during the expansion in the nozzle. The former doesn't consider further chemical reactions in the nozzle, so the gas composition at the exit is the same as that at the entrance. This makes the computation easier for the code and it is suitable when the fluid dynamic characteristic time is much lower than the chemical characteristic time (especially in the divergent part of the nozzle, where the gas reaches supersonic velocities). In reality, some chemical reactions occur during the expansion, so the composition of reaction products may noticeably change along the nozzle, and the "shifting" condition takes into consideration this aspect. Extra energy is released in the nozzle due to the recombination of free-radicals and atoms species. Shifting equilibrium makes more enthalpy available for conversion to kinetic energy, obtaining higher performances (higher specific impulse or characteristic velocity) and higher exit temperature. The difference between frozen and shifting equilibrium conditions can be substantial.
As for the assignment of assumptions, also the analysis of the problem considers separately the two systems. The objective of the analysis of the combustion chamber conditions is to determine the theoretical flame temperature, the theoretical composition of reaction products and the physical properties of combustion gases (specific heat, molecular weight, density). In order to get theoretical results, chemical equilibrium programs apply equations for conservation of energy and mass. Conservation of energy is attained considering the heat created by the combustion equal to the heat required to adiabatically raise the temperature of gaseous products to their final combustion temperature. This means that the heat of reaction of combustion must equal the enthalpy change of the product gases.

$$\Delta_r H = \sum_{j=1}^{m} n_j \int_{T_{ref}}^{T1} c_{pj} dT \tag{4.1}$$

Conservation of mass states that the mass of any atomic species present in the reactants must equal that of the same species in the products.
The analysis of the supersonic nozzle focuses on the adiabatic, reversible expansion process. Along the nozzle the thermal energy is converted into kinetic energy, so a substantial drop of temperature and pressure can be appreciated. CEA studies the nozzle expansion in the simplest way, applying these assumptions:

- Frozen equilibrium composition;
- One-dimensional flow;
- Isentropic flow;
- Effects of friction, divergence angle, heat losses, shock waves and non equilibrium are neglected;
- Condensed species are assumed to have zero volume and to be in kinetic and thermal equilibrium with the gas flow.

Some of these effects can be considered during the postprocessing phase in order to get more realistic results. In the next chapter will be treated only numerical results obtained with the aforementioned programs [7].

4.2 How Do Approximations Affect Rocket Performances

As mentioned before, chemical equilibrium programs apply some approximations in order to study the rocket problem analytically. These assumptions tend to overstimate the real performances of the rocket, so corrections in postprocessing could be required in order to get more realistic results.
Before performing calculations with CEA code, the user can choose to apply frozen or shifting equilibrium

conditions. Other approximations are intrinsic in the code. Frozen condition makes the problem simpler since no chemical reactions or phase changes occur during the expansion. Thus, products composition at the exit of the nozzle is the same to that of the combustion chamber. This condition tends to understimate the system's performance typically by 1 to 4 %.
When chemical reactions and phase changes take place during the expansion along the nozzle, it is suggested to apply shifting equilibrium condition. This makes the analysis more complex and tends to overstimate real performance values by 1 to 4 % [7].
Chemical equilibrium program does not consider the effects of condensed species in the combustion products. When diameter of condensed particles produced by combustion is greater than 0.1 μm, thermal lag and velocity lag affect the performances. For example, solid propellants with aluminum oxide in the exhaust gases lead to losses from 1 to 3 %.
Another source of error comes from the non consideration of boundary layer effects, which means that the code is neglecting viscous drag that in reality converts part of the kinetic energy of the flow into thermal energy, causing performance losses.When the flow is turbulent, this approximation affects the results with a higher error. Fig. 4.1 shows the real profiles of velocity and temperature near the wall.

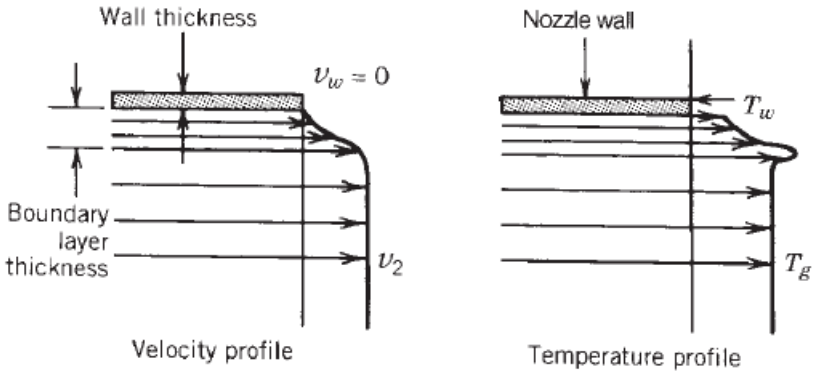

Figure 4.1: Velocity and temperature profiles near the nozzle wall [7].

Furthermore, in reality the nozzle flow is not isentropic because the expansion process is only partly reversible. To avoid this error, losses due to friction, shock waves and turbulence should be considered. Chemical equilibrium programs do not take into consideration these aspects which in reality lead to a higher average exhaust temperature and a decrease in specific impulse [7].

If the purpose of the research is to make a relative grading between two or more mixtures, these kind of results are quite good in order to have an idea of which mixture exhibits the best performances, otherwise one has to perform some corrections during the post-processing phase in order to have more realistic results.
In order to correct theoretical results, one can choose two ways:

- Use an empirical correction factor based on experimental data;
- Develop more accurate algorithms.

The last solution requires a lot of time and a higher computational cost.
Solid rocket propulsion involves a lot of physical and chemical processes. It is difficult to take into consideration all these aspects, even during the post-processing phase. The only way is to list all these processes and find which ones have a major impact on the performances of the rocket, the other ones can be neglected.
In real conditions, principal losses occurring during the expansion in the nozzle are:

- Divergence of the flow: losses due to the fact that the flow of combustion products doesn't exit from the nozzle entirely parallel to the rocket's flight direction. This loss varies as a function of the cosine of the divergence angle;
- Low nozzle contraction ratio: causes pressure losses in combustion chamber, leading to a slight reduction in thrust and exhaust velocity as reported in Tab. 4.1;

- Boundary layers: the reduction of velocity near the wall of the nozzle leads to a reduction of the average exhaust velocity by 0.5 to 1.5%;
- Condensed species: solid particles and/or liquid droplets in the exhaust gases may cause losses up to 5%, depending on particle size and shape;
- Unsteady combustion and/or flow oscillations: typically lead to small losses;
- Chemical reactions within nozzle flows: change composition, properties and temperature of the gas composition. Typically lead to 0.5% of losses;
- Transient operations: during start, stop or pulsing operations, overall performance is lower;
- Erosion of the throat: it increases the throat diameter. This typically reduces chamber pressure and thrust by 1 to 6%; even the specific impulse, usually less than 0.7%;
- Non uniform gas composition: incomplete mixing or incomplete combustion may reduce performances;
- Real gas properties: slightly reduce performances, from 0.2 to 0.7%;
- Flying at non optimal altitudes: reduces thrust and specific impulse for nozzles of fixed area ratios. This condition can lead up to 10% of losses on thrust, and may reduces flight performances between 1 and 5%, figure.

Chamber-to-Throat Area Ratio	Throat Pressure (%)	Thrust Reduction (%)	Specific Impulse Reduction (%)
∞	100	0	0
3.5	99	1.5	0.31
2.0	96	5.0	0.55
1.0	81	19.5	1.34

Table 4.1: Estimated Losses for Small-Diameter Chambers

In a preliminary phase of analysis it is difficult to account all these conditions. Some of them require experimental research in order to be assessed. For the other ones, the huge experience in rocket propulsion systems development allows to consider an average of the impacts [7].

4.3 Input Parameters

In order to get the results from chemical equilibrium programs, some input parameters are required. First of all, CEA allows to select between different kind of problems, and each of them gives information about different thermochemical properties of considered reaction. The problem selected in order to get the results listed in this document is the rocket problem, which allows to calculate performances of a particular mixture inside an ideal system made by a combustion chamber and a nozzle. Selecting the rocket problem, some parameters are requested to the user, such as pressure in combustion chamber, expansion ratio of the nozzle or ratio between the internal pressure and the pressure at the exit of the nozzle. User can also choose to consider frozen or shifting conditions during the expansion in the nozzle. Once the conditions in which the reaction has to occur are set, user has to select the reactants. Elements involved in the reaction can be chosen from the library available in CEA or can be manually inserted by knowing their chemical formula and standard enthalpy of formation. The amount of each reactant can be expressed in terms of moles or in terms of relative weight. Even the temperature at which each element is considered to be stored before the reaction has to be set. Further settings about products composition and structure of the output file can be modified, but this is not mandatory. Once the problem is set, user can run the simulation and get the results.

A deep research through scientific papers about microthrusters has been conducted in order to find the most suitable parameters required by chemical equilibrium programs. Since the interest about this topic is spreading very fast, a lot of researches and results are available, so it is difficult to find overall values

for the required parameters, such as pressure in combustion chamber and expansion ratio. However, it is worth reminding that the aim of this document is not to obtain realistic results, but to perform a relative grading between the most interesting mixtures that are under the magnifying glass of the research. Thus, it is not so important to set real conditions before running the simulation, but it is required to set the same initial conditions for each simulation in order to see how different mixtures react when subjected to the same environment.
Results for this research are obtained from CEA by setting a pressure of 10 *bar* in combustion chamber, an expansion ratio equal to 15, and considering shifting conditions in the nozzle. These parameters are extrapolated from the results of real experiments reported in scientific papers, as shown in Fig.4.2 and Fig.4.3, in which geometric parameters of the microthruster are reported. It is fair to remember that not all microthrusters are developed with the same geometry, so these values can vary.

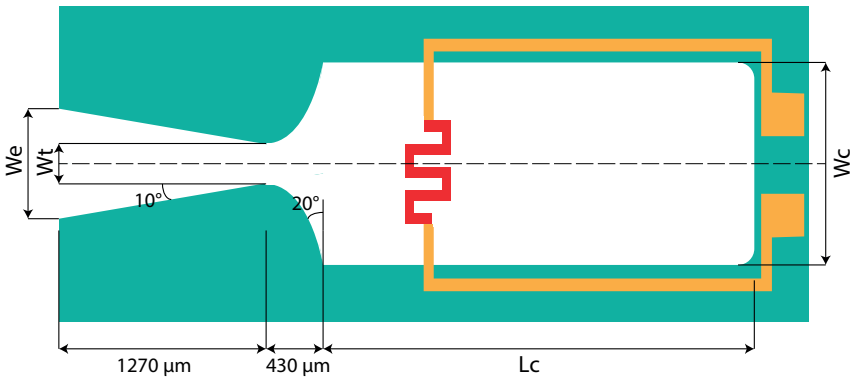

Figure 4.2: Schematic top view of a single microthruster with the geometric dimensions (this figure is adapted from Ref. [6]).

Since not all the elements involved in the reactions analysed in this document are available in CEA, some of them need to be studied with TERRA. Basically TERRA is similar to CEA and they perform the same analysis, but they differ in some aspects, including problem settings. For example, TERRA doesn't allow to set an expansion ratio for the rocket problem. Furthermore, some mixtures cannot be studied in TERRA setting a pressure in combustion chamber lower than 20 *bar*. For this reason, in order to compare CEA and TERRA results, further calculations are performed with CEA by setting the same parameters of TERRA. Thus, in this document, the best mixtures obtained with CEA are directly compared with the ones of TERRA by setting a pressure of 20 *bar* and a ratio between internal pressure and external pressure equal to 66.667, which means having a pressure equal to 0.03 MPa at the nozzle exit. Results obtained with programs are listed in following chapters.

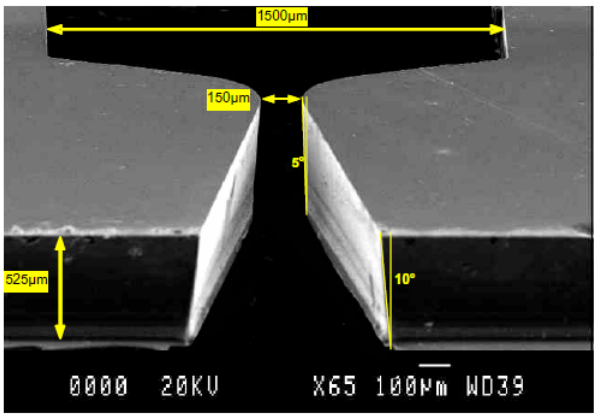

Figure 4.3: SEM image of a micro-nozzle [6].

Chapter 5

Analysis and Results

This thesis focuses on the analysis of the performances of different mixtures of thermite of great interest for space micropropulsion systems and for other aerospace purposes. As mentioned before, properties of thermite can be exploited for different applications: welding, weapons, gas generations, solid rocket propellants, biocidal systems. The main characteristic of these mixtures is the high energy density, which means that a small amount of compound can release large quantities of enthalpy. This property feats very well with the need to generate gaseous products with very high temperatures in solid rocket motors. The only drawback of these mixtures is the small mass fractions of gaseous combustion products, which is an important aspect for the rocket performances. Thus, the aim of this paper is to collect the most interesting thermite systems analysed in the last decades, find the best ones in terms of performances and study alternative additives in order to improve their performances.

5.1 Analysed Mixtures

Thermite systems are not typically considered for gas generation since the amount of gas produced by the reaction is not comparable to other solid propellants. However, special thermite compositions can generate a huge amount of gas. The most widely investigated are Al/Fe_2O_3, Al/MoO_3, Al/CuO, Al/Bi_2O_3 and Al/I_2O_5. Recent studies demonstrate that energetic gas generators based on bismuth and iodine show interesting reaction characteristics such as high gas discharge and fast energy release [9]. Moreover, these properties are followed by reduced ignition delay and reaction times, and high heat transfer rate. Improvement of some performances can be obtained with special additives: addition of carbon, for example, increases the enthalpy release and the produced gas mass fractions of all the formulations, while decreases the maximum pressure peak obtained during the reaction; otherwise, addition of boron increases the pressure peak [9].
Another interesting application is the micropropulsion. Nanostructured energetic materials can be used as propellants for microthrusters in order to produce the required thrust to correct the attitude of microsatellites. Microsatellites require thrusts of the order of mN, and chemical microthrusters provide thrust in a range from 0.1 mN to 100 N, with a specific impulse usually lower than 200 s. The performances of chemical thrusters are mainly determined by the choice of the solid propellant. Due to their high energy release, thermite systems are very interesting for this purpose, even though they do not produce a large amount of gas. In order to compensate this problem, thermite-based propellants are meant to be a mix between a heat source (thermite) and a gas-generating agent, such as RDX, HMX, nitrocellulose (NC), nitroglycerin (NG) and ammonium perchlorate [5]. The heat releases of possible thermite-based solid propellants are listed in Tab 5.1. According to Tab 5.1 and experimental results, the system Al/CuO:HMX:NC = 45:50:5 releases more heat and produces a higher amount of gas than other composites. Al/CuO/NC-based composites are suitable propellants for microthrusters, in which NC acts as an energetic binder and a gas generator. Experimental results about performances of this system are shown in Tab 5.2. Experimental results show that energy and specific impulse are lower than theoretical values because of the activity of aluminum, thermal losses at the microscale and combustion efficiency.

Composition at mass ratio	Enthalpy Release per Unit Mass, J/g
Al/CuO	918.8
Al/CuO:HMX:NC = 85:10:5	745.34
Al/CuO:HMX:NC = 45:50:5	1006.30
Al/Bi_2O_3	348.86
Al/Bi_2O_3:HMX:NC = 85:10:5	400.74
Al/Bi_2O_3:HMX:NC = 45:50:5	696.38

Table 5.1: Heat releases of thermite-based propellants [5].

Propellant	Thrust, N	Specific Impulse, s
Al/CuO (MM)	0.479	10.2±3.3
Al/CuO/NC (2.5 wt%, MM)	0.574	17.7±2.5
Al/CuO/NC (5.0 wt%, MM)	0.500	14.6±4.4
Al/CuO/NC (2.5 wt%, ES)	0.495	17.1±2.7
Al/CuO/NC (5.0 wt%, ES)	0.645	24.3±3.5
Al/CuO/NC (10.0 wt%, ES)	0.605	27.2±4.4

Table 5.2: Experimental results for the mixture Al/CuO. (MM, Mechanical Mixing; ES, Electrospray) [5].

Further research shows that hydroxide-based thermites are interesting due to their ability to produce a large amount of gas. For example, $Al/Bi(OH)_3$ generates more than twice the amount of gaseous products produced by the corresponding oxide system Al/Bi_2O_3 [5]. Considering the following reactions based on nanothermite systems:

$$Bi_2O_3 + 2Al = Al_2O_3 + 2Bi - 15.2kJ/m^3 \tag{5.1}$$

$$2Bi(OH)_3 + 2Al = Al_2O_3 + 2Bi + 3H_2O - 8.83kJ/m^3 \tag{5.2}$$

Reaction 5.1 has larger heat release, while reaction 5.2 produces a higher amount of gas with a lower atomic weight, as reported in Tab 5.3.

Nanothermite system	$T_{ad}(K)$	Gaseous Products	$M_W(g/mol)$	$\sqrt{\frac{T_{ad}}{M_W}}$
I_2O_5-Al	3830	I	127	5.5
Bi_2O_3-Al	3250	Bi	209	3.96
$Bi(OH)_3$-Al	2970	2Bi + $3H_2O$	93.2	5.65

Table 5.3: Theoretical impulse estimation for nanothermite reaction [5].

Theoretical notions about chemical rockets say that the specific impulse is directly proportional to the square root of the ratio between the temperature in the combustion chamber and the molecular weight of gas products. Therefore with reaction 5.2 one can generate 43% higher specific impulse with respect to the first reaction. This result confirms that hydroxide-based thermite systems releases a larger volume of gas.
The aforementioned mixtures will be analysed in the next sections. Theoretical results will be provided in order to get a general overview on these interesting systems, trying to figure out which path the research has to follow in order to obtain the best system for a microthruster.

5.2 Superthermite

Thermite systems are supposed to be a mix between a metal fuel and a metal oxidizer. Dimensions of the particles constituting the system are of huge relevance when trying to obtain a high energy release during the reaction. In the last decades, many researches focused on the effects of the reduction of the

particles size for a solid rocket propellant. Results showed that the reduction of dimensions from micron to nano-range increases the reaction rate due to the increase of the particle specific surface area [5]. Moreover, the burning rate of tested propellants increased up to 50% in some cases, but at the same time also the pressure exponent increased. It was also noticed that the total energy content of the propellant decreased due to the higher mass content of aluminum oxide (Al_2O_3). For this reason numerous efforts have been done towards developing a method of producing nanometal particles without a passivating layer, but the technical difficulties were great so the problem remained unsolved. Another important drawback is the cost of production of nanoparticles, which in some cases, especially for the aerospace field, is too high.
Despite the results about nanoparticles present some drawbacks, many researches carried out in the last decades show that nanotechnology can be exploited in order to enhance the performances of thermite systems. When at least one of the components of a thermite system has dimensions included in the nanometric range, the mixture is called superthermite. The increased intimacy between the fuel and the oxidizer reduces the diffusion limitations, which affect a lot the traditional thermite systems. This leads to a huge increase of the rate of the energy release during the reaction. Thus, superthermite is considered a suitable system for micropropulsion, since a small amount of propellant can release a lot of energy thanks to its high volumetric energy density, which can exceed the existing traditional monomolecular explosives by a factor of two, and the energy density can reach up to 27.5 kJ/m^3 [5]. Figure 5.1 shows a comparison between the peaks of pressure generated by different nanoenergetic formulations.

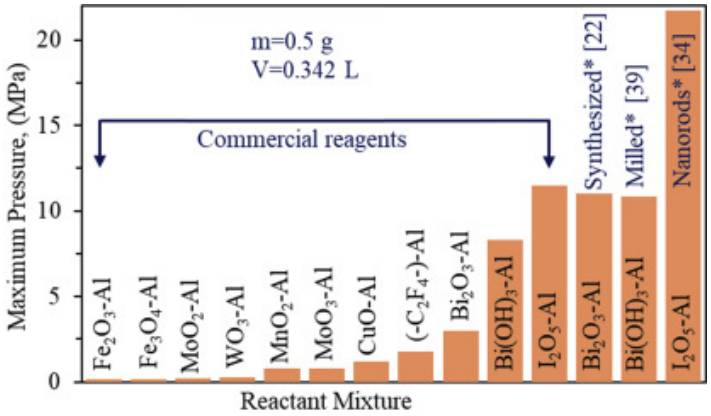

Figure 5.1: Peak pressure values generated during the explosion of different nanoenergetic thermites [5].

5.3 Additives

Thermite systems release high energy during the reaction but usually are not able to generate high amount of gas. For this reason, thermite is not directly used as propellant for solid rocket motors. Thermite-based propellants consist of a thermite as the heat source and a gas-generating agent as the work substance, such as RDX, HMX, nitrocellulose, nitroglycerin, and ammonium perchlorate.
In the following subsections will be reported a brief description of these additives.

5.3.1 RDX and HMX

RDX, also known as cyclonite or hexogen, is a very explosive powder. It was investigated for the first time in the 1930s by the Royal Arsenal, and was widely used as an explosive during World War II, often mixed with TNT (Trinitrotoluene). The RDX is an organic compound with chemical formula $(O_2NNCH_2)_3$. The main hazards that characterise this compound are its high toxicity and its explosiveness.
HMX, also known as octogen and cyclotetramethylene-tetranitramine, is another powerful, yet relatively insensitive explosive. Produced for the first time in 1930, it is chemically similar to RDX. Its chemical formula is $C_4H_8N_8O_8$ and it presents a low sensitivity to shocks. Mainly used in military applications, such as detonator in nuclear weapons or polymer-bonded explosive, it can also be used as in solid rocket propellants [30]. Physical and chemical properties of RDX and HMX are collected in Tab. 5.4.

Compound	Chemical Formula	Density, g/cm^3	Molecular Weight, g/mol	Std Enthalpy of Formation, kJ/mol
RDX	$(O_2NNCH_2)_3$	1.82	222.12	92.6
HMX	$C_4H_8N_8O_8$	1.91	296.16	104.8

Table 5.4: Physical and chemical properties of RDX and HMX [30]

Since the library of NASA CEA code has not information about these components, data presented in Tab. 5.4 are useful in order to insert manually RDX and HMX inside the mixtures.
For several years research put much efforts in desensitizing explosives against accidental initiation. Nanostructuring of explosives was a promising idea of research in order to reach this goal. Many methods were used to produce nanocrystalline grades of RDX, for example spray flash-evaporation process, reprecipitation method or the rapid expansion of supercritical solutions process. Impact and shock sensitivity tests revealed that the nanocrystalline grades of RDX were less sensitive with respect to the coarser ones. But the most interesting result is that the sensitivity is not directly proportional to the size of the powders [5]. There is an unexpected minimum, which occurs at a mean crystal size in the vicinity of 500 nm. For coarser grades of RDX, as one can expect shock sensitivity increases with the crystal syze. Even for size lower than 500 nm there is a markedly higher sensitivity to shock and impact stimuli [5].

5.3.2 Nitrocellulose

Nitrocellulose, also called cellulose nitrate, is a mixture of nitric esters of cellulose. It is a highly flammable compound, originally used as a propellant or low-order explosive. It is obtained from the nitration of cellulose. Cellulose is a natural polymer obtained from wood pulp or the short fibers that adhere to cotton seeds.
Different types of nitrocellulose can be produced depending on the content of nitrogen. Nitrocellulose with 12.6-13.4% nitrogen content is used in energetic formulations such as propellants and dynamite. Pyroxilin, a high flammable mixture of nitrocellulose, is a mixture that was used as a rocket propellant in the 1930s [30]. Pyroxilin contains 11.5-12.3% of nitrogen, its chemical formula is $C_{18}H_{21}N_{11}O_{38}$, and its molecular weight is 999.4 g/mol.
As for RDX and HMX, also nitrocellulose information are not listed in the library of CEA. It is difficult to find in literature a precise value for the standard enthalpy of formation for this compound. In ref. [31] are reported many experiments about cellulose and nitrocellulose, including one in which the standard enthalpy of formation is evaluated for a nitrocellulose obtained from cotton linters with different percentages of nitrogen content. For the one with 12.60% of nitrogen (same content as for pyroxylin), a ΔH_f^o equal to -2579,97 kJ/mol is obtained.

5.3.3 Nitroglycerin

Nitroglycerin, also known as trinitroglycerin or glyceryl trinitrate, is an organic nitrate compound with chemical formula $C_3H_5N_3O_9$. Its molecular weight is 227.09 g/mol [32]. It has been mostly used as ingredient for explosives, especially dynamite. Double base propellants are made by mixing nitrocellulose, nitroglycerin and a minor percentage of additives [7]. NG is used also in medicine thanks to its vasodilator activity. Information about NG are not collected in the chemical library of CEA, so they must be inserted manually. Its standard enthalpy of formation is equal to -370 kJ/mol [32].

5.3.4 Ammonium Perchlorate

Ammonium perchlorate is an inorganic compound with chemical formula NH_4ClO_4. It appears as a white, crystalline solid. Its molecular weight is 117.49 g/mol [32]. It is the most widely used crystalline oxidizer in solid propellants thanks to its compatibility with other propellants, good performance, low sensitivities and large availability. Its oxidizing potential is high so it is a suitable oxidizer for high-specific-impulse propellants [7].
The AP decomposes before melting, producing hydrogen chloride, nitrogen, oxygen and water. When it reacts with fuels, ammonium perchlorate generates gaseous HCl and other toxic and corrosive chlorine compounds. Its handling requires measures of safety to safeguard operating personnel. Its properties

(chemical formula and standard enthalpy of formation) are already available in chemical library of CEA [7]
.

5.3.5 Compatibility Tests

Energetic materials such as those analysed in this document must be handled with care and respect on the safety rules. Neglecting this aspects could lead to serious consequences. For this reason, before carrying out experiments aimed at evaluating the performances of these mixtures, stability, compatibility and safety tests must be performed. This allows to know if a particular mixture made with energetic materials can be safely produced, stored, transported, handled and tested.
There are several methods to evaluate compatibility, the most commonly used are the VST (Vacuum Stability Test) and the DSC (differential thermal analysis) methods [5]. The VST method evaluates the gas released by the system, at a specified temperature and heating time. This method uses the following equation to evaluate the compatibility:

$$R = C - (A + B) \tag{5.3}$$

where R is the net amount of gases released by the system, C is the amount of gases released by the system, and A, B are the amount of gases released by the two materials expressed in mL. The larger is R, the easier is the reaction between the two materials, so when R exceeds a certain value the two materials are considered incompatible. The criteria are: R $< 0.60\ mL$, compatible; $0.60 \leq$ R $\leq 1.0\ mL$, medium compatible; R $> 1.0\ mL$, incompatible [5].
VST has been applied to many mixed systems, as showed in Tab 5.5.

Mixed systems (0.5/0.5 g)	R (mL)	Rating
Al/PbO-NC	-0.04	Compatible
Al/PbO-NC + NG	0.39	Compatible
Al/PbO-RDX	0.27	Compatible
Al/CuO-NC	0.22	Compatible
Al/CuO-NC + NG	3.87	Incompatible
Al/CuO-RDX	2.01	Incompatible
Al/Bi_2O_3-NC	-0.07	Compatible
Al/Bi_2O_3-NC + NG	-0.03	Compatible
Al/Bi_2O_3-RDX	0.15	Compatible

Table 5.5: Vacuum stability test results on different mixed systems [5].

Sometimes VST method is not suitable to calculate compatibility for certain materials, especially polymers and energetic compounds, which do not release gases.
Since almost all interactions have thermal effects, a thermal analysis is more suitable in assessing compatibility. With DSC methods, mixtures like Al/CuO-NC/NG and Al/CuO-RDX resulting incompatible with VST analysis, are found to be compatible or slightly sensitive. So they are also considered in this research as suitable systems for a micropropulsion device [5].

5.4 Thermite Systems

The results obtained with chemical equilibrium programs (CEA and TERRA) for different thermite systems are listed in this chapter. Additives are not considered, their effects will be analysed in the following section.
As mentioned in previous chapters, thermite mixtures are not suitable if used as propellants for rocket propulsion due to the small mass amount of gaseous species released. Thus, research nowadays is focused on the combination of the high energy release of thermite systems with the high gas generation of other consolidated systems (DB propellants, other additives).
The results are resumed in tables in which physical and performance parameters, and the composition of gas products are reported. These data allows to make a relative grading between the mixtures, aiming to understand which system shows the best performances in terms of rocket propulsion. The comparison is based on values of specific impulses and the percentage of condensed species in gas products. Good

mixtures tend to have higher specific impulse and higher capability of generating gas products.
Since the analysed materials generate high energetic systems which in some cases tend to be highly sensitive to external stimuli, the mass fractions considered in this document are limited to be close to values find in reference experimental works. Part of the considered mixtures has been tested as reported in different scientific papers; the rest has been at least studied with compatibility tests, reaching good results.
Each mixture is briefly described in dedicated sections, before discussing a full comparison at the end of the chapter.

5.4.1 Al/PbO

Lead oxide is an inorganic compound with chemical formula PbO. It is toxic if swallowed or inhaled, it causes damages to organs through prolonged or repeated exposure and it is dangerous for the environment. Its molecular weight is 223 g/mol [32].
Reference [5] reports that metal oxide can be used as combustion catalyst in order to enhance combustion properties of solid propellants. As a kind of combustion catalyst, nano-PbO could increase the burning rate of propellant in the high pressure range and at the same time could decrease the pressure exponent. The further addition of a metal fuel, such as aluminum, to the propellant, generating a thermite mixture with PbO, can even improve the performances [5]. Experimental results show that double base (DB) propellants containing a superthermite mixture like Al/PbO exhibit excellent combustion performances. Thus, a mixture of DB propellant and Al/PbO could be interesting for micropropulsion systems.
The stoichiometric reaction between aluminum and lead oxide is written as:

$$2\mathrm{Al} + 3\mathrm{PbO} \rightarrow \mathrm{Al_2O_3} + 3\mathrm{Pb} \tag{5.4}$$

This means that 3 moles of PbO completely react with 2 moles of Al, so the stoichiometric ratio for this reaction is:

$$\left.\frac{Ox}{Fu}\right|_{mol,stech} = \frac{3}{2} = 1.5 \tag{5.5}$$

The mass ratio considered in this document for the mixture Al/PbO is 12.23/87.77, the same reported in Ref. [5]. In order to obtain the molar ratio, one has to consider the molecular weight of the components. In this case molecular weight of aluminum is 26.98 g/mol, while, as mentioned before, molecular weight of PbO is 223 g/mol. Thus,

$$\frac{Ox}{Fu} = \frac{\frac{87.77g}{223g/mol}}{\frac{12.23g}{26.98g/mol}} = 0.868 \tag{5.6}$$

The equivalence ratio is:

$$\Phi = \frac{\frac{Ox}{Fu}}{\frac{Ox}{Fu}|_{mol,stech}} = \frac{0.868}{1.5} = 0.578 \tag{5.7}$$

Thus the mixture has a lower content of oxidant with respect to the stoichiometric conditions.

5.4.2 Al/CuO

Copper oxide is an inorganic compound with chemical formula CuO. It is a black solid, and it is available in nature as a mineral, known as tenorite. Its molecular weight is 79.55 g/mol [32].
Usually it is mixed with aluminum in order to produce an incendiary thermite, which is used to weld large quantities of copper without the need of an external energy source. Thanks to its high heat release per unit volume, small critical diameter of combustion, low cost and environment friendliness, the mixture Al/CuO is a suitable thermite system that can be used as a heat source for solid propellant. Mixing this system with some additives (such as HMX, nitrocellulose, ammonium perchlorate) allows to produce an interesting mixture for micropropulsion systems.
Addition of superthermite acts as a combustion catalyst to improve the combustion performances of DB

propellants and it was found that addition of n-Al/CuO is able to enhance combustion [5] [33].
The stoichiometric reaction between aluminum and copper oxide is written as:

$$2\mathrm{Al} + 3\mathrm{CuO} \rightarrow \mathrm{Al_2O_3} + 3\mathrm{Cu} \tag{5.8}$$

This means that 3 moles of CuO completely react with 2 moles of Al, so the stoichiometric ratio for this reaction is:

$$\left.\frac{Ox}{Fu}\right|_{mol,stech} = \frac{3}{2} = 1.5 \tag{5.9}$$

In this document two systems of Al/CuO are considered, as suggested in different scientific papers. The first system has a mass ratio of 25.03/74.97 as reported in Ref. [5], the second one is 28.8/71.2 as in ref [33].
Knowing the molecular weight it is possible to evaluate the molar ratio for these two systems. For the system with mass ratio 25.03/74.97:

$$\left.\frac{Ox}{Fu}\right|_{25.03/74.97} = \frac{\frac{74.97g}{79.55g/mol}}{\frac{25.03g}{26.98g/mol}} = 1.015 \tag{5.10}$$

The equivalence ratio is:

$$\Phi = \frac{\frac{Ox}{Fu}}{\frac{Ox}{Fu}|_{mol,stech}} = \frac{1.015}{1.5} = 0.677 \tag{5.11}$$

For the system with mass ratio 28.8/71.2:

$$\left.\frac{Ox}{Fu}\right|_{28.8/71.2} = \frac{\frac{71.2g}{79.55g/mol}}{\frac{28.8g}{26.98g/mol}} = 0.838 \tag{5.12}$$

The equivalence ratio is:

$$\Phi = \frac{\frac{Ox}{Fu}}{\frac{Ox}{Fu}|_{mol,stech}} = \frac{0.838}{1.5} = 0.558 \tag{5.13}$$

Thus, both mixtures have an excess of fuel and they are far from the stoichiometric conditions.

5.4.3 Al/I_2O_5

Iodine pentoxide is a chemical compound with chemical formula I_2O_5. It is produced by dehydration of iodic acid at 240°C:

$$2\mathrm{HIO_3} \rightarrow \mathrm{I_2O_5} + \mathrm{H_2O} \tag{5.14}$$

It appears as white crystals, with a density equal to 4.98 g/cm^3, molecular weight 333.81 g/mol and it is highly soluble in water.
Iodine pentoxide is a strong oxidizing agent which can react with several substances. For example, it oxidizes carbon monoxide to carbon dioxide [34].
In the last few years, iodine-based composites have attracted research interest not only for the aerospace field but also for other purposes. For example, these kind of mixtures are studied as systems able to inactivate harmful aerosolized spores and bacteria. Energetic formulations containing halogens (e.g. iodine) can be used as munitions to defeat stockpiles of biological weapons [35].
Researches on systems based on the mixture Al/I_2O_5 found interesting results for aerospace purposes. The reaction of this mixture releases a large amount of gas and generates a fast moving thermal wave.
The stoichiometric reaction between aluminum and iodine pentoxide is written as:

$$10\mathrm{Al} + 3\mathrm{I_2O_5} \rightarrow 5\mathrm{Al_2O_3} + 6\mathrm{I} \tag{5.15}$$

This means that 3 moles of I_2O_5 completely react with 10 moles of Al. The enthalpy release of this reaction is equal to 6.22 kJ/g, and it is higher than that of common stoichiometric thermite reactions, such as Al/Fe_2O_3 (3.97 kJ/g), Al/MoO_3 (4.72 kJ/g), Al/WO_3 (2.92 kJ/g), Al/CuO (4.09 kJ/g) and

Al/Bi_2O_3 (2.12 kJ/g).
The stoichiometric ratio for this reaction is:

$$\left.\frac{Ox}{Fu}\right|_{mol,stech} = \frac{3}{10} = 0.3 \tag{5.16}$$

In this document the mass ratio considered for the mixture is 22/78, which generates the highest amount of gaseous products compared to other ratios [36]. Knowing the molecular weight of the components it is possible to evaluate the molar ratio for the system:

$$\frac{Ox}{Fu} = \frac{\frac{78}{333.81g/mol}}{\frac{22g}{26.98g/mol}} = 0.286 \tag{5.17}$$

The equivalence ratio is:

$$\Phi = \frac{\frac{Ox}{Fu}}{\frac{Ox}{Fu}|_{mol,stech}} = \frac{0.286}{0.3} = 0.955 \tag{5.18}$$

Thus the system has a slight excess of fuel.

5.4.4 Al/Bi_2O_3

Bismuth oxide is a chemical compound with chemical formula Bi_2O_3. It can be found naturally as mineral bismite while commercially is made from bismuth subnitrate. It is a yellow monoclinic crystal, with density 8.90 g/cm^3, molecular weight 465.959 g/mol and it is not soluble in water [34].
Ref. [9] reports that the system Al/Bi_2O_3 is able to generate a higher pressure and a higher gas discharge with rispect to other thermite systems. It can also be used as a combustion catalyst in order to improve performances of DB propellants. Nanothermite system Al/Bi_2O_3 is able to increase effectively the burning rate of propellants. However its combustion shows a high-pressure exponent [5]. A possible explanation for its capability of generating a high amount of gas is that reaction product (bismuth) boils at temperature of 1833 K, which is lower than the maximum reaction temperature. This causes bismuth evaporation and increases the released gas pressure [15].
The stoichiometric reaction between aluminum and bismuth oxide is written as:

$$2Al + Bi_2O_3 \rightarrow Al_2O_3 + 2Bi \tag{5.19}$$

This means that 1 mole of Bi_2O_3 completely reacts with 2 moles of Al. The stoichiometric ratio is:

$$\left.\frac{Ox}{Fu}\right|_{mol,stech} = \frac{1}{2} = 0.5 \tag{5.20}$$

In this document the mass ratio considered for this system is 7.15/92.85, as reported in Ref. [5]. Knowing molecular weight of the components it is possible to evaluate the molar ratio for the system:

$$\frac{Ox}{Fu} = \frac{\frac{92.85}{465.959g/mol}}{\frac{7.15g}{26.98g/mol}} = 0.752 \tag{5.21}$$

The equivalence ratio is:

$$\Phi = \frac{\frac{Ox}{Fu}}{\frac{Ox}{Fu}|_{mol,stech}} = \frac{0.752}{0.5} = 1.503 \tag{5.22}$$

Thus the system has an excess of oxidizer.
Since CEA program does not allow to perform calculations for mixtures that involve bismuth, results for this system are obtained thanks to TERRA program. It should be noted that TERRA does not allow to set the same parameters as in CEA. For example, it is not possible to set an expansion ratio, and for this kind of mixture is not possible to assume a pressure lower than 20 *bar* in the combustion chamber. For this reason it is not possible to directly compare previous results with results obtained for bismuth-based mixtures. In order to get a comparison, further calculations are performed with CEA, setting the same parameters as in TERRA. Results will be listed in following chapters.

5.4.5 Al/Bi(OH)$_3$

Bismuth hydroxide is a chemical compound with chemical formula $Bi(OH)_3$. It is produced by precipitation, obtained by adding sodium hydroxide to a solution of bismuth nitrate. It is a yellowish-white amorphous powder, with density 4.96 g/cm^3, molecular weight 260.00 g/mol, and it is insoluble in water [34].
Hydroxide-based nanothermites are very interesting due to their capability of generating large volumes of gas. Experimental tests showed that the corresponding oxide system Al/Bi_2O_3 generates a larger heat release ($\Delta H = -15.2 kJ/cm^3$) with respect to the hydroxide-based system ($\Delta H = -8.83 kJ/cm^3$). On the other hand, the system $Al/Bi(OH)_3$ yields a larger mass fraction of gaseous combustion products [5]. This makes this mixture very interesting for propulsion systems.
The stoichiometric reaction between aluminum and bismuth hydroxide is written as:

$$2Al + 2Bi(OH)_3 \rightarrow Al_2O_3 + 2Bi + 3H_2O \tag{5.23}$$

This means that 2 moles of Bi_2O_3 completely react with 2 moles of Al. The stoichiometric ratio is:

$$\left.\frac{Ox}{Fu}\right|_{mol,stech} = \frac{2}{2} = 1 \tag{5.24}$$

In this document the mass ratio considered for this system is 20/80, as reported in Ref. [5]. Knowing molecular weight of the components it is possible to evaluate the molar ratio for the system:

$$\frac{Ox}{Fu} = \frac{\frac{80}{260.00 g/mol}}{\frac{20.00 g}{26.98 g/mol}} = 0.415 \tag{5.25}$$

The equivalence ratio is:

$$\Phi = \frac{\frac{Ox}{Fu}}{\frac{Ox}{Fu}|_{mol,stech}} = \frac{0.415}{1} = 0.415 \tag{5.26}$$

Thus the mixture has an excess of fuel.
Also for this system, results are obtained with TERRA. Thus, direct comparison with previous results are reported in following chapters.

5.4.6 Results for Thermite Systems

Results obtained with chemical equilibrium programs are listed in the following tables. For each simulated reaction several thermophysical properties of gas products are computed in combustion chamber, throat section and nozzle exit. The composition of gas products is also shown in tables.
Even if the structure of the results coming from TERRA is quite different with respect to CEA structure, it is still possible to compare the most important parameters for a rocket propellant. As already mentioned, it is worth noting that the input parameters for TERRA are different from the ones for CEA. In order to make a relative grading, further computations have been performed for the best mixtures obtained with CEA using the same input parameters as in TERRA.
Tab.5.6 shows the results for the mixture Al/PbO (Ox/Fu = 0.868, $\Phi = 0.578$) with mass ratio 12.23/87.77. Tab. 5.7 and Tab. 5.8 collect the results for Al/CuO thermite. The former has a mass ratio equal to 25.03/74.97, a Ox/Fu equal to 1.015 and Φ equal to 0.677, the latter has a mass ratio 28.8/71.2, with Ox/Fu equal to 0.838 and Φ equal to 0.558. Tab. 5.9 lists the results for the mixture Al/I_2O_5 (Ox/Fu = 0.286, $\Phi = 0.955$) with mass ratio 22/78. Tab. 5.10 collects the results for the same mixture of Tab. 5.9, but with different operating conditions, in order to be able to compare this mixture with the ones studied with TERRA. In Tab. 5.11 are presented the results for the mixture Al/Bi_2O_3 (Ox/Fu = 0.752, $\Phi = 1.503$) with mass ratio 7.15/92.85. In conclusion, Tab. 5.12 lists the results for mixture $Al/Bi(OH)_3$ (Ox/Fu = 0.415, $\Phi = 0.415$) with mass ratio 20/80.

	Location		
Parameters	Combustion Chamber	Throat Section	Nozzle Exit
Pressure ratio, p_{inf}/p	1.00	1.70	71.51
Pressure, p, MPa	1.00	0.58	0.01
Temperature, T, K	2527	2390	1704
Density, ρ, kg/m^3	24.50	13.66	0.29
Molecular weight, M_W, g/mol	143.54	142.84	139.92
Specific heat, C_p, $kJ/(kg \cdot K)$	0.380	0.380	0.331
Sonic vel., c, m/s	206.5	211.9	229.5
Mach number, M	0.00	1.00	2.90
Characteristic vel., c^*, m/s	NA	345.3	345.3
Thrust coeff., C_F	NA	0.61	1.92
Specific impulse, I_s, m/s	NA	413.9	737.4
Mass fractions of gas mixture			
Al	0.00135	0.00113	0.00016
Al_2	0.00003	0.00002	0.00000
Al_2O	0.01967	0.01609	0.00080
Pb	0.33367	0.38977	0.70036
Al(liquid)	0.04007	0.04214	0.05099
Al_2O_3(solid)	0.00000	0.00000	0.13326
Al_2O_3(liquid)	0.12409	0.12583	0.00000
Pb(liquid)	0.48111	0.42502	0.11443
and a small amount of other gases			

Table 5.6: Results obtained for the mixture Al/PbO, Ox/Fu = 0.868, $\Phi = 0.578$, mass ratio 12.23/87.77 (NASA CEA, chamber pressure 1.0 MPa, nozzle exhaust-to-throat area ratio 15, shifting equilibrium).

	Location		
Parameters	Combustion Chamber	Throat Section	Nozzle Exit
Pressure ratio, p_{inf}/p	1.00	1.64	76.44
Pressure, p, MPa	1.00	0.60	0.01
Temperature, T, K	3109	3003	2327
Density, ρ, kg/m^3	11.29	6.81	0.15
Molecular weight, M_W, g/mol	70.15	70.12	69.81
Specific heat, C_p, $kJ/(kg \cdot K)$	2.70	3.17	0.00
Sonic vel., c, m/s	294.6	297.2	213.4
Mach number, M	0.00	1.00	4.09
Characteristic vel., c^*, m/s	NA	493.7	493.7
Thrust coeff., C_F	NA	0.60	1.77
Specific impulse, I_s, m/s	NA	597.8	970.6
Mass fractions of gas mixture			
Al	0.01235	0.01271	0.01511
AlO	0.00020	0.00016	0.00001
Al_2	0.00032	0.00024	0.00004
Al_2O	0.13222	0.13172	0.12761
Al_2O_2	0.00035	0.00026	0.00001
Cu	0.06514	0.07444	0.12514
Cu_2	0.00513	0.00515	0.00261
Al_2O_3(solid)	0.00000	0.00000	0.01082
Al_2O_3(liquid)	0.25566	0.25600	0.24749
Cu(liquid)	0.52863	0.51932	0.47116

Table 5.7: Results obtained for the mixture Al/CuO, Ox/Fu = 1.015, $\Phi = 0.677$, mass ratio 25.03/74.97 (NASA CEA, chamber pressure 1.0 MPa, nozzle exhaust-to-throat area ratio 15, shifting equilibrium).

	Location		
Parameters	Combustion Chamber	Throat Section	Nozzle Exit
Pressure ratio, p_{inf}/p	1.00	1.64	68.10
Pressure, p, MPa	1.00	0.60	0.01
Temperature, T, K	2858	2749	2231
Density, ρ, kg/m^3	12.41	7.47	0.17
Molecular weight, M_W, g/mol	67.036	67.431	68.269
Specific heat, C_p, $kJ/(kg \cdot K)$	err	err	3.57
Sonic vel., c, m/s	0.00	283.7	301.3
Mach number, M	0.00	1.00	2.77
Characteristic vel., c^*, m/s	NA	471.5	471.5
Thrust coeff., C_F	NA	0.60	1.77
Specific impulse, I_s, m/s	NA	570.7	938.1
Mass fractions of gas mixture			
Al	0.01198	0.01265	0.01984
AlO	0.00004	0.00003	0.00000
Al_2	0.00052	0.00044	0.00010
Al_2O	0.17880	0.18827	0.20818
Al_2O_2	0.00010	0.00007	0.00001
Cu	0.02336	0.02437	0.06032
Cu_2	0.00132	0.00117	0.00099
Al(liquid)	0.02253	0.01708	0.00000
Al_2O_3(solid)	0.00000	0.00000	0.20308
Al_2O_3(liquid)	0.21724	0.21268	0.00000
Cu(liquid)	0.54411	0.54325	0.50748

Table 5.8: Results obtained for the mixture Al/CuO, Ox/Fu = 0.838, $\Phi = 0.558$, mass ratio 28.8/71.2 (NASA CEA, chamber pressure 1.0 MPa, nozzle exhaust-to-throat area ratio 15, shifting equilibrium).

	Location		
Parameters	Combustion Chamber	Throat Section	Nozzle Exit
Pressure ratio, p_{inf}/p	1.00	1.70	93.37
Pressure, p, MPa	1.00	0.58	0.01
Temperature, T, K	4335	4197	3388
Density, ρ, kg/m^3	3.13	1.92	0.04
Molecular weight, M_W, g/mol	88.55	88.87	124.56
Specific heat, C_p, $kJ/(kg \cdot K)$	18.88	19.40	22.25
Sonic vel., c, m/s	589.9	576.5	492.9
Mach number, M	0.00	1.00	3.16
Characteristic vel., c^*, m/s	NA	902.0	902.0
Thrust coeff., C_F	NA	0.63	1.73
Specific impulse, I_s, m/s	NA	1106.1	1705.6
Mass fractions of gas mixture			
Al	0.01309	0.01355	0.01692
AlI	0.03544	0.03110	0.01083
AlI_2	0.00048	0.00031	0.00001
AlO	0.04856	0.04688	0.03398
AlO_2	0.00400	0.00317	0.00050
Al_2	0.00002	0.00002	0.00000
Al_2O	0.03010	0.02972	0.02388
Al_2O_2	0.02071	0.01884	0.00798
Al_2O_3	0.00040	0.00031	0.00003
I	0.56247	0.56648	0.58409
I_2	0.00094	0.00066	0.00004
O	0.02374	0.02349	0.02115
O_2	0.01086	0.01010	0.00551
Al_2O_3(liquid)	0.24919	0.25537	0.29507

Table 5.9: Results obtained for the mixture Al/I_2O_5, Ox/Fu = 0.286, $\Phi = 0.955$, mass ratio 22/78 (NASA CEA, chamber pressure 1.0 MPa, nozzle exhaust-to-throat area ratio 15, shifting equilibrium).

	Location		
Parameters	Combustion Chamber	Throat Section	Nozzle Exit
Pressure ratio, p_{inf}/p	1.00	1.70	66.66
Pressure, p, MPa	2.00	1.17	0.03
Temperature, T, K	4516	4366	3556
Density, ρ, kg/m^3	6.18	3.80	0.12
Molecular weight, M_W, g/mol	90.00	90.26	92.47
Specific heat, C_p, $kJ/(kg \cdot K)$	16.12	16.65	19.37
Sonic vel., c, m/s	594.3	580.7	501.9
Mach number, M	0.00	1.00	3.03
Characteristic vel., c^*, m/s	NA	908.2	908.2
Thrust coeff., C_F	NA	0.64	1.67
Specific impulse, I_s, m/s	NA	580.7	1520.3
Mass fractions of gas mixture			
Al	0.01152	0.01197	0.01499
AlI	0.04147	0.03656	0.01432
AlI_2	0.00091	0.00058	0.00002
AlO	0.04641	0.04497	0.03425
AlO_2	0.00483	0.00385	0.00073
Al_2	0.00003	0.00002	0.00000
Al_2O	0.02798	0.02784	0.02394
Al_2O_2	0.02121	0.01945	0.00933
Al_2O_3	0.00052	0.00039	0.00005
I	0.55648	0.56129	0.58115
I_2	0.00158	0.00111	0.00009
O	0.02199	0.02179	0.01992
O_2	0.01080	0.01007	0.00586
Al_2O_3 (liquid)	0.25428	0.26011	0.29534

Table 5.10: Results obtained for the mixture Al/I_2O_5, Ox/Fu = 0.286, Φ = 0.955, mass ratio 22/78 (NASA CEA, chamber pressure 2.0 MPa, nozzle exit pressure 0.03 MPa).

	Location		
Parameters	Combustion Chamber	Throat Section	Nozzle Exit
Pressure, p, MPa	2.00	1.19	0.03
Temperature, T, K	2435	2349	1826
Molecular weight, M_W, g/mol	264.87	260.30	230.82
Specific heat, C_p, $kJ/(kg \cdot K)$	0.38	0.38	0.33
Mach number, M	0.00	1.00	1.01
Specific impulse, I_s, m/s	NA	455.67	753.70
Condensed species ratio, Z	0.31	0.30	0.25

Table 5.11: Results obtained for the mixture Al/Bi_2O_3, Ox/Fu = 0.752, $\Phi = 1.503$, mass ratio 7.15/92.85 (TERRA, chamber pressure 2.0 MPa, nozzle exit pressure 0.03 MPa).

	Location		
Parameters	Combustion Chamber	Throat Section	Nozzle Exit
Pressure, p, MPa	2.00	1.17	0.03
Temperature, T, K	2828	2695	2230
Molecular weight, M_W, g/mol	84.54	84.35	82.07
Specific heat, C_p, $kJ/(kg \cdot K))$	0.75	0.74	0.68
Mach number, M	0.00	1.00	2.86
Specific impulse, I_s, m/s	NA	871.52	1340.72
Condensed species ratio, Z	0.28	0.28	0.28

Table 5.12: Results obtained for the mixture $Al/Bi(OH)_3$, Ox/Fu = 0.415, $\Phi = 0.415$, mass ratio 20/80 (TERRA, chamber pressure 2.0 MPa, nozzle exit pressure 0.03 MPa).

5.4.7 Comparison Between Thermite Systems

Simulations for simple thermite systems give some interesting results. This kind of analysis allows to verify which reaction tends to produce the highest performances in ideal conditions. From tables listed in the previous chapter it is possible to extrapolate the most interesting parameters, like temperature in combustion chamber, molecular weight of gas products, specific impulse and percentage of condensed species. In order to make a rapid comparison between mixtures, these parameters have been collected in Fig. 5.2 and Fig.5.3.

Fig.5.3 shows a comparison based on two important parameters. A good propellant for rocket propulsion has to produce very high specific impulse with low amount of condensed species. The high interest on the specific impulse is due to the fact that it gives us a quick way to evaluate the thrust of a rocket knowing the mass flow rate of propellant, and it is an indicator of engine efficiency. The system characterized by the highest specific impulse produces the highest thrust with the same amount of propellant. At the same time, also the production of condensed species is an important aspect. The higher is the amount of condensed species produced, the higher is the reduction of real performances and the higher is the risk of particles settling in the throat of the nozzle.

Thus, Fig.5.3 shows that among the mixtures studied with CEA, the one made by aluminum and iodine pentoxide is the best both for specific impulse and for the production of condensed species. Performances

are way better with respect to the other mixtures, so this system is very interesting for micropropulsion applications.

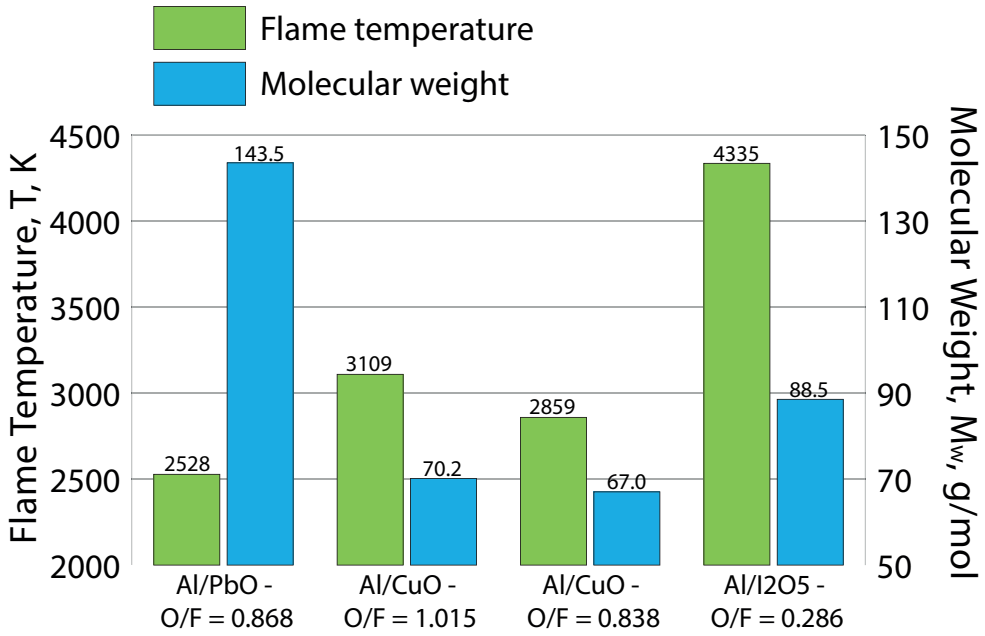

Figure 5.2: Comparison of temperatures and molecular weights of tested mixtures (NASA CEA, 1.0 Mpa, nozzle exhaust-to-throat area ratio 15, shifting equilibrium).

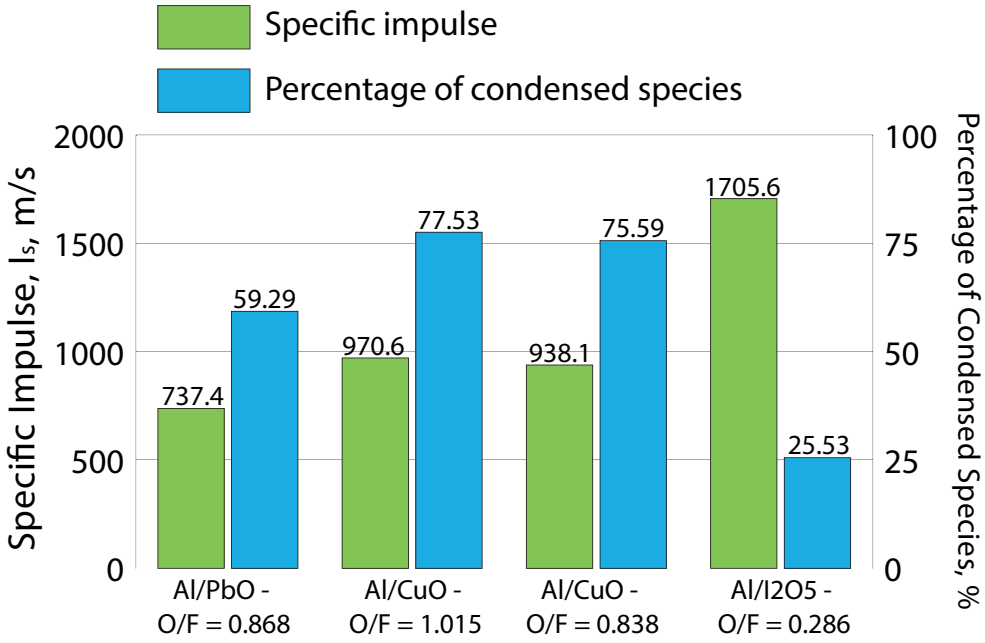

Figure 5.3: Comparison of specific impulses and percentages of condensed species at throat section of tested mixtures (NASA CEA, 1.0 Mpa, nozzle exhaust-to-throat area ratio 15, shifting equilibrium).

It should be noted that in Fig.5.2 and Fig.5.3 are not collected bismuth-based mixtures results, since they have been studied with TERRA so they cannot be directly compared with the ones studied with CEA. For this reason, one more simulation has been performed for mixture Al/I_2O_5 with the same input parameters used in TERRA, and results have been compared in Fig.5.4.

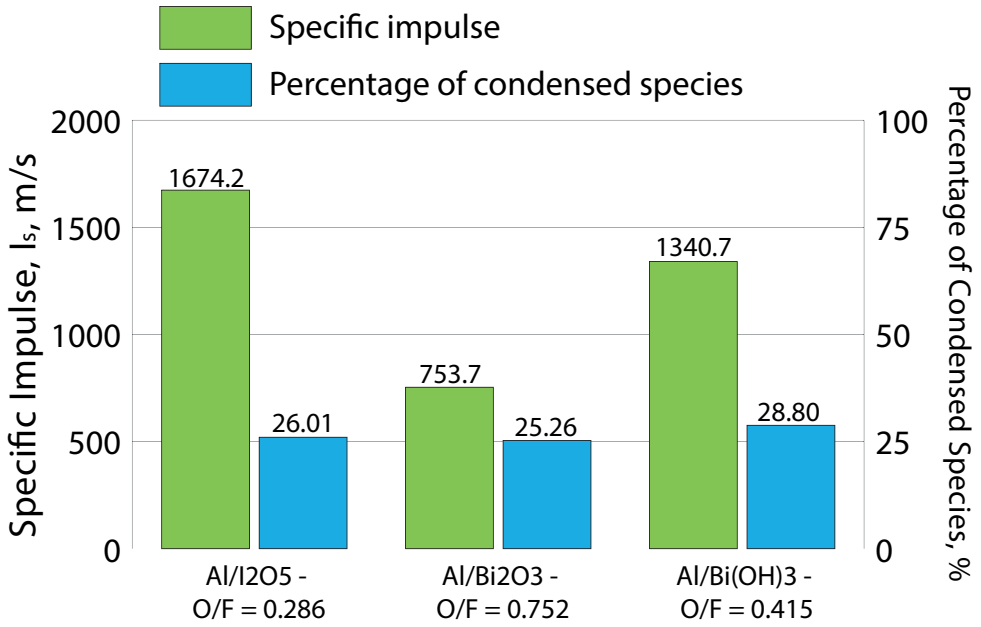

Figure 5.4: Comparison of specific impulses and percentages of condensed species at throat section of tested mixtures (mixture Al/I_2O_5 studied with CEA, other mixtures studied with TERRA, 2.0 MPa, exit pressure 0.03 MPa, shifting equilibrium in CEA).

Even if bismuth-based mixtures show interesting performances, system with iodine pentoxide still remains the best one. Results from this first analysis on simple thermite systems allow to make some important considerations. Iodine- and bismuth-based thermite systems show interesting performances with respect to the other "conventional" thermite systems. These compounds have high energy density, and experiments proved that they release a higher amount of gases with respect to other systems, reaching very high values of peak pressure. A possible explanation for the high pressure rise and the higher release of gases is that the boiling temperature of the reaction products (457 K for iodine, and 1833 K for bismuth) is much lower than the maximum reaction temperature $\sim$2273 K. Several advantages have been highlighted thanks to experimental analysis: (i) reduced ignition delay and reaction times; (ii) higher heat transfer rates; (iii) enhanced density impulse. Moreover, the use of hydroxide-based system tends to produce almost twice the specific impulse than the corresponding oxide system producing a slightly higher amount of condensed species [5] [15].
These results are very interesting but research on thermite systems for micropropulsion states that performances of these kind of systems are not enough for the purpose, especially for gas production. The need to increase gas production led to the emerging and promising idea of mixing thermite with gas-generating additives. Analysis and results about this novelty are shown in the following chapter.

5.5 Results for Thermite Systems with Additives

In this section are listed all the results obtained for mixtures that exploit thermite systems as heat source and the gas-generating capability of some additives like HMX, RDX, nitrocellulose, nitroglycerin, and ammonium perchlorate. Compatibility test results for these mixtures are shown in previous chapters except for the one with iodine pentoxide. This one has been analysed since the results of the simple thermite system are very promising.

5.5.1 Al/PbO with Additives

In this section the NASA CEA results for Al/PbO thermite in combination with different additives are presented. Results are obtained for a chamber pressure equal to 1.0 MPa, an expansion ratio equal to 15 and shifting equilibrium in the nozzle. In Tab. 5.13 results for the system Al/PbO/NC with Ox/Fu equal to 0.893 are listed. In this mixture, aluminum mass fraction is 11%, and the PbO/NC mass ratio is 7.9. Tab. 5.14 collects the results for the mixture Al/PbO/RDX with Ox/Fu equal to 1.866. Aluminum

appears with a mass fraction of 6.10%, and the PbO/RDX mass ratio is 0.87. In conclusion, Tab. 5.15 shows the results for the mixture Al/PbO/NC/NG with OX/Fu equal to 1.34. Aluminum has a mass fraction of 6.10%, PbO has a mass fraction of 43.90%, and the NC/NG mass ratio is equal to 2.0. All the mixtures considered in this section are studied with the same mass ratios presented in Ref. [5].

	Location		
Parameters	Combustion Chamber	Throat Section	Nozzle Exit
Pressure ratio, p_{inf}/p	1.00	1.72	91.47
Pressure, p, MPa	1.00	0.58	0.01
Temperature, T, K	2950	2796	2114
Density, ρ, kg/m^3	5.56	3.42	0.085
Molecular weight, M_W, g/mol	110.10	110.26	110.53
Specific heat, C_p, $kJ/(kg \cdot K)$	0.69	0.66	4.69
Sonic vel., c, m/s	447.6	435.5	370.6
Mach number, M	0.00	1.00	3.13
Characteristic vel., c^*, m/s	NA	671.1	671.1
Thrust coeff., C_F	NA	0.64	1.72
Specific impulse, I_s, m/s	NA	825.5	1270.5
Mass fractions of gas mixture			
Al	0.00240	0.00236	0.00284
AlH	0.00030	0.00027	0.00015
AlOH	0.00236	0.00171	0.00020
Al_2O	0.01424	0.01452	0.01405
CO	0.05039	0.05040	0.05042
H	0.00011	0.00009	0.00003
H_2	0.00193	0.00197	0.00208
N_2	0.01541	0.01540	0.01533
Pb	0.73311	0.73323	0.73331
AlN(liquid)	0.00000	0.00000	0.00022
Al_2O_3(solid)	0.00000	0.00000	0.18135
Al_2O_3(liquid)	0.17921	0.17976	0.00000

Table 5.13: Results obtained for the mixture Al/PbO/NC, Ox/Fu = 0.893, aluminum mass fraction 11%, PbO/NC mass ratio 7.9 (NASA CEA, chamber pressure 1.0 MPa, nozzle exhaust-to-throat area ratio 15, shifting equilibrium).

	Location		
Parameters	Combustion Chamber	Throat Section	Nozzle Exit
Pressure ratio, p_{inf}/p	1.00	1.73	125.04
Pressure, p, MPa	1.00	0.57	0.01
Temperature, T, K	3206	3017	1661
Density, ρ, kg/m^3	1.63	1.00	0.02
Molecular weight, M_W, g/mol	41.61	41.95	42.80
Specific heat, C_p, $kJ/(kg \cdot K)$	2.35	2.06	1.03
Sonic vel., c, m/s	835.4	808.3	611.6
Mach number, M	0.00	1.00	3.41
Characteristic vel., c^*, m/s	NA	1226.1	1226.1
Thrust coeff., C_F	NA	0.65	1.70
Specific impulse, I_s, m/s	NA	1513.3	2234.2
Mass fractions of gas mixture			
Al	0.00002	0.00001	0.00000
AlO	0.00013	0.00005	0.00000
AlOH	0.00162	0.00080	0.00000
$Al(OH)_2$	0.00010	0.00004	0.00000
$Al(OH)_3$	0.00008	0.00005	0.00000
CO	0.16096	0.15885	0.14049
CO_2	0.04429	0.04761	0.07646
H	0.00071	0.00054	0.00000
H_2	0.00527	0.00528	0.00639
H_2O	0.06430	0.06694	0.06449
NO	0.00204	0.00125	0.00000
N_2	0.18822	0.18860	0.18918
O	0.00094	0.00051	0.00000
OH	0.00675	0.00472	0.00000
O_2	0.00100	0.00057	0.00000
Pb	0.37086	0.37755	0.40686
PbO	0.03935	0.03215	0.00058
Al_2O_3(solid)	0.00000	0.00000	0.11554
Al_2O_3(liquid)	0.11328	0.11446	0.00000

Table 5.14: Results obtained for the mixture Al/PbO/RDX, Ox/Fu = 1.866, aluminum mass fraction 6.10%, PbO/RDX mass ratio 0.878 (NASA CEA, chamber pressure 1.0 MPa, nozzle exhaust-to-throat area ratio 15, shifting equilibrium).

	Location		
Parameters	Combustion Chamber	Throat Section	Nozzle Exit
Pressure ratio, p_{inf}/p	1.00	1.72	105.34
Pressure, p, MPa	1.00	0.58	0.01
Temperature, T, K	3131	2988	2014
Density, ρ, kg/m^3	1.98	1.21	0.03
Molecular weight, M_W, g/mol	48.74	49.20	51.01
Specific heat, C_p, $kJ/(kg \cdot K)$	2.87	2.72	1.13
Sonic vel., c, m/s	750.9	729.5	599.8
Mach number, M	0.00	1.00	3.22
Characteristic vel., c^*, m/s	NA	1124.5	1124.5
Thrust coeff., C_F	NA	0.64	1.71
Specific impulse, I_s, m/s	NA	1383.3	2092.3
Mass fractions of gas mixture			
AlO	0.00003	0.00001	0.00000
AlOH	0.00027	0.00016	0.00000
$Al(OH)_2$	0.00004	0.00002	0.00000
$Al(OH)_3$	0.00009	0.00006	0.00000
CO	0.13224	0.12574	0.09282
CO_2	0.15369	0.16391	0.21562
H	0.00028	0.00023	0.00002
$HAlO_2$	0.00001	0.00001	0.00000
HO_2	0.00001	0.00001	0.00000
H_2	0.00148	0.00141	0.00137
H_2O	0.07474	0.07686	0.08360
NO	0.00375	0.00283	0.00003
N_2	0.08042	0.08085	0.08216
O	0.00209	0.00152	0.00001
OH	0.01056	0.00861	0.00028
O_2	0.00930	0.00735	0.00003
Pb	0.29725	0.30701	0.39273
PbO	0.11865	0.10813	0.01579
Al_2O_3(solid)	0.00000	0.00000	0.11554
Al_2O_3(liquid)	0.11508	0.11528	0.00000

Table 5.15: Results obtained for the mixture Al/PbO/NC/NG, Ox/Fu = 1.340, aluminum mass fraction 6.10%, PbO mass fraction 43.90%, NC/NG mass ratio 2 (NASA CEA, chamber pressure 1.0 MPa, nozzle exhaust-to-throat area ratio 15, shifting equilibrium).

5.5.2 Al/CuO with Additives

In this section the NASA CEA results for Al/CuO thermite in combination with different additives are presented. Results are obtained for a chamber pressure equal to 1.0 MPa, an expansion ratio equal to 15 and shifting equilibrium in the nozzle. Tab. 5.16, Tab. 5.17 and Tab. 5.18 show the behaviour of performances of the mixture Al/CuO/NC with the increase of the NC content. In Tab. 5.16 the Ox/Fu is equal to 1.015, with aluminum mass fraction equal to 24.4 % and CuO/NC mass ratio equal to 29.24. In Tab. 5.17 the Ox/Fu is equal to 0.992, with aluminum mass fraction of 23.77% and CuO/NC mass ratio of 14.24. In Tab. 5.18 the mixture has a Ox/Fu equal to 1.025, aluminum mass fraction of 22.52% and CuO/NC ratio of 6.75. Mass ratios for these mixtures are collected from Ref. [5].
Tab. 5.19 and Tab. 5.20 shows the effects of the increase of AP in the mixture Al/CuO/NC/AP. In Tab. 5.19 the Ox/Fu is equal to 0.881 and the mass composition is 26.64/65.86/2.5/5.0. In Tab. 5.20 AP mass fraction increases up to 10%, NC content is kept constant, Al/CuO mass composition is 25.2/62.3 and the Ox/Fu is equal to 0.93. Mass ratios for these mixtures are collected from Ref. [33]
Tab. 5.21 and Tab. 5.22 show the effects of the increase of HMX content from 10% to 50% in the mixture Al/CuO/HMX/NC. In Tab. 5.21 the mixture has a Ox/Fu equal to 1.061, the aluminum mass fraction is 21.28% and CuO/HMX/NC mass composition is 63.72/10/5. In Tab. 5.22 the mixture has a Ox/Fu equal to 1.428, aluminum mass fraction is 11.2% and CuO/HMX/NC mass composition is 33.74/50/5. Tab. 5.23 collects the results for the same mixture studied in Tab. 5.22 but with different operating conditions. This mixture will be compared with the ones studied with TERRA.
Tab. 5.24 collects the results for the mixture Al/CuO/RDX/NC with Ox/Fu equal to 1.563, aluminum mass fraction equal to 11.26% and CuO/RDX/NC mass composition 33.74/50/5. Tab. 5.25 lists the results for the same mixture, without NC. Ox/Fu is equal to 1.50, aluminum mass fraction is 12.5% and CuO/RDX mass ratio is 0.75. Mass ratios for these mixtures are collected from Ref. [5].
In conclusion, Tab. 5.26 presents the results for the mixture Al/CuO/NC/NG with Ox/Fu equal to 1.243, aluminum mass fraction of 12.5%, CuO mass fraction 37.5% and NC/NG mass ratio of 2.0.

	Location		
Parameters	Combustion Chamber	Throat Section	Nozzle Exit
Pressure ratio, p_{inf}/p	1.00	1.65	78.08
Pressure, p, MPa	1.00	0.60	0.01
Temperature, T, K	3136	3020	2327
Density, ρ, kg/m^3	8.54	5.17	0.12
Molecular weight, M_W, g/mol	67.76	67.74	67.50
Specific heat, C_p, $kJ/(kg \cdot K)$	3.71	4.32	0.00
Sonic vel., c, m/s	343.2	343.7	236.8
Mach number, M	0.00	1.00	4.15
Characteristic vel., c^*, m/s	NA	561.8	561.8
Thrust coeff., C_F	NA	0.61	1.75
Specific impulse, I_s, m/s	NA	682.5	1091.2
Mass fractions of gas mixture			
Al	0.01178	0.01204	0.01411
AlH	0.00068	0.00061	0.00028
AlO	0.00028	0.00021	0.00001
AlOH	0.00255	0.00218	0.00051
Al_2	0.00021	0.00016	0.00003
Al_2O	0.10968	0.10962	0.10730
Al_2O_2	0.00041	0.00029	0.00001
CO	0.01260	0.01260	0.01261
Cu	0.09427	0.10402	0.16026
Cu_2	0.00767	0.00735	0.00334
H	0.00007	0.00007	0.00004
H_2	0.00038	0.00039	0.00047
H_2O	0.00001	0.00001	0.00000
N_2	0.00385	0.00385	0.00385
Al_2O_3(solid)	0.00000	0.00000	0.06318
Al_2O_3(liquid)	0.27350	0.27397	0.21361
Cu(liquid)	0.48203	0.47260	0.42037

Table 5.16: Results obtained for the mixture Al/CuO/NC, Ox/Fu = 1.015, aluminum mass fraction 24.4%, CuO/NC mass ratio 29.24 (NASA CEA, chamber pressure 1.0 MPa, nozzle exhaust-to-throat area ratio 15, shifting equilibrium).

	Location		
Parameters	Combustion Chamber	Throat Section	Nozzle Exit
Pressure ratio, p_{inf}/p	1.00	1.67	79.44
Pressure, p, MPa	1.00	0.59	0.01
Temperature, T, K	3156	3032	2327
Density, ρ, kg/m^3	6.82	4.14	0.09
Molecular weight, M_W, g/mol	65.60	65.59	65.38
Specific heat, C_p, $kJ/(kg \cdot K)$	4.84	5.55	0.00
Sonic vel., c, m/s	388.1	386.4	257.9
Mach number, M	0.00	1.00	4.20
Characteristic vel., c^*, m/s	NA	623.9	623.9
Thrust coeff., C_F	NA	0.61	1.73
Specific impulse, I_s, m/s	NA	759.9	1201.3
Mass fractions of gas mixture			
Al	0.01087	0.01106	0.01281
AlH	0.00081	0.00073	0.00033
AlO	0.00035	0.00025	0.00002
AlOH	0.00396	0.00333	0.00074
Al_2	0.00014	0.00011	0.00002
Al_2O	0.08927	0.08945	0.08815
Al_2O_2	0.00046	0.00032	0.00001
CO	0.02520	0.02521	0.02522
CO_2	0.00003	0.00002	0.00000
Cu	0.12628	0.13594	0.19610
Cu_2	0.01052	0.00977	0.00408
H	0.00012	0.00011	0.00006
HCN	0.00001	0.00000	0.00000
H_2	0.00081	0.00084	0.00097
H_2O	0.00004	0.00003	0.00000
N_2	0.00770	0.00770	0.00771
Al_2O_3(solid)	0.00000	0.00000	0.11560
Al_2O_3(liquid)	0.29118	0.29180	0.17934
Cu(liquid)	0.43223	0.42332	0.36885

Table 5.17: Results obtained for the mixture Al/CuO/NC, Ox/Fu = 0.992, aluminum mass fraction 23.77%, CuO/NC mass ratio 14.24 (NASA CEA, chamber pressure 1.0 MPa, nozzle exhaust-to-throat area ratio 15, shifting equilibrium).

	Location		
Parameters	Combustion Chamber	Throat Section	Nozzle Exit
Pressure ratio, p_{inf}/p	1.00	1.68	81.29
Pressure, p, MPa	1.00	0.59	0.01
Temperature, T, K	3181	3048	2327
Density, ρ, kg/m^3	4.83	2.95	0.07
Molecular weight, M_W, g/mol	61.75	61.74	61.59
Specific heat, C_p, $kJ/(kg \cdot K)$	7.28	8.14	0.00
Sonic vel., c, m/s	468.0	462.1	295.5
Mach number, M	0.00	1.00	4.26
Characteristic vel., c^*, m/s	NA	733.6	733.6
Thrust coeff., C_F	NA	0.63	1.71
Specific impulse, I_s, m/s	NA	896.6	1396.7
Mass fractions of gas mixture			
Al	0.00805	0.00815	0.00933
AlH	0.00072	0.00065	0.00030
AlO	0.00045	0.00031	0.00002
AlOH	0.00581	0.00479	0.00100
Al_2	0.00005	0.00004	0.00001
Al_2O	0.05178	0.05215	0.05207
Al_2O_2	0.00047	0.00031	0.00001
CO	0.05037	0.05040	0.05044
CO_2	0.00010	0.00007	0.00000
Cu	0.19352	0.20202	0.26843
Cu_2	0.01658	0.01480	0.00559
H	0.00022	0.00020	0.00009
H_2	0.00172	0.00177	0.00199
H_2O	0.00014	0.00010	0.00001
N_2	0.01541	0.01541	0.01541
OH	0.00001	0.00001	0.00000
Al_2O_3(solid)	0.00000	0.00000	0.22273
Al_2O_3(liquid)	0.32557	0.32655	0.10750
Cu(liquid)	0.32897	0.32225	0.26505

Table 5.18: Results obtained for the mixture Al/CuO/NC, Ox/Fu = 1.025, aluminum mass fraction 22.52%, CuO/NC mass ratio 6.75 (NASA CEA, chamber pressure 1.0 MPa, nozzle exhaust-to-throat area ratio 15, shifting equilibrium).

	Location		
Parameters	Combustion Chamber	Throat Section	Nozzle Exit
Pressure ratio, p_{inf}/p	1.00	1.68	77.34
Pressure, p, MPa	1.00	0.59	0.01
Temperature, T, K	3141	3015	2327
Density, ρ, kg/m^3	5.57	3.39	0.08
Molecular weight, M_W, g/mol	64.24	64.23	64.02
Specific heat, C_p, $kJ/(kg \cdot K)$	5.61	6.31	0.00
Sonic vel., c, m/s	433.5	429.2	289.0
Mach number, M	0.00	1.00	4.08
Characteristic vel., c^*, m/s	NA	685.6	685.6
Thrust coeff., C_F	NA	0.62	1.71
Specific impulse, I_s, m/s	NA	836.9	1312.0
Mass fractions of gas mixture			
Al	0.01245	0.01261	0.01467
AlCl	0.02392	0.02433	0.02599
AlH	0.00128	0.00115	0.00051
AlO	0.00039	0.00027	0.00002
AlOH	0.00624	0.00518	0.00117
Al_2	0.00015	0.00012	0.00002
Al_2O	0.10167	0.10183	0.09955
Al_2O_2	0.00051	0.00034	0.00002
CO	0.01260	0.01260	0.01261
Cu	0.14725	0.15604	0.23450
CuCl	0.00277	0.00239	0.00068
Cu_2	0.01206	0.01097	0.00488
H	0.00019	0.00018	0.00009
HCl	0.00041	0.00034	0.00008
H_2	0.00184	0.00189	0.00211
N_2	0.00981	0.00981	0.00981
Al_2O_3(solid)	0.00000	0.00000	0.25288
Al_2O_3(liquid)	0.30113	0.30216	0.05408
Cu(liquid)	0.36503	0.35758	0.28631

Table 5.19: Results obtained for the mixture Al/CuO/NC/AP, Ox/Fu = 0.881, aluminum mass fraction 26.64%, CuO/NC/AP mass composition 65.86/2.5/5.0 (NASA CEA, chamber pressure 1.0 MPa, nozzle exhaust-to-throat area ratio 15, shifting equilibrium).

	Location		
Parameters	Combustion Chamber	Throat Section	Nozzle Exit
Pressure ratio, p_{inf}/p	1.00	1.69	90.75
Pressure, p, MPa	1.00	0.59	0.01
Temperature, T, K	3237	3097	2327
Density, ρ, kg/m^3	3.90	2.38	0.05
Molecular weight, M_W, g/mol	62.77	62.74	62.46
Specific heat, C_p, $kJ/(kg \cdot K)$	12.37	13.85	0.00
Sonic vel., c, m/s	523.2	515.2	292.5
Mach number, M	0.00	1.00	4.81
Characteristic vel., c^*, m/s	NA	813.6	813.6
Thrust coeff., C_F	NA	0.63	1.72
Specific impulse, I_s, m/s	NA	995.6	1541.4
Mass fractions of gas mixture			
Al	0.00632	0.00622	0.00584
AlCl	0.03587	0.03791	0.04913
AlH	0.00067	0.00059	0.00023
AlO	0.00064	0.00043	0.00002
AlOH	0.00852	0.00696	0.00122
Al_2O	0.03283	0.03196	0.02594
Al_2O_2	0.00054	0.00035	0.00001
CO	0.01258	0.01259	0.01261
Cl	0.00041	0.00032	0.00003
Cu	0.28570	0.29648	0.33206
CuCl	0.01843	0.01649	0.00458
Cu_2	0.02599	0.02306	0.00692
H	0.00039	0.00035	0.00014
HCl	0.00261	0.00229	0.00060
H_2	0.00322	0.00333	0.00376
N_2	0.01577	0.01577	0.01578
Al_2O_3(solid)	0.00000	0.00000	0.05610
Al_2O_3(liquid)	0.37424	0.37658	0.32920
Cu(liquid)	0.17413	0.16754	0.15577
and a small amount of other gases			

Table 5.20: Results obtained for the mixture Al/CuO/NC/AP, Ox/Fu = 0.93, aluminum mass fraction 25.2%, CuO/NC/AP mass composition 62.3/2.5/10 (NASA CEA, chamber pressure 1.0 MPa, nozzle exhaust-to-throat area ratio 15, shifting equilibrium).

	Location		
Parameters	Combustion Chamber	Throat Section	Nozzle Exit
Pressure ratio, p_{inf}/p	1.00	1.70	83.66
Pressure, p, MPa	1.00	0.58	0.01
Temperature, T, K	3147	3012	2300
Density, ρ, kg/m^3	3.62	2.22	0.05
Molecular weight, M_W, g/mol	56.06	56.05	55.98
Specific heat, C_p, $kJ/(Kg \cdot K)$	8.20	8.93	18.57
Sonic vel., c, m/s	547.0	536.1	486.4
Mach number, M	0.00	1.00	2.97
Characteristic vel., c^*, m/s	NA	840.0	840.0
Thrust coeff., C_F	NA	0.63	1.71
Specific impulse, I_s, m/s	NA	1029.6	1589.0
Mass fractions of gas mixture			
Al	0.00630	0.00636	0.00740
AlH	0.00069	0.00062	0.00029
AlO	0.00043	0.00028	0.00001
AlOH	0.00717	0.00581	0.00114
Al_2O	0.03528	0.03567	0.03587
Al_2O_2	0.00038	0.00025	0.00001
CO	0.06294	0.06297	0.06304
CO_2	0.00014	0.00010	0.00001
Cu	0.23089	0.23558	0.29592
Cu_2	0.01903	0.01648	0.00578
H	0.00032	0.00028	0.00013
HCN	0.00002	0.00001	0.00001
H_2	0.00323	0.00332	0.00362
H_2O	0.00033	0.00022	0.00001
N_2	0.04553	0.04553	0.04554
OH	0.00002	0.00001	0.00000
Al_2O_3(solid)	0.00000	0.00000	0.33385
Al_2O_3(liquid)	0.32809	0.32945	0.00000
Cu(liquid)	0.25913	0.25699	0.20737

Table 5.21: Results obtained for the mixture Al/CuO/HMX/NC, Ox/Fu = 1.061, aluminum mass fraction 21.28%, CuO/HMX/NC mass composition 63.72/10/5 (NASA CEA, chamber pressure 1.0 MPa, nozzle exhaust-to-throat area ratio 15, shifting equilibrium).

	Location		
Parameters	Combustion Chamber	Throat Section	Nozzle Exit
Pressure ratio, p_{inf}/p	1.00	1.74	101.96
Pressure, p, MPa	1.00	0.57	0.01
Temperature, T, K	3022	2824	2067
Density, ρ, kg/m^3	1.50	0.92	0.02
Molecular weight, M_W, g/mol	34.98	35.16	35.31
Specific heat, C_p, $kJ/(kg \cdot K)$	2.24	1.99	7.23
Sonic vel., c, m/s	874.8	845.9	676.9
Mach number, M	0.00	1.00	3.24
Characteristic vel., c^*, m/s	NA	1276.9	1276.9
Thrust coeff., C_F	NA	0.66	1.71
Specific impulse, I_s, m/s	NA	1577.5	2380.8
Mass fractions of gas mixture			
AlO	0.00003	0.00001	0.00000
AlOH	0.00069	0.00029	0.00000
CO	0.17905	0.17711	0.16881
CO_2	0.05550	0.05855	0.07160
Cu	0.25445	0.25503	0.1244
CuO	0.00120	0.00066	0.0000
CuOH	0.00179	0.00132	0.00006
Cu_2	0.01269	0.01291	0.00126
H	0.00046	0.00032	0.00007
H_2	0.00564	0.00572	0.00634
H_2O	0.07399	0.07552	0.07374
NO	0.00111	0.00056	0.00002
N_2	0.19637	0.19663	0.19688
O	0.00037	0.00015	0.00000
OH	0.00421	0.00253	0.00020
O_2	0.00043	0.00018	0.00000
Al_2O_3(solid)	0.00000	0.00000	0.21282
Al_2O_3(liquid)	0.21188	0.21243	0.00000
Cu(liquid)	0.00000	0.00000	0.14377

Table 5.22: Results obtained for the mixture Al/CuO/HMX/NC, Ox/Fu = 1.428, aluminum mass fraction 11.26%, CuO/HMX/NC mass composition 33.74/50/5 (NASA CEA, chamber pressure 1.0 MPa, nozzle exhaust-to-throat area ratio 15, shifting equilibrium).

	Location		
Parameters	Combustion Chamber	Throat Section	Nozzle Exit
Pressure ratio, p_{inf}/p	1.00	1.73	66.66
Pressure, p, MPa	2.00	1.15	0.03
Temperature, T, K	3093	2940	2198
Density, ρ, kg/m^3	2.96	1.83	0.06
Molecular weight, M_W, g/mol	35.10	35.15	35.30
Specific heat, C_p, $kJ/(kg \cdot K)$	7.47	7.37	6.29
Sonic vel., c, m/s	875.5	846.1	698.4
Mach number, M	0.00	1.00	3.04
Characteristic vel., c^*, m/s	NA	1290.7	1290.7
Thrust coeff., C_F	NA	0.65	1.64
Specific impulse, I_s, m/s	NA	846.1	2123.6
Mass fractions of gas mixture			
AlO	0.00003	0.00001	0.00000
AlOH	0.00070	0.00040	0.00001
$Al(OH)_2$	0.00007	0.00003	0.00000
$Al(OH)_3$	0.00011	0.00006	0.00000
CO	0.17939	0.17802	0.17067
CO_2	0.05498	0.05713	0.06868
Cu	0.23441	0.21781	0.11775
CuO	0.00136	0.00082	0.00002
CuOH	0.00239	0.00167	0.00011
Cu_2	0.01813	0.01385	0.00176
H	0.00040	0.00033	0.00009
$HAlO_2$	0.00001	0.00000	0.00000
H_2	0.00564	0.00569	0.00620
H_2O	0.07460	0.07552	0.07478
NO	0.00107	0.00070	0.00003
N_2	0.19639	0.19656	0.19687
O	0.00029	0.00018	0.00001
OH	0.00387	0.00285	0.00031
O_2	0.00034	0.00021	0.00001
Al_2O_3(solid)	0.00000 0.00000	0.21281	
Al_2O_3(liquid)	0.21183	0.21227	0.00000
Cu(liquid)	0.01400	0.03588	0.14990

Table 5.23: Results obtained for the mixture Al/CuO/HMX/NC, Ox/Fu = 1.428, aluminum mass fraction 11.26%, CuO/HMX/NC mass composition 33.74/50/5 (NASA CEA, chamber pressure 2.0 MPa, nozzle exit pressure 0.03 MPa).

	Location		
Parameters	Combustion Chamber	Throat Section	Nozzle Exit
Pressure ratio, p_{inf}/p	1.00	1.74	102.13
Pressure, p, MPa	1.00	0.57	0.01
Temperature, T, K	3036	2838	2069
Density, ρ, kg/m^3	1.49	0.92	0.02
Molecular weight, M_W, g/mol	34.95	35.13	35.31
Specific heat, C_p, $kJ/(kg \cdot K)$	2.27	2.01	7.39
Sonic vel., c, m/s	876.9	848.0	678.1
Mach number, M	0.00	1.00	3.24
Characteristic vel., c^*, m/s	NA	1280.8	1280.8
Thrust coeff., C_F	NA	0.66	1.71
Specific impulse, I_s, m/s	NA	1582.2	2386.0
Mass fractions of gas mixture			
AlO	0.00004	0.00001	0.00000
AlOH	0.00074	0.00031	0.00000
CO	0.17923	0.17727	0.16885
CO_2	0.05523	0.05831	0.07154
Cu	0.25484	0.25552	0.12786
CuO	0.00125	0.00070	0.00001
CuOH	0.00179	0.00133	0.00006
Cu_2	0.01226	0.01239	0.00131
H	0.00048	0.00034	0.00007
H_2	0.00563	0.00571	0.00633
H_2O	0.07375	0.07537	0.07375
NO	0.00117	0.00061	0.00002
N_2	0.19634	0.19660	0.19688
O	0.00040	0.00017	0.00000
OH	0.00443	0.00269	0.00020
O_2	0.00047	0.00020	0.00000
Al_2O_3(solid)	0.00000	0.00000	0.21282
Al_2O_3(liquid)	0.21181	0.21240	0.00000
Cu(liquid)	0.00000	0.00000	0.14028

Table 5.24: Results obtained for the mixture Al/CuO/RDX/NC, Ox/Fu = 1.563, aluminum mass fraction 11.26%, CuO/RDX/NC mass composition 33.74/50/5 (NASA CEA, chamber pressure 1.0 MPa, nozzle exhaust-to-throat area ratio 15, shifting equilibrium).

	Location		
Parameters	Combustion Chamber	Throat Section	Nozzle Exit
Pressure ratio, p_{inf}/p	1.00	1.72	100.70
Pressure, p, MPa	1.00	0.57	0.01
Temperature, T, K	3026	2843	2102
Density, ρ, kg/m^3	1.57	0.97	0.02
Molecular weight, M_W, g/mol	36.33	36.47	36.59
Specific heat, C_p, $kJ/(kg \cdot K)$	2.11	9.56	8.75
Sonic vel., c, m/s	853.8	818.4	665.4
Mach number, M	0.00	1.00	3.22
Characteristic vel., c^*, m/s	NA	1248.8	1248.8
Thrust coeff., C_F	NA	0.65	1.71
Specific impulse, I_s, m/s	NA	1541.2	2330.3
Mass fractions of gas mixture			
AlOH	0.00082	0.00038	0.00000
$Al(OH)_2$	0.00005	0.00002	0.00000
$Al(OH)_3$	0.00005	0.00003	0.00000
CO	0.16472	0.16348	0.15728
CO_2	0.03840	0.04034	0.05009
Cu	0.28127	0.27783	0.15830
CuO	0.00101	0.00058	0.00001
CuOH	0.00159	0.00117	0.00007
Cu_2	0.01611	0.01540	0.00180
H	0.00048	0.00035	0.00009
H_2	0.00612	0.00622	0.00675
H_2O	0.06054	0.06164	0.06046
NO	0.00081	0.00044	0.00002
N_2	0.18880	0.18897	0.18917
O	0.00027	0.00013	0.00000
OH	0.00328	0.00208	0.00020
O_2	0.00024	0.00011	0.00000
Al_2O_3(solid)	0.00000	0.00000	0.23646
Al_2O_3(liquid)	0.23537	0.23598	0.00000
Cu(liquid)	0.00000	0.00484	0.13930

Table 5.25: Results obtained for the mixture Al/CuO/RDX, Ox/Fu = 1.50, aluminum mass fraction 12.5%, CuO/RDX mass ratio 0.75 (NASA CEA, chamber pressure 1.0 MPa, nozzle exhaust-to-throat area ratio 15, shifting equilibrium).

	Location		
Parameters	Combustion Chamber	Throat Section	Nozzle Exit
Pressure ratio, p_{inf}/p	1.00	1.71	97.2
Pressure, p, bar	1.00	0.58	0.01
Temperature, T, K	3007	2874	2161
Density, ρ, kg/m^3	1.85	1.13	0.02
Molecular weight, M_W, g/mol	41.82	42.00	42.46
Specific heat, C_p, $kJ/(kg \cdot K)$	2.70	10.42	11.68
Sonic vel., c, m/s	776.5	754.3	629.6
Mach number, M	0.00	1.00	3.17
Characteristic vel., c^*, m/s	NA	1163.8	1163.8
Thrust coeff., C_F	NA	0.64	1.71
Specific impulse, I_s, m/s	NA	1431.3	2179.4
Mass fractions of gas mixture			
AlOH	0.00015	0.00009	0.00000
$Al(OH)_2$	0.00002	0.00001	0.00000
$Al(OH)_3$	0.00008	0.00005	0.00000
CO	0.12968	0.12513	0.11040
CO_2	0.15771	0.16485	0.18800
Cu	0.27349	0.27095	0.21659
CuO	0.00484	0.00334	0.00012
CuOH	0.00427	0.00326	0.00028
Cu_2	0.01872	0.01572	0.00293
H	0.00021	0.00017	0.00006
H_2	0.00149	0.00146	0.00162
H_2O	0.07657	0.07809	0.08071
NO	0.00234	0.00169	0.00010
N_2	0.08108	0.08139	0.08213
O	0.00106	0.00073	0.00003
OH	0.00724	0.00572	0.00079
O_2	0.00481	0.00348	0.00015
Al_2O_3(solid)	0.00000	0.00000	0.23646
Al_2O_3(liquid)	0.23620	0.23631	0.00000
Cu(liquid)	0.00000	0.00755	0.07962

Table 5.26: Results obtained for the mixture Al/CuO/NC/NG, Ox/Fu = 1.243, aluminum mass fraction 12.5%, CuO mass fraction 37.5%, NC/NG mass ratio 2.0 (NASA CEA, chamber pressure 1.0 MPa, nozzle exhaust-to-throat area ratio 15, shifting equilibrium).

5.5.3 Al/I_2O_5 with Additives

In this section the NASA CEA results for Al/I_2O_5 thermite in combination with different additives are presented. Results are obtained for a chamber pressure equal to 1.0 MPa, an expansion ratio equal to 15 and shifting equilibrium in the nozzle. Tab. 5.27 and Tab. 5.28 show the results for the mixture Al/I_2O_5/HMX/NC. In Tab. 5.27 the Ox/Fu is equal to 0.341, aluminum mass fraction is 18.7% and I_2O_5/HMX/NC mass composition is 66.3/10/5. In Tab. 5.28 the Ox/Fu is equal to 0.758, aluminum mass fraction is 9.9% and I_2O_5/HMX/NC mass composition is 35.1/50/5. Tab. 5.10 collects the results for the same mixture presented in Tab. 5.28 but with different operating conditions. This mixture will be compared with the ones studied with TERRA.

	Location		
Parameters	Combustion Chamber	Throat Section	Nozzle Exit
Pressure ratio, p_{inf}/p	1.00	1.70	95.00
Pressure, p, MPa	1.00	0.58	0.01
Temperature, T, K	4093	3959	3139
Density, ρ, kg/m^3	2.18	1.34	0.03
Molecular weight, M_W, g/mol	62.20	62.48	64.74
Specific heat, C_p, $kJ/(kg \cdot K)$	9.44	9.23	6.10
Sonic vel., c, m/s	708.4	691.5	586.5
Mach number, M	0.00	1.00	3.18
Characteristic vel., c^*, m/s	NA	1079.2	1079.2
Thrust coeff., C_F	NA	0.64	1.72
Specific impulse, I_s, m/s	NA	1324.1	2035.7
Mass fractions of gas mixture			
Al	0.00527	0.00494	0.00170
AlI	0.01500	0.01232	0.00175
AlO	0.02333	0.02093	0.00603
AlOH	0.01577	0.01449	0.00533
CO	0.05828	0.05839	0.05855
HI	0.01053	0.00908	0.00289
H_2O	0.00505	0.00499	0.00489
I	0.48056	0.48443	0.49977
NO	0.00650	0.00578	0.00233
N_2	0.04245	0.04280	0.04445
O	0.01879	0.01827	0.01373
OH	0.01081	0.01028	0.00694
O_2	0.01039	0.00975	0.00636
Al_2O_3(liquid)	0.26709	0.27694	0.33331
and a small amount of other gases			

Table 5.27: Results obtained for the mixture Al/I_2O_5/HMX/NC, Ox/Fu = 0.341, aluminum mass fraction 18.7%, I_2O_5/HMX/NC mass composition 66.3/10/5 (NASA CEA, chamber pressure 1.0 MPa, nozzle exhaust-to-throat area ratio 15, shifting equilibrium).

	Location		
Parameters	Combustion Chamber	Throat Section	Nozzle Exit
Pressure ratio, p_{inf}/p	1.00	1.72	107.10
Pressure, p, MPa	1.00	0.58	0.01
Temperature, T, K	3550	3391	2333
Density, ρ, kg/m^3	1.27	0.78	0.02
Molecular weight, M_W, g/mol	35.31	35.71	38.32
Specific heat, C_p, $kJ/(kg \cdot K)$	4.10	4.75	1.98
Sonic vel., c, m/s	938.9	910.8	733.3
Mach number, M	0.00	1.00	3.27
Characteristic vel., c^*, m/s	NA	1399.7	1399.7
Thrust coeff., C_F	NA	0.65	1.71
Specific impulse, I_s, m/s	NA	1723.0	2597.0
Mass fractions of gas mixture			
Al	0.00016	0.00009	0.00000
AlI	0.00069	0.00039	0.00000
AlO	0.00161	0.00091	0.00000
AlOH	0.00620	0.00411	0.00003
$Al(OH)_2$	0.00032	0.00019	0.00000
Al_2O_2	0.00021	0.00009	0.00000
CO	0.17912	0.17593	0.14949
CO_2	0.05540	0.06041	0.10195
H	0.00160	0.00143	0.00027
HI	0.01405	0.01241	0.00668
H_2	0.00434	0.00428	0.00409
H_2O	0.06377	0.06775	0.09058
I	0.25220	0.25411	0.26022
NO	0.00931	0.00762	0.00033
N_2	0.19251	0.19332	0.19674
O	0.00837	0.00684	0.00016
OH	0.02241	0.01990	0.00208
O_2	0.01056	0.00938	0.00032
Al_2O_3(liquid)	0.17640	0.18038	0.18702
and a small amount of other gases			

Table 5.28: Results obtained for the mixture Al/I_2O_5/HMX/NC, Ox/Fu = 0.758, aluminum mass fraction 9.9%, I_2O_5/HMX/NC mass composition 35.1/50/5 (NASA CEA, chamber pressure 1.0 MPa, nozzle exhaust-to-throat area ratio 15, shifting equilibrium).

	Location		
Parameters	Combustion Chamber	Throat Section	Nozzle Exit
Pressure ratio, p_{inf}/p	1.00	1.72	66.66
Pressure, p, MPa	2.00	1.15	0.03
Temperature, T, K	3649	3479	2472
Density, ρ, kg/m^3	2.50	1.54	0.06
Molecular weight, M_W, g/mol	35.65	36.04	38.28
Specific heat, C_p, $kJ/(kg \cdot K)$	4.50	4.27	2.05
Sonic vel., c, m/s	948.2	919.3	754.7
Mach number, M	0.00	1.00	3.07
Characteristic vel., c^*, m/s	NA	1410.3	1410.3
Thrust coeff., C_F	NA	0.65	1.64
Specific impulse, I_s, m/s	NA	1736.6	2351.8
Mass fractions of gas mixture			
Al	0.00014	0.00007	0.00000
AlO	0.00142	0.00080	0.00000
AlO_2	0.00016	0.00007	0.00000
$Al(OH)_2$	0.00045	0.00026	0.00000
Al_2O	0.00011	0.00005	0.00000
CO	0.17786	0.17464	0.15137
CO_2	0.05737	0.06243	0.09900
H	0.00138	0.00123	0.00028
HI	0.01794	0.01591	0.00913
H_2	0.00427	0.00420	0.00399
H_2O	0.06651	0.07047	0.09082
I	0.24812	0.25049	0.25776
I_2	0.00029	0.00022	0.00006
NO	0.00952	0.00771	0.00051
N_2	0.19241	0.19327	0.19665
O	0.00702	0.00565	0.00022
OH	0.02155	0.01896	0.00270
O_2	0.00934	0.00817	0.00045
Al_2O_3(liquid)	0.17667	0.18058	0.18698
and a small amount of other gases			

Table 5.29: Results obtained for the mixture Al/I_2O_5/HMX/NC, Ox/Fu = 0.758, aluminum mass fraction 9.9%, I_2O_5/HMX/NC mass composition 35.1/50/5 (NASA CEA, chamber pressure 2.0 MPa, nozzle exit pressure 0.03 MPa).

5.5.4 Al/Bi_2O_3 with Additives

In this section the TERRA results for Al/Bi_2O_3 thermite in combination with different additives are presented. Results are obtained for a chamber pressure equal to 2.0 MPa and pressure at the nozzle exit equal to 0.03 MPa. Tab. 5.30 and Tab. 5.31 collect the results for the mixture Al/Bi_2O_3/HMX/NC. In Tab. 5.30 the Ox/Fu is equal to 0.934, the aluminum mass fraction is 6% and the Bi_2O_3/HMX/NC mass composition is 79/10/5. In Tab. 5.31 Ox/Fu is equal to 2.251, aluminum mass fraction is 3.15% and the Bi_2O_3/HMX/NC is 41.85/50/5.
Tab. 5.32 collects the results for the mixture Al/Bi_2O_3/NC/NG, with Ox/Fu equal to 1.583, aluminum mass fraction equal to 3.5%, Bi_2O_3 mass fraction equal to 46.5% and NC/NG mass ratio equal to 2.0. Mass ratios considered for these mixtures are collected from Ref. [5].

	Location		
Parameters	Combustion Chamber	Throat Section	Nozzle Exit
Pressure, p, MPa	2.00	1.16	0.03
Temperature, T, K	2772	2629	1895
Molecular weight, M_W, g/mol	98.17	98.51	99.75
Specific heat, C_p, $kJ/(kg \cdot K)$)	0.55	0.55	0.51
Mach number, M	0.00	1.00	3.02
Specific impulse, I_s, m/s	NA	888.8	1322.5
Condensed species ratio, Z	0.11	0.11	0.11

Table 5.30: Results obtained for the mixture Al/Bi_2O_3/HMX/NC, Ox/Fu = 0.934, aluminum mass fraction 6%, Bi_2O_3/HMX/NC mass composition 79/10/5 (TERRA, chamber pressure 2.0 MPa, nozzle exit pressure 0.03 MPa).

	Location		
Parameters	Combustion Chamber	Throat Section	Nozzle Exit
Pressure, p, MPa	2.00	1.14	0.03
Temperature, T, K	3093	2893	1658
Molecular weight, M_W, g/mol	38.86	39.15	39.86
Specific heat, C_p, $kJ/(kg \cdot K)$)	1.14	1.13	1.04
Mach number, M	0.00	1.00	3.16
Specific impulse, I_s, m/s	NA	1524.3	2142.5
Condensed species ratio, Z	0.05	0.05	0.05

Table 5.31: Results obtained for the mixture Al/Bi_2O_3/HMX/NC, Ox/Fu = 2.251, aluminum mass fraction 3.15%, Bi_2O_3/HMX/NC mass composition 41.85/50/5 (TERRA, chamber pressure 2.0 MPa, nozzle exit pressure 0.03 MPa).

	Location		
Parameters	Combustion Chamber	Throat Section	Nozzle Exit
Pressure, p, MPa	2.00	1.16	0.03
Temperature, T, K	3010	2870	1988
Molecular weight, M_W,g/mol	48.27	48.73	50.59
Specific heat, C_p, $kJ/(kg \cdot K)$)	1.03	1.02	0.97
Mach number, M	0.00	1.00	3.03
Specific impulse, I_s, m/s	NA	1354.5	1981.0
Condensed species ratio, Z	0.06	0.06	0.06

Table 5.32: Results obtained for the mixture Al/Bi_2O_3/NC/NG, Ox/Fu = 1.583, aluminum mass fraction 3.5%, Bi_2O_3 mass fraction 46.5%, NC/NG mass ratio 2.0 (TERRA, chamber pressure 2.0 MPa, nozzle exit pressure 0.03 MPa).

5.5.5 Comparison Between Thermite Systems with Additives

In previous sections results about several systems made by mixing thermite and gas-generating substances have been listed. The most interesting parameters for each mixture have been collected and represented in Fig. 5.5 and Fig. 5.6. From these graphs it is possible not only to compare different mixtures but also to see the behaviour of performance parameters with the increase of the percentage of gas-generating substances; in fact, Fig. 5.5 shows that for some of these mixtures, an increase of the mass percentage of the additive corresponds to an increase of the specific impulse, and at the same time the percentage of condensed species decreases. Moreover, performances obtained by each mixture containing additives are way better with respect to the corresponding simple thermite mixture. This important result states that the idea of mixing thermite with gas-generating additives could be the right way to go in order to enhance performances of a solid microthruster.

The simple thermite system Al/PbO with mass ratio 12.23/87.77 produces a specific impulse equal to 737.4 m/s with a production of 59.29% of condensed species. If the same system is mixed with 10% of NC, performances increase a lot. Specific impulse rises up to 1270.5 m/s (+72% w.r.t. the system without additive) and the production of condensed species drops to 17.97%. Thus, it is enough to add a small quantity of additive to generate a huge increase of performances. Results are even more interesting when Al/PbO is mixed with RDX or with a mixture of nitrocellulose and nitroglicerine. Keeping the same mass ratio between Al and PbO, addition of RDX with an overall mass percentage equal to 50% produces 2234.2 m/s (+200% w.r.t. the system without additive) of specific impulse with a generation of 11.44 % of condensed species. Another composition exploits the addition of a mixture of NC and NG. The ratio between NC and NG is the same that is maintained in order to produce DB propellants (2/3 NC, 1/3 NG). Addition of this mixture with an overall mass percentage equal to 50% produces 2092.3 m/s (+183% w.r.t. the system without additive) of specific impulse with a generation of 11.52% of condensed species.

Moving to the mixture with Al/CuO it is possible to see that the situation is quite different. The simple thermite system Al/CuO with mass ratio 25.03/74.97 produces 970.6 m/s and 77.53% of condensed species. Addition of a small amount of gas-generating substances does not generate a high increase of performances like that seen for Al/PbO, especially when trying to reduce the production of condensed species. A first analysis has been carried on by studying the effects of the increase of NC in the overall mass percentage. As the percentage of NC increases, specific impulse increases up to 1396.7 m/s (+43% w.r.t. the system without additive) with production of 64.88% of condensed species when using 10% of NC. Another analysis involves the use of ammonium perchlorate mixed with Al/CuO and 2.5% of NC. Also in this case specific impulse increases (1541.4 m/s,+58% w.r.t. the system without additive) but condensed species, even if they are reduced, still remain too high (54.41%). Interesting results come with the addition of higher amounts of additives, especially when using HMX. A particular compound of Al/CuO with a fixed amount of NC (5%) mixed with a variable quantity of HMX has been analysed.

The addition of 50% of HMX allows to obtain a specific impulse equal to 2380.8 m/s (+145% w.r.t. the system without additive) with generation of 21.24% of condensed species. Substituting HMX with RDX and keeping the same mass percentages, no effects are noticed in terms of thermochemical euqilibrium results. These mixtures seem to be the best in terms of performances, since the remaining ones containing 50% of RDX and 50% of NC/NG produce slightly lower performances.

The last mixture analysed with CEA is the one with Al/I_2O_5 and it is the only mixture of which there is no information about compatibility tests, but since it showed the best performances compared to other simple thermite systems, it is interesting to analyse its behaviour when mixed with additives. A hypothetical mixture made by adding 50% of HMX and 5% of NC has been simulated. Results obtained are the best in terms of performances, since the specific impulse reaches 2597 m/s (+52% w.r.t. the system without additive) and the production of condensed species is 18.03%. If compatibility between Al/I_2O_5 and HMX is assured, this would be the best mixture. Tab 5.33 shows a direct comparison between the results of simple thermite systems and systems with additives studied with CEA.

Also in this case, bismuth-based mixtures required the use of TERRA. Results about some mixtures made with Bi_2O_3 and additives are showed in Fig.5.6, in which they are compared with results obtained for other 2 mixtures previously studied with CEA (Al/CuO/HMX/NC and Al/I_2O_5/HMX/NC). Also in this case the best choice is to add a high quantity of additives, especially HMX. The mixture Al/Bi_2O_3/HMX/NC with mass ratio 3.15/41.85/50.00/5.00 generates a specific impulse equal to 2142.5 % (+184% w.r.t. the system without additive), which is lower with respect to the ones obtained for other compounds. However, the percentage of condensed species is equal to 5.95%, the lowest value obtained in the overall research.

Mixtures without additives				Mixtures with additives			
Mixture	Mass Percentage	I_s (m/s)	Percentage of cond. spec.	Mixture	Mass Percentage	I_s (m/s)	Percentage of cond. spec.
Al/PbO	12.23/87.77	737.4	59.29	Al/PbO/ RDX	6.10/43.90/ 50.00	2234.2	11.44
				Al/PbO/ NC/NG	6.10/43.90/ 33.50/16.50	2092.3	11.52
				Al/PbO/ NC	11.0/79.0/ 10.0	1270.5	17.97
Al/CuO	25.03/74.97	970.6	77.53	Al/CuO/ RDX/NC	11.26/33.74/ 50.00/5.00	2386.0	21.24
				Al/CuO NC	22.52/67.48/ 10.00	1396.7	64.88
				Al/CuO NC/AP	25.20/62.30/ 2.50/10.00	1541.4	54.41
				Al/CuO/ NC/NG	12.50/37.50/ 33.50/16.50	2179.4	23.63
Al/I_2O_5	22.00/78.00	1705.6	25.53	Al/I_2O_5/ HMX/NC	9.90/35.10/ 50.00/5.00	2597.0	18.03

**: mixtures analysed with TERRA.*

Table 5.33: Comparison between thermite mixtures and mixtures with additives.

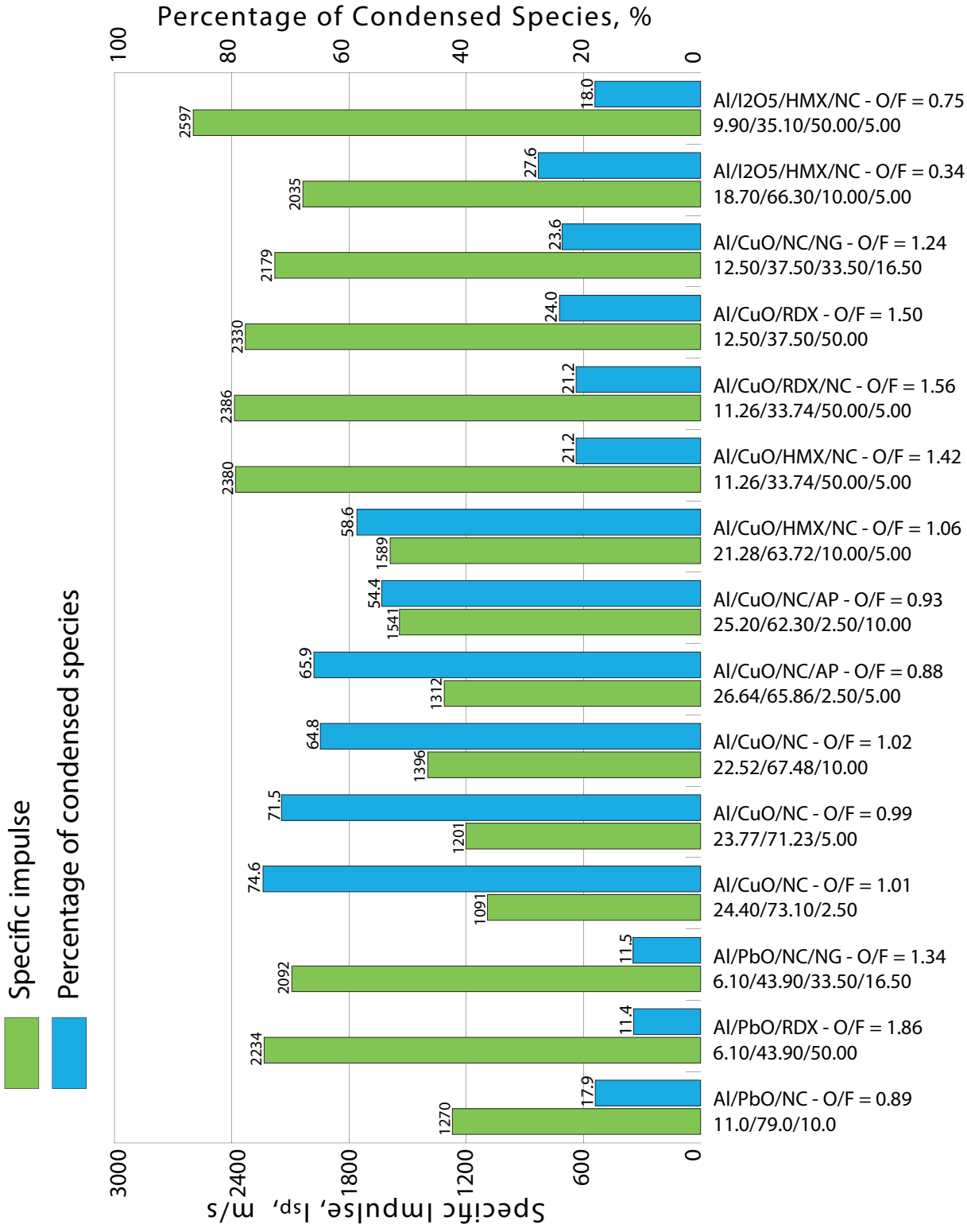

Figure 5.5: Comparison of specific impulses and percentages of condensed species of thermite systems with additives (NASA CEA, 1.0 MPa, nozzle exhaust-to-throat area ratio 15, shifting equilibrium).

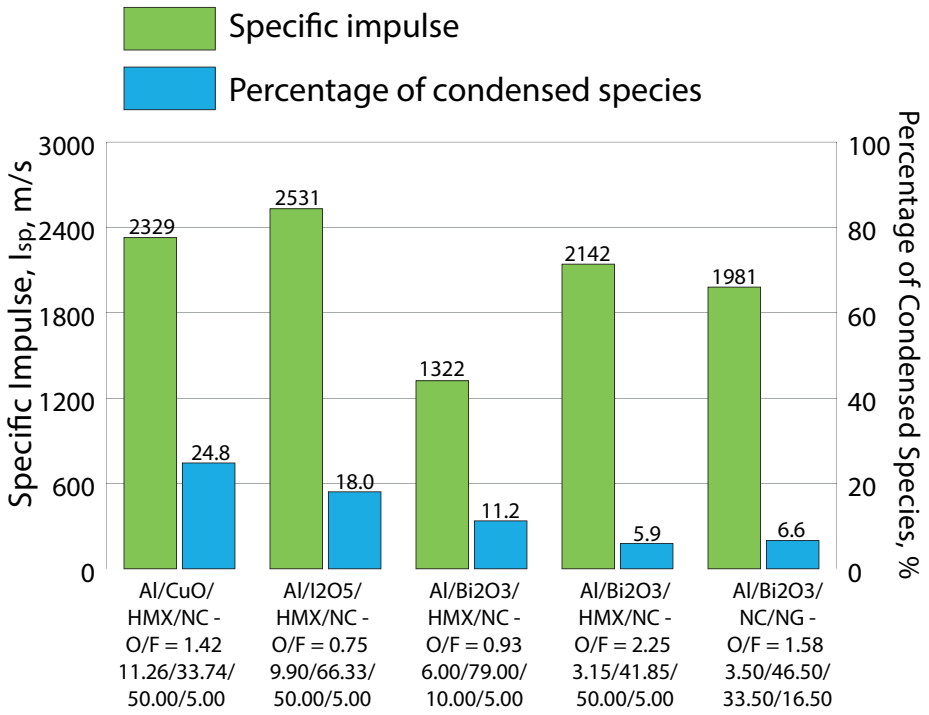

Figure 5.6: Comparison of specific impulses and percentages of condensed species at throat section of mixtures with additives (mixtures with CuO and I_2O_5 studied with CEA, other mixtures with TERRA, 2.0 MPa, exit pressure 0.03 MPa, shifting equilibrium in CEA).

5.6 Discussion of Results

Analysis with chemical equilibrium programs suggests that the idea of a thermite-based propellant consisting of thermite as the heat source and a gas-generating agent as the work substance is very interesting for space micropropulsion. The Table 5.33 clearly shows that mixtures containing additives greatly enhance the specific impulse with respect to the corresponding simple thermite system, and at the same time they tend to lower the percentage of condensed species inside the combustion products. Among the additives analysed in this document, HMX and NC are the most interesting. The latter, especially, is a good gas-generating substance thanks to its igniting and combustion performance. Using nitrocellulose additives improves the specific impulse, but in some cases NC would represent a barrier between the fuel and the oxidizer, decreasing the reaction rate and the sensitivity of the mixture. For example, a concentration of NC higher than 10% in the mixture Al/CuO/NC results in insensitive propellant, difficult to be ignited [5]. Results listed in tables show that an increase of NC content in the mixture leads to a decrease in the molecular weight of gas products, promoting the increase of the specific impulse.
Better performances can be achieved by increasing the amount of the gas-generating agent. Experiments have been successfully performed for mixtures containing 50% of HMX with 5% of NC used as an energetic binder. CEA results follow this trend; each mixture studied with this particular composition exhibits the best performances.

Chemical equilibrium programs apply some assumptions in order to be able to solve the complexity of a problem like a chemical reaction. All these assumptions can be found in Chapter 4. Most of them do not affect heavily the results, especially when studying propellants for a large scale rocket motor, but when the problem refers to a microscale system like in this case, the assumption of adiabatic process leads to huge errors in the results. Heat dissipation in a microthruster mainly occurs via thermal conductivity, which means that the physics is governed by the Fourier's Law. This law states that the heat flow through a solid is directly proportional to the cross-sectional area, the time, and the temperature difference across the material, but is inversely proportional to the thickness of the material as follow:

$$Q = KA(T_2 - T_1)\frac{t}{x} \tag{5.27}$$

where Q is the rate of heat flow, A is the cross-sectional area, $T_2 - T_1$ is the temperature drop, t is the time, x is the thickness, and K is the coefficient of thermal conductivity. Microthrusters are thought to be produced using plastics, polymers or glasses, since these kind of materials possess the lowest coefficients of thermal conductivity, so they reduce the heat dissipation with the external environment. But this is not enough because dimensions of some systems are of the order of microns, and the smaller is the thickness of the material, the higher is the heat flow through it. This means that the temperature computed by chemical equilibrium programs (adiabatic flame temperature) is far from the real one since it is considered that the heat generated by the reaction warms up only combustion products, while in real cases a great part of it flows outside.
Another factor is the time of combustion. Since dimensions are small, the quantity of propellant inside the system is small too. Once the mixture is ignited, it takes few milliseconds to entirely burn. This means that temperature of gas generated has not time enough to reach the theoretical temperature simulated. All these aspects make the temperature reached in real cases in combustion chamber much lower than the theoretical one, with an impact on performances of the system. A much lower temperature means also that chemical reactions occurring through the entire systems are different from the ones computed with programs, and this means also that mass percentages of combustion products are different from the ones predicted.
Furthermore, even the method used to prepare the powders affects the real performances of the mixture. An example is reported in Tab. 5.2, in which two systems made with the same elements and with the same mass percentages but produced with two different methods (MM: Mechanical Mixing; ES: Electrospray) generate slightly different thrust and specific impulse.
However, the purpose of this research is not to get the real results, but to make a relative grading based on performances between the most interesting energetic materials studied nowadays for space micropropulsion. This kind of research, as already mentioned, can be seen as a preliminary analysis in order to find which mixture could be potentially the best choice for a microthruster. After this, an experimental research should be performed in order to validate theoretical results.

After this analysis it is not possible to chose which mixture would be the best one for a micropropulsion system. The best one in terms of specific impulse is Al/I_2O_5/HMX/NC with mass ratio 9.90/35.10/50.00 /5.00, but it must be remembered that this is the only one that has not results about compatibility tests. This means that it is not sure that it is possible to produce a mixture like this. In case it is not possible, the best performances are obtained by the mixture Al/CuO/HMX/NC with mass ratio 11.26/33.74/50.00/5.00.
Nowadays it is well known the importance of condensed species generation. Solid and liquid particles moving through the nozzle reduce the performances of the rocket by adding a kinetic lag and settling in the throat section, changing the expansion ratio of the nozzle. Moreover, space pollution is another critical aspect, and solid particles exiting from the nozzle could deposit on spacecraft surfaces like solar panels, reducing their efficiency. Considering this aspects, the best choice would be the mixture Al/Bi_2O_3/HMX/NC with mass ratio 3.15/41.85/50.00/5.00, which produces only 5.95% of condensed species.
Mixtures with PbO generate good performances, but toxicity of Pb makes these systems less attractive for micropropulsion. Another aspect that has to be considered is the cost of materials. Sigma-Aldrich Corporation, an American company involved in biochemicals and biotechnology, provides a website in which chemical compounds are available for the online purchase. Considering this website as a valid reference, it is possible to evaluate costs of materials. CuO can be purchased for 5.48 €/g, PbO for 7.6 €/g, I_2O_5 for 2.74 €/g, Bi_2O_3 for 5.87 €/g. Thus, from an economical point of view, iodine pentoxide-based mixture is the cheapest. This confirms that, if compatibility tests about system with iodine get positive results, this mixture would be an interesting choice for space micropropulsion [5] [37].

Chapter 6

Conclusions

In this document several potential mixtures for space micropropulsion have been investigated. A deep research through the large amount of available scientific papers focused on this topic allowed to collect many different mixtures that can be used as solid propellants for microthrusters. In order to get an overall idea on which of these systems could be the best choice for space micropropulsion, a relative grading between these mixtures has been performed thanks to the use of chemical equilibrium software like CEA and TERRA. The results obtained are not to be considered real since this kind of programs apply some strong approximations in order to get a solution, and moreover some important processes occurring at microscale are not considered. However, if input parameters are the same, results obtained from different compositions can be compared, highlighting which of the considered mixtures can potentially generate higher performances.
Most of the results come from CEA, while the remaining part, involving compositions made with bismuth, comes from TERRA. Mixtures studied with CEA are supposed to react in an ideal rocket engine (made by a combustion chamber, a nozzle and considering the process to be adiabatic) with pressure in combustion chamber equal to 1.0 MPa, expansion ratio equal to 15 and shifting conditions in the nozzle. It is not possible to replicate the same conditions in TERRA, either because it is not possible to study mixtures with bismuth with a pressure in combustion chamber lower than 2.0 MPa or because it is not possible to set the expansion ratio. For this reason, the best mixtures obtained with CEA are then subjected to further calculations, setting the same conditions as in TERRA (2.0 MPa in combustion chamber and 0.03 MPa at the nozzle exit).
The research has been divided into 2 steps:

- Calculations for simple thermite systems;
- Calculations for thermite systems with gas-generating additives.

Among the large amount of available thermite systems, the most interesting for micropropulsion according with different researches are: Al/PbO, Al/CuO, Al/I_2O_5, Al/Bi_2O_3, Al/$Bi(OH)_3$. Results for these mixtures show that simple thermite systems are not suitable to produce high rocket performances. It is well known that thermite reactions can release a huge amount of heat but generating a small quantity of gas products. However, mixtures with iodine pentoxide and bismuth oxide are very interesting since they are able to generate higher amount of gas with respect to other thermite systems. From results it is easy to see that the most interesting thermite system is Al/I_2O_5 (Ox/Fu = 0.286, $\Phi = 0.955$), with mass ratio 22/78, which generates the highest adiabatic temperature (4335.60 K), the highest specific impulse (1705.6 m/s, computed with CEA) and a percentage of condensed species comparable with bismuth-based systems.

The idea of considering a mixture made with a heat source (thermite) and a gas-generating additive (HMX, RDX, NC, NG, AP) is very interesting. Most of these additives are explosives, so before performing experiments on them, compatibility tests are required. Mixtures studied in this document are certified to be safe (except for the mixture with iodine pentoxide and additives), so usable for experiments. Results demonstrate that addition of gas-generating agents allows to obtain higher performances with respect to simple thermite. The most interesting mixtures are those generated adding HMX, NC and NG to thermite systems like Al/CuO, Al/Bi_2O_3, and Al/I_2O_5. It should be noted that the last

system based on iodine pentoxide is the only system proposed by the author of this document, since the results of the simple thermite are promising and there are not information about addition of additives to this system. Thus, compatibility test results about this system are not available. Results obtained with additives are very interesting. As the percentage of HMX in the mixture increases, the specific impulse increases too. It is difficult to find the best mixtures among all the ones studied with additives. The reason is that there is not a mixture which prevails over the others in every single performance parameter. Results from TERRA show that the highest specific impulse (2531.8 m/s) would be produced by the mixture Al/I_2O_5/HMX/NC (Ox/Fu = 0.758) with mass composition 9.9/35.1/50/5 and mass ratio between Al and I_2O_5 equal to 22/78, with a percentage of condensed species in combustion products equal to 18.05%. This confirms that, if compatibility of additives with Al/I_2O_5 is ensured, this mixture would be the most performing. Otherwise, the most performing mixture in terms of specific impulse is Al/CuO/HMX/NC (Ox/Fu = 1.563) with mass composition 11.26/33.74/50/5 and ratio between Al and CuO equal to 25.03/74.97, which produces 2329.1 m/s of specific impulse with a percentage of condensed species equal to 24.81%. System Al/Bi_2O_3/HMX/NC (Ox/Fu = 2.251) with mass composition 3.15/41.85/50/5 and with ratio between Al and Bi_2O_3 equal to 7/93 do not reach the highest specific impulse (2142.59 m/s, still comparable to the others) but produces only 5.95% of condensed species in combustion products, which is very low with respect to the other mixtures. This aspect is very important because condensed species can both reduce the real performances of the thruster and, if released in space, can accidentally cover important surfaces of the satellite such as solar panels, reducing their efficiency.

The choice of a propulsion system is not only based on the performances. Costs, environmental pollution and requirements of the mission are other important aspects that have to be considered. Usually, one of these aspects overcomes the others in importance, so it helps to choose among the available propulsion systems (electric thruster, cold gas thruster, chemical thruster).
In conclusion, it should be remembered that results obtained in this research are not to be considered as real performance parameters of a micropropulsion system. The aim of the research was to collect different mixtures from many researches, compute theoretical parameters and make a relative grading. This kind of work can be seen as a preliminary research of a project aimed at finding the best propellants for microthrusters. Future developments could be focused on different aspects. Experimental tests should be performed in order to see if the trend of theoretical results is confirmed, trying to investigate all that processes that can not be considered with chemical software, like the heat dissipation in the micro-scale world. Moreover, it would be interesting to study in depth the kinetic of the reaction, the time-to-ignition and the energy required for the ignition of the propellants. The extensive research among the many scientific articles available for this topic found that several geometries for these systems are under development. Thus, optimization of geometry for a microthruster would be another interesting research.

Appendix A

Thermite Systems for Gas Propulsion

As a conclusion to this research it was thought to briefly analyse the use of energetic materials in a different way. In previous chapters thermite systems have been studied as propellants, so the aim of the research was to investigate the improvement of propulsion performances through the addition of gas-generating agents. Since thermite is well known thanks to its capability of releasing huge amounts of heat, it would be interesting to exploit this characteristic in order to warm up a gas which flows through a nozzle generating thrust. The idea comes from the well consolidated cold gas propulsion. This system generates thrust by making a propellant flowing out from the thruster in gaseous phase while no combustion occurs. It is simple, robust, safe and clean. The drawback is the low temperature of gases, which doesn't allow to generate high specific impulses.
For this reason, it would be interesting to exploit the heat generated by thermite reaction in order to increase the temperature of the flowing gas before entering in the nozzle and expanding. This leads to an increase of the complexity of the system, but at the same time the specific impulse would increase, depending on the properties of the gas adopted as a propellant.
In this chapter, the conceptual design of a heating chamber is presented with a brief analysis on performances of different gases. The aim is not to find which gas would generate the highest specific impulse, but which one would obtain more benefit by using a system like this.

A.1 Concept and Model of the System

Cold gas propulsion system is appreciated for its simplicity. It basically consists in a high-pressure tank, pipelines and a nozzle, so it requires small space inside the spacecraft. The tank stores the propellant in solid, liquid or gas phase at high pressure. Once the system is activated, the propellant must be warmed up in order to become gas if the initial phase is solid or liquid. Then it flows through the pipeline in which pressure is regulated by valves, until it reaches the nozzle in which it expands and generates thrust.

The concept of a cold gas propulsion system equipped with a heating chamber is based on the system reported in Ref. [38], in which the propulsion unit of a satellite occupies 2U of volume (where 1U is 10x10x10 cm^3). A hypothetical heating chamber, with cylindrical geometry, would occupy no more than 1U of volume, so its limit in length would be 10 cm, and considering that part of the volume could be occupied by other components, the limit for the external diameter could be 5 cm. The chamber is covered by an external case filled with thermite, which, once ignited, warms up the chamber. The gas coming from the tank flows inside the chamber and raises its temperature before expanding in the nozzle. Fig. A.1 shows the schematic of the hypothetical system.

Even if the system seems simple, the physics involved in the process is not. An accurate model would require a deep analysis through the fluid dynamics and the thermodynamics of the problem. The most important aspects regard the possibility to apply a continuum approach, the no slip conditions at the wall, thermal creep, viscous dissipation, and shear stress. Such analysis would require a lot of time, thus, also in this case a simplified model is applied to the system.

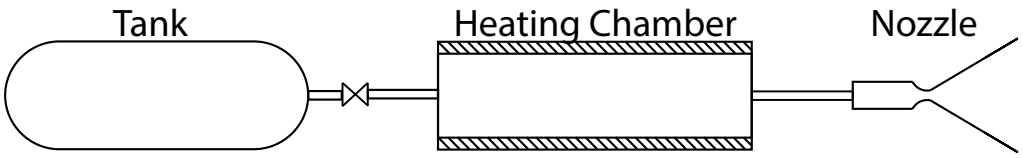

Figure A.1: Schematic of the cold gas propulsion system with a heating chamber

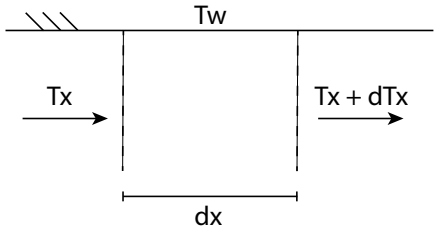

Figure A.2: Infinitesimal length of the duct

In order to get an approximated solution, the problem can be studied as a forced convection in a duct, with fixed wall temperature. The flow is considered completely developed inside the duct and heat exchange occurs through convection. The governing equation follows the Newton's Law, which states that the heat flow is proportional to the area of the wall and to the temperature difference between the wall and the flow:

$$Q = -hA(T_w - T_f) \tag{A.1}$$

where Q is the heat flux, A is the wall area, T_w is the wall temperature, T_f is the fluid temperature and h is the convective coefficient. This coefficient is an important parameter, it depends on many factors: thermophysical properties of the fluid (density, specific heat, dynamic viscosity and thermal conductivity), characteristic length of the geometry and the flow velocity. Considering the numerous factors that affect the value of this coefficient, its evaluation is not simple. In order to simplify it, dimensionless numbers are used:

- Nusselt number : $Nu = \frac{hD_c}{\lambda_f}$. Ratio between convective heat exchange and conductive heat exchange;
- Reynolds number: $Re = \frac{\rho_f w D_c}{\mu_f}$. Ratio between inertia forces and viscous forces;
- Prandtl number: $Pr = \frac{\mu_f c_{pf}}{\lambda_f}$. Ratio between kinematic diffusivity and thermal diffusivity.

Where D_c is the characteristic length of the geometry (in our case it is the diameter of the duct), λ_f is the thermal conductivity of the fluid, ρ_f is the density of the fluid, μ_f is the dynamic viscosity of the fluid, c_{pf} is the specific heat of the fluid and w is the flow velocity. Knowing these parameters, one can compute the Reynolds number. For forced convection in a duct, if the flow is laminar (Re < 2000), Nu $= 3.66$, otherwise if the flow is turbulent (Re > 2000), Nu $= 0.023 \cdot Re^{0.8} \cdot Pr^{0.33}$. Knowing the Nusselt number it is possible to compute h and then solve the Newton's equation. Considering an infinitesimal length of the duct dx, as shown in Fig. A.2, the equation can be written as:

$$\dot{m} c_{pf}(T_x + dT_x - T_x) = h 2\pi R_i dx (T_w - T_x) \tag{A.2}$$

where $\dot{m}$ is the mass flow rate, R_i is the radius of the duct, T_x is the temperature of the flow at the entrance of the infinitesimal portion of the duct and dT_x is the variation of temperature along this portion. Integrating along the entire length L of the heating chamber:

$$T_{out} = T_w - \frac{T_w - T_{in}}{exp(\frac{2\pi h R_i L}{\dot{m} c_{pf}})} \tag{A.3}$$

The objective is to get the highest possible variation of temperature, and as can be seen from Eq. A.3, the exit temperature depends on geometry of the problem and characteristics of the fluid.
This kind of analysis has been applied to different gases considered for space propulsion, results are reported in the following section.

A.2 Results

The aim of the research is to find which gas gains more benefits from the use of a heating chamber and see how performances change with variation of geometrical parameters of the chamber and its wall temperature. Initial data for this problem are collected from Ref. [38]. Temperature of the gas at the inlet of the chamber is 293.15 K, the pressure inside is 0.2 MPa and the pressure at the nozzle exit is 0.03 MPa. The mass flow rate is 0.5 g/s.
Many different gases are considered for this problem, most of them are listed in Fig. 2.5. Their properties are collected in Tab. A.1.

Gas	Density, kg/m^3	Specific Heat Ratio	Molecular Weight g/mol	Specific Heat, $kJ/(kg \cdot K)$	Dynamic Viscosity $\mu Pa \cdot s$	Thermal Conductivity, $W/(m \cdot K)$
H_2	0.089	1.405	2.016	14.307	8.90	0.182
He	0.178	1.667	4.003	5.192	19.85	0.153
Ne	0.900	1.667	20.183	1.029	31.75	0.049
N_2	1.250	1.400	28.013	1.039	17.96	0.024
Ar	1.784	1.667	39.948	0.520	22.61	0.017
Kr	3.708	1.660	83.800	0.248	25.30	0.009
Xe	5.900	1.650	131.293	0.158	23.08	0.005
CF_4	3.720	1.183	88.004	0.659	17.32	0.016
CH_4	0.679	1.310	16.000	2.209	10.74	0.032
NH_3	0.728	1.320	17.031	2.166	9.72	0.024
N_2O	1.872	1.285	44.013	0.873	14.36	0.017
C_3H_8	1.898	1.141	44.100	1.643	7.87	0.017
C_4H_{10}	2.532	1.110	58.120	1.650	7.25	0.015
CO_2	1.871	1.299	44.010	0.841	14.44	0.015
SF_6	6.170	1.100	146.06	0.652	1.45	0.012

Table A.1: Thermophysical properties of different gases

Results obtained for a wall temperature equal to 1500 K and a duct with diameter equal to 3 cm and length 8 cm are reported in Tab. A.2. It can be seen that the three gases that obtain the highest values of ΔI_{sp} are hydrogen, helium and neon.

Gas	I_s without heating, s	I_s with heating, s	T_{out}, K	ΔI_s, s
H_2	191.6	200.5	321.05	8.9
He	129.7	143.1	356.83	13.4
Ne	57.7	67.0	394.68	9.3
N_2	51.4	55.7	343.36	4.3
Ar	41.0	45.9	366.76	4.9
Kr	28.3	32.0	374.43	3.7
Xe	22.7	25.5	370.51	2.8
CF_4	30.7	33.4	345.87	2.7
CH_4	69.5	73.2	325.43	3.7
NH_3	67.2	70.0	317.57	2.8
N_2O	42.2	45.2	337.19	3.0
C_3H_8	44.0	45.7	316.19	1.7
C_4H_{10}	38.8	40.1	314.28	1.3
CO_2	42.0	44.9	334.25	2.9
SF_6	24.5	26.3	335.57	1.8

Table A.2: Performances with wall temperature equal to 1500K and length of the chamber equal to 8 cm.

Now it is interesting to see the effects of wall temperature and geometry on the performances of these three gases. A first simulation keeps the length of the chamber fixed (8 cm), and studies the behaviour of performances when the wall temperature increases from 500 K until 3000 K. A second simulation keeps the wall temperature fixed (1500 K) while the length of the chamber changes from 5 cm until 9 cm. Results are reported in Fig. A.3, Fig. A.4 and Fig. A.5. It is easily predictable that an increment of wall temperature or an increment of the chamber length lead to an increment of performances. Figures show that neon is the gas that reacts in the best way for what concern the outlet temperature, helium is the one that gets the highest increment of specific impulse and hydrogen is the one that generates the highest specific impulse.

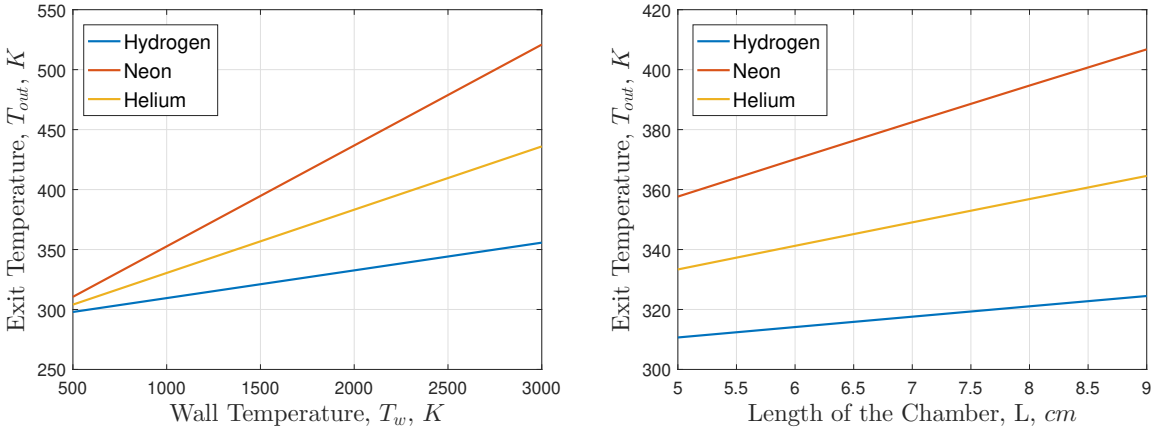

Figure A.3: Trend of the outlet temperature with increasing of the wall temperature and with length of the chamber equal to 8 cm (left); trend of the outlet temperature with increasing of the chamber length and with wall temperature equal to 1500 K (right).

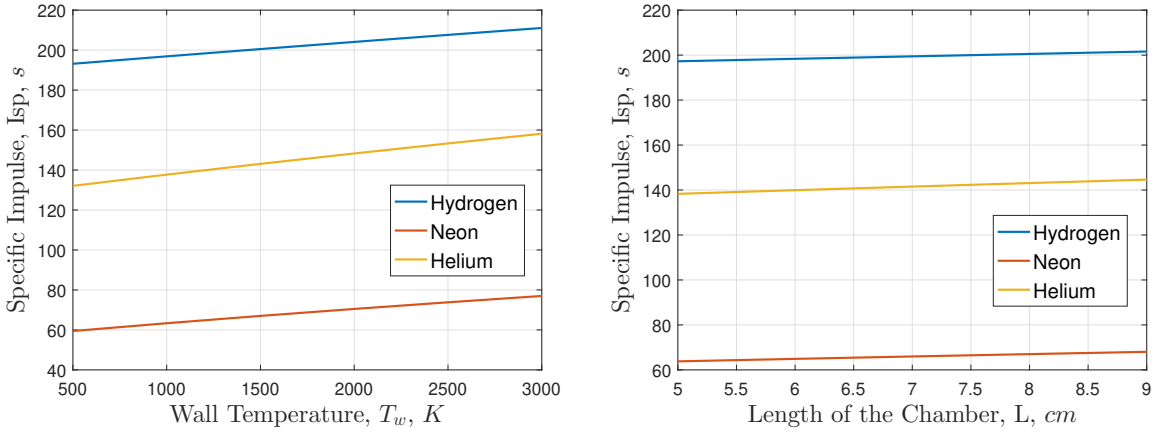

Figure A.4: Trend of the specific impulse with increasing of the wall temperature and with length of the chamber equal to 8 cm (left); trend of the specific impulse with increasing of the chamber length and with wall temperature equal to 1500 K (right).

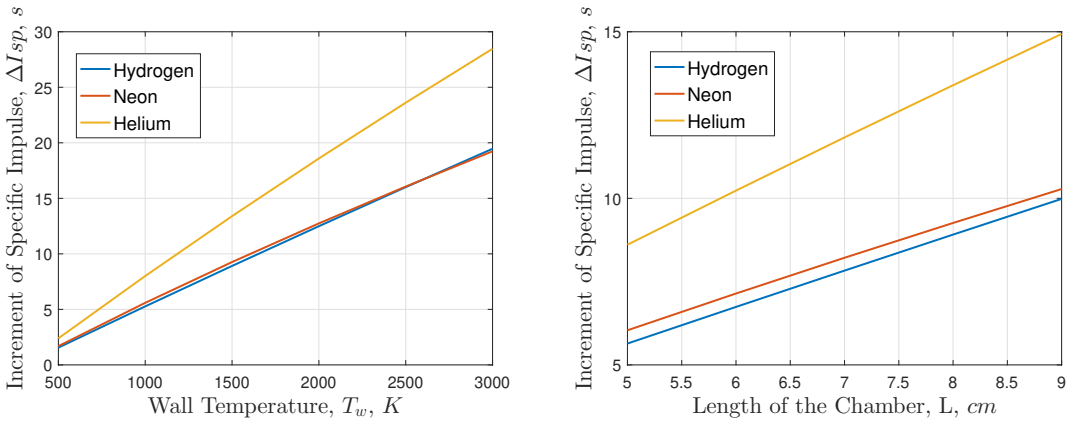

Figure A.5: Trend of the variation of specific impulse with increasing of the wall temperature and with length of the chamber equal to 8 cm (left); trend of the variation of specific impulse with increasing of the chamber length and with wall temperature equal to 1500 K (right).

A.3 Discussion

Analysis about the system shows that among the several gases considered, hydrogen, helium and neon are the ones that react in the best way to the introduction of a heating chamber before the expansion in the nozzle. The explanation to this behaviour can be found in Tab. A.1. Looking at Eq. A.3, an increase of the outlet temperature can be achieved by increasing radius or length of the chamber, by selecting a gas with higher convective coefficient and lower specific heat or by reducing the mass flow inside the chamber. He, H_2 and Ne are the gases with the highest values of thermal conductivity, and this means that they have highest values of convective coefficient h. Fig. A.3 shows that neon is the gas that most increases the outlet temperature. This is due to the fact that in addition to a high thermal conductivity, it has a relatively low specific heat (1.029 $kJ/(kg \cdot K)$) with respect to helium (5.192 $kJ/(kg \cdot K)$) and hydrogen (14.307 $kJ/(kg \cdot K)$, the highest among all the considered gases). Despite the good thermal properties, neon is not the best gas in terms of propulsion performances. The highest specific impulse is achieved by hydrogen, but the highest increment of specific impulse is obtained with helium. This trend is due to the fact that helium and hydrogen have the lowest values of molecular weight, at least one order of magnitude lower with respect to other gases. Specific impulse depends on values of the exhaust velocity, which is mainly characterized by the ratio between the total temperature inside the chamber and the molecular weight of the gas. This means that lower values of molecular weight generate higher specific impulses.

This preliminary analysis allows to understand which gases would obtain more benefits from the addition of a heating chamber. Results show that neon is the one that most increases the outlet temperature, hydrogen generates the highest specific impulse with a considerable increment of specific impulse, helium generates a very high specific impulse with the highest increment of specific impulse. Among the numerous gases studied, these are the ones that mostly exploit the insertion of the heating chamber.
Obviously this research is not enough in order to understand if these gases are suitable for this kind of system. Here only the thermodynamic of the system has been analysed. Other aspects would be considered in further studies.
First of all, numerical modeling and experimentation about the physical processes occurring in real cases are necessary. As already mentioned, some aspects like thermal creep, viscous dissipation and shear stress could affect the performances of the thruster. Furthermore, it must be ensured that thermite reaction warms up properly the case of the heating chamber. For low wall temperatures the increment of specific impulse probably is not worth the increase in the complexity of the system. This requires further studies not only about type and quantity of thermite, but also about the material of the structure, trying to avoid excessive dissipation of heat in the surrounding. In conclusion, it must be considered also the storage of the gas. From that point of view it is preferable to store a propellant with higher density and moderate low boiling point and melting temperature. Moreover, the storage in solid phase is preferable with respect to liquid or gas phase. In this way problems regarding sloshing can be avoided.
All these aspects allow to understand the complexity of the system, and a simple research about ther-

modynamic of the system is not enough, but at least allows to make a first consideration about the best propellants for gas propulsion.

Bibliography

[1] Lonsdale, C. P., "Thermite rail welding: history, process developments, current practices and outlook for the 21st century." *Proc. AREMA 1999 Annu. Conf.*, 1999.

[2] National Aeronautics and Space Administration. https://www.nasa.gov/. Last Visit: February 2020

[3] Levchenko, I., Bazaka, K., Ding, Y., Raitses, Y., Mazouffre, S., Henning, T., and Kim, M., "Space micropropulsion systems for Cubesats and small satellites: from proximate targets to furthermost frontiers." *Applied Physics Reviews*, 5.1, 2018.

[4] Nguyen, H., Köhler, J., and Stenmark, L., "The merits of cold gas micropropulsion in state-of-the-art space missions." *The 53rd International Astronautical Congress, IAC 02-S*, 2.07, Houston, Texas, 2002.

[5] Yan, Q. L., He, G. Q., Liu, P. J., and Gozin, M., *Nanomaterials in rocket propulsion systems*, Elsevier, 2018.

[6] Chaalane, A., Chemam, R., Houabes, M., Yahiaoui, R., Metatla, A., Ouari, B., and Esteve, D., "A MEMS-based solid propellant microthruster array for space and military applications." *Journal of Physics: Conference Series*, Vol. 660, No. 1, IOP Publishing, 2015.

[7] Sutton, G. P., and Biblarz, O., *Rocket Propulsion Elements*, John Wiley Sons, 2016.

[8] Jayaraman, K., Chakravarthy, S., and Sarathy, R., "Behaviour of Nano-Aluminum in Solid Propellant Combustion.", *44th AIAA/ASME/SAE/ASEE Joint Propulsion Conference and Exhibit*, 2008.

[9] Martirosyan, K. S., Wang, L., Vicent, A., and Luss, D., "Nanoenergetic Gas-Generators: Design and Performance.", *Propellants, Explosives, Pyrotechnics: An International Journal Dealing with Scientific and Technological Aspects of Energetic Materials*, 2009, p. 532-538.

[10] Davenas, A., *Solid rocket propulsion technology*, Elsevier, 2012.

[11] Richard Nakka's Experimental Rocketry Web Site. https://www.nakka-rocketry.net/igniter.html. Last visit: October 2019.

[12] White Sands Missile Range Museum. http://www.wsmr-history.org/Photos/ASP.jpg. Last visit: October 2019.

[13] White Sands Missile Range Museum.http://www.wsmr-history.org/Photos/ParkPhotos/Loki.jpg. Last visit: October 2019.

[14] Astronautix. https://web.archive.org/web/20100102233831/http://astronautix.com/lvs/loki.htmchrono. Last visit: October 2019.

[15] Martirosyan, K. S., "Nanoenergetic gas-generators: principles and applications.", *Journal of Materials Chemistry*, 21.26, 2011, p. 9400-9405.

[16] American Welding Society. https://awo.aws.org/2015/07/welding-in-space/. Last visit: October 2019.

[17] Assembly Magazine. https://www.assemblymag.com/articles/94007-friction-stir-welding-expands-its-reach. Last visit: October 2019.

[18] NASA Technology Transfer Program. https://technology.nasa.gov/patent/TOP8-95. Last visit: October 2019.

[19] NASA Technology Transfer Program. https://technology.nasa.gov/patent/MFS-TOPS-5. Lasr visit: October 2019.

[20] Oxford dictionaries - English. lexico.com/en/definition/regolith. Last visit: October 2019.

[21] Álvarez, F., Delgado, A., Frias, J., Rubio, M., White, C., Narayana Swamy, A. K., and Shafirovich, E., "Combustion of thermites in reduced gravity for space applications." *Journal of thermophysics and heat transfer*, 27.3, 2013.

[22] French, B. M., Heiken, G., Vaniman, D., and Schmitt, J., *Lunar sourcebook: A user's guide to the Moon*, CUP Archive, 1991.

[23] Bagatti, F., Corradi, E., Desco, A., and Ropa, C., Chimica, Zanichelli, 2017.

[24] Job, G., and Herrmann, F., "Chemical potential: a quantity in search of recognition." *European journal of physics*, 27.2, 2006.

[25] Gordon, S., and McBride, J. B., "Computer program for calculation of complex chemical equilibrium compositions and applications. Part 1: Analysis", NASA Lewis Research Center, 1994.

[26] Kornilov, S., Rempe, N., Smirnyagina, N., Khaltanova, V., and Lapina, A., "Thermodynamic Modelling of High-temperature Synthesis of the Titan and Chrome Carbides on an Alloyed Steel for Electron-Beam Melting of Modifying Coatings.", *MATEC Web of Conferences*, Vol. 79., EDP Sciences, 2016.

[27] Kosanke, K. L., Kosanke, B. J., and Jennings-White, C., "Lecture notes for pyrotechnic chemistry", *Journal of Pyrotechnics*, 2004.

[28] Wang, L., Munir, Z. A., and Maximov, Y. M., "Thermite reactions: their utilization in the synthesis and processing of materials.", *Journal of Materials Science*, 28.14, 1993.

[29] Brown, M. E., and Gallagher, P. K., *Handbook of Thermal Analysis and Calorimetry: Applications to inorganic and miscellaneous materials*, Elsevier, 2003.

[30] De Luca, L. T., Shimada, T., Sinditskii, V. P., and Calabro, M., *Chemical rocket propulsion: A comprehensive survey of energetic materials*, Springer, 2016.

[31] Jessup, R. S., and Prosen, E., "Heats of combustion and formation of cellulose and nitrocellulose (cellulose nitrate).", *J. Res. Natl. Bur. Stand*, 44, 1950, p. 387-393.

[32] U.S. National Library of Medicine, PubChem. https://pubchem.ncbi.nlm.nih.gov/. Last visit: March 2020.

[33] Dai, J., Wang, F., Ru, C., Xu, J., Wang, C., Zhang, W., and Shen, R., "Ammonium perchlorate as an effective additive for enhancing the combustion and propulsion performance of Al/CuO nanothermites.", *The Journal of Physical Chemistry*, C 122.18, 2018.

[34] Patnaik, P., *Handbook of inorganic chemicals*, Vol. 529, New York: McGraw-Hill, 2003.

[35] Wang, S., Abraham, A., Zhong, Z., Schoenitz, M., and Dreizin, E. L., "Ignition and combustion of boron-based Al· B· I2 and Mg· B· I2 composites.", *Chemical Engineering Journal*, 293, 2016, p. 112-117.

[36] Martirosyan, K. S., Wang, L., and Luss, D., "Novel nanoenergetic system based on iodine pentoxide.", *Chemical Physics Letters*, 483.1-3, 2009, p. 107-110.

[37] Ru, C., Wang, F., Xu, J., Dai, J., Shen, Y., Ye, Y., and Shen, R., "Superior performance of a MEMS-based solid propellant microthruster (SPM) array with nanothermites.", *Microsystem Technologies*, 23.8, 2017.

[38] Zaberchik, M., Lev, D. R., Edlerman, E., and Kaidar, A., "Fabrication and Testing of the Cold Gas Propulsion System Flight Unit for the Adelis-SAMSON Nano-Satellites.", *Aerospace*, 6.8, 2019.